

RAPID AND SENSITIVE DETECTION OF FOODBORNE PATHOGENS  
USING BIO-NANOCOMPOSITES FUNCTIONALIZED ELECTROCHEMICAL  
IMMUNOSENSOR WITH DIELECTROPHORETIC ATTRACTION

A DISSERTATION SUBMITTED TO THE GRADUATE DIVISION OF THE  
UNIVERSITY OF HAWAII AT MĀNOA IN PARTIAL FULFILLMENT OF THE  
REQUIREMENTS FOR THE DEGREE OF

DOCTOR OF PHILOSOPHY  
IN  
MOLECULAR BIOSCIENCES AND BIOENGINEERING

DECEMBER 2017

By  
Inae Lee

Dissertation Committee:

Soojin Jun, Chairperson  
Qing X. Li  
Samir Kumar Khanal  
Wei-Wen Winston Su  
Yong Li

Keywords: biosensor, carbon nanotubes, dielectrophoresis, impedance, microfabrication, virus

© 2017, Inae Lee

## ACKNOWLEDGEMENT

This accomplishment would not have been possible without help, support, and encouragement from my family, friends, academic advisor, committee members, and people around me. I wish to take this opportunity to convey my appreciation to all of them.

Firstly, I would like to express my heartfelt gratitude to my advisor, Dr. Soojin Jun, for the continuous support of my Ph.D. study and related research, for his patience, motivation, and immense knowledge. His guidance helped me in all the time of research and writing of this dissertation. I could not have imagined having a better advisor and mentor for my Ph.D. study.

I would like to appreciate Dr. Yong Li who kindly provided bacterial strains and allowed me to work in Food Microbiology Lab. I would also like to acknowledge the rest of my committee members: Dr. Qing X. Li, Dr. Samir Kumar Khanal, and Dr. Wei-Wen Winston Su, for their insightful comments and encouragement, but also for the hard question which incited me to widen my research from various perspectives.

Many sincere thanks go out to previous and current labmates at Food Processing Lab for their friendly assistance and for all the fun we have had in the last four years. I am also pleased to thank my friends and research coworkers in Korea. In particular, I am grateful to Dr. Sanghoon Ko for enlightening me the first glance of research, as well as for the tremendous help, advice, and mentorship on my academic life and future.

Last but not the least, I must express my profound gratitude to my parents, my brother, and sister, and to *Junho Jung*, for providing me with unfailing support and continuous encouragement throughout my years of study and through the process of researching and writing this dissertation.

## ABSTRACT

The rapid detection and identification of potentially harmful microorganisms in food are essential to prevent foodborne outbreaks and ensure our safety. The faster response time and relatively high sensitivity and selectivity of biosensor-based detection methods, as compared to conventional methods, have increased the attention towards alternative approaches for the early inspection of foodborne pathogens in a variety of food products. The recent advances in micro- and nanotechnologies are attributed to the improvement of the sensor's performance. The methods of using single-walled carbon nanotubes (SWCNTs) to enhance the sensing signal response, as well as dielectrophoresis (DEP) and fluidics techniques to improve bioaffinity reactions, create unique bio-nano sensing devices for fast and reliable microbial analysis. The goal of this study was to develop SWCNT functionalized electrochemical immunosensors for the rapid and sensitive detection of foodborne pathogens assisted with dielectrophoretic and fluidic technologies. The biosensor design, which involved electrode configuration, electrode surface modification, and detection mode, were gradually transformed to achieve the sensitive, selective, specific, or simultaneous detection of bacteria and viruses.

The functionalized microwire-based electrochemical immunosensor (MEI sensor) was designed and fabricated for the selective detection of target bacteria from non-target bacteria. The *Escherichia coli* specific MEI sensor was prepared to test the functionalization process and the *Staphylococcus aureus* specific MEI sensor was used to validate the proposed sensor concept for other bacteria. The combination of double-layered SWCNTs and 5% bovine serum albumin coating contributed to signal enhancement and cell binding specificity. The selective capture of *E. coli* or *S. aureus* cells was achieved when the electric field was generated at a frequency of 3

MHz and 20Vpp. A linear trend in the change of electron transfer resistance ( $\Delta R_{et}$ ) was observed as *E. coli* concentrations increased from  $5.32 \times 10^2$  to  $1.30 \times 10^8$  CFU/mL ( $R^2 = 0.976$ ) and *S. aureus* concentrations from  $8.90 \times 10^2$  to  $3.45 \times 10^7$  CFU/mL ( $R^2 = 0.983$ ). Both MEI sensors could detect target bacteria cells without interfering with the other bacteria in the mixed suspensions. The detection time was 10 min including cell concentration and signal measurement.

The developed MEI sensor was evaluated for its detection of target bacteria from non-target materials in food. The *E. coli* specific sensor and the *Salmonella* specific sensor were fabricated to individually detect *E. coli* K12 and *S. Typhimurium* contaminated baby spinach. The estimated concentrations of *E. coli* in the spinach extracts corresponded well with the concentrations determined by the plate counting method, with an  $R^2$  value of 0.972 and a detection range from  $8.33 \times 10^2$  to  $7.97 \times 10^5$  CFU/g for the surface contamination method. A linear relationship was observed between  $\Delta R_{et}$  and *S. Typhimurium* concentrations from  $1.43 \times 10^3$  to  $1.67 \times 10^7$  CFU/g with an  $R^2$  value of 0.942. Both *E. coli* and *Salmonella* MEI sensors are specific towards the target bacteria in the sample despite the interference of spinach debris and non-target bacteria.

The continuous flow multi-junction biosensor was fabricated and characterized for the simultaneous detection of *E. coli* and *S. aureus*. The developed continuous flow junction sensor showed an increase of sensing sensitivity by a factor of 10 in the detection of *E. coli* K12, as compared to the stationary sensor. A linear regression was observed for both the *E. coli* and *S. aureus* functionalized multi-junction array sensors with a detection range of  $10^2$  to  $10^5$  CFU/mL. Multiplexed detection of bacteria at sensing levels as low as  $10^2$  CFU/mL for *E. coli* K12 and *S. aureus* were accomplished within 2 min.

Lastly, the flow-based dielectrophoretic biosensor was designed and tested for the

detection of bacteriophage MS2 as a norovirus surrogate. The cyclic voltammogram showed that the current for the PEI-SWCNTs electrode was higher than the current of the PEI film surface, and was followed by a decrease in the current after antibody immobilization and MS2 attachment. Antibody immobilization on the detector with electric field applied to the fluidic channel at 10 V<sub>pp</sub> and 1 MHz showed higher current changes by antibody-MS2 complexes than the assay without antibody immobilization and DEP. The changes in current signal displayed a dependence on the concentration of MS2 in the sample solution. The total assay was completed within 15 min.

The developed MEI sensor with DEP-assisted cell trapping has the potential for fast, simple, and selective detection of low levels of target bacteria in the presence of mixed bacteria communities and food matrices. The CNTs functionalization and continuous flow assay could offer advances in sensitivity and detection time. The proposed sensing technology and the device can have a beneficial influence on the food industry by offering the rapid detection of multiple pathogens in food. It will also result in the development of new approaches to monitor and control biological hazards, which can be incorporated into food production and processing facilities to improve the safety of our food products.

## TABLE OF CONTENTS

<b>ACKNOWLEDGEMENT</b> .....	<b>i</b>
<b>ABSTRACT</b> .....	<b>ii</b>
<b>LIST OF FIGURES</b> .....	<b>ix</b>
<b>LIST OF TABLES</b> .....	<b>xiv</b>
<b>LIST OF ABBREVIATIONS</b> .....	<b>xv</b>
<b>Chapter 1.</b> .....	<b>1</b>
<b>INTRODUCTION</b> .....	<b>1</b>
<b>Chapter 2.</b> .....	<b>6</b>
<b>LITERATURE REVIEW</b> .....	<b>6</b>
<b>2.1. Introduction</b> .....	<b>6</b>
2.1.1. Foodborne pathogens and illness outbreaks .....	6
2.1.2. Current detection methods .....	8
<b>2.2. Biosensors for detection of foodborne pathogens</b> .....	<b>11</b>
2.2.1. Biosensor classification .....	11
2.2.2. Electrochemical immunosensor.....	14
<b>2.3. Advanced technologies incorporated to electrochemical immunosensors</b> .....	<b>19</b>
2.3.1. Functionalization of the biosensor with nanomaterials .....	19
2.3.2. Manipulation of microorganism movement by dielectrophoresis .....	22
2.3.3. Microfabricated biosensor devices .....	30
<b>2.4. Conclusion</b> .....	<b>32</b>
<b>Chapter 3.</b> .....	<b>34</b>
<b>Selective detection of <i>Escherichia coli</i> K12 and <i>Staphylococcus aureus</i> in mixed bacterial communities using a functionalized electrochemical immunosensor with dielectrophoretic concentration</b> .....	<b>34</b>
<b>ABSTRACT</b> .....	<b>34</b>
<b>3.1. Introduction</b> .....	<b>36</b>
<b>3.2. Materials and methods</b> .....	<b>39</b>

3.2.1. Materials and instruments.....	39
3.2.2. Microbial preparation .....	40
3.2.3. Functionalization of microwire surface.....	42
3.2.4. Bacterial cell capture by dielectrophoresis .....	42
3.2.5. Impedance measurement .....	43
3.2.6. Data analysis.....	44
3.2.7. FESEM visualization and validation .....	44
<b>3.3. Results and discussion.....</b>	<b>44</b>
3.3.1. Surface morphology of bare and functionalized microwires.....	44
3.3.2. Effect of SWCNTs coating on signal enhancement .....	46
3.3.3. Effect of BSA solution on blocking the non-specific binding.....	47
3.3.4. Detection of <i>E. coli</i> K12 in pure and mixed solution .....	49
3.3.5. Application of developed MEI sensor for detection of <i>S. aureus</i> in pure and mixed solution .....	52
<b>3.4. Conclusion.....</b>	<b>55</b>
<b>Chapter 4. ....</b>	<b>56</b>
<b>Microwire-based electrochemical immunosensing technique combined with dielectrophoresis for rapid detection of <i>Escherichia coli</i> K12 and <i>Salmonella</i> Typhimurium in baby spinach.....</b>	<b>56</b>
<b>ABSTRACT.....</b>	<b>56</b>
<b>4.1. Introduction .....</b>	<b>58</b>
<b>4.2. Materials and methods .....</b>	<b>60</b>
4.2.1. Bacterial cultures preparation.....	60
4.2.2. Inoculation of <i>E. coli</i> K12 and <i>S. Typhimurium</i> into spinach leaves.....	61
4.2.3. Functionalization of microwire surface.....	62
4.2.4. Detection of <i>E. coli</i> K12 and <i>S. Typhimurium</i> in contaminated spinach leaves .....	62
4.2.5. Impedance measurement .....	63
4.2.6. Data analysis.....	64
4.2.7. FESEM visualization.....	64
<b>4.3. Results .....</b>	<b>65</b>



4.3.1. Detection of <i>E. coli</i> K12 in spinach leaves using the <i>E. coli</i> specific sensor .....	65
4.3.2. Specificity test of the <i>Salmonella</i> specific sensor against <i>E. coli</i> K12 in buffer .....	67
4.3.3. Detection of <i>S. Typhimurium</i> in spinach leaves using the <i>Salmonella</i> specific sensor.....	69
<b>4.4. Discussion.....</b>	<b>71</b>
4.4.1. Sensitivity of the <i>E. coli</i> and the <i>Salmonella</i> sensors .....	72
4.4.2. Specificity of the <i>E. coli</i> and the <i>Salmonella</i> sensors.....	73
4.4.3. Application of developed biosensing for detection of other bacteria species .....	74
4.4.4. Detection of bacteria in food sample.....	75
<b>4.5. Conclusion.....</b>	<b>76</b>
<b>Chapter 5. ....</b>	<b>77</b>
<b>Simultaneous detection of <i>Escherichia coli</i> K12 and <i>Staphylococcus aureus</i> using a continuous flow multi-junction biosensor.....</b>	<b>77</b>
<b>ABSTRACT.....</b>	<b>77</b>
<b>5.1. Introduction .....</b>	<b>78</b>
<b>5.2. Materials and methods .....</b>	<b>81</b>
5.2.1. Junction sensor fabrication .....	81
5.2.2. Microbial preparation .....	82
5.2.3. Continuous flow detection.....	83
5.2.4. Sensitivity and selectivity test .....	84
5.2.5. Data analysis.....	85
<b>5.3. Results and discussion.....</b>	<b>85</b>
5.3.1. Detection <i>E. coli</i> K12 with a single junction sensor in a continuous flow mode.....	85
5.3.2. Sensitivity and selectivity of multi-junction sensors.....	89
5.3.3. Simultaneous detection of <i>E. coli</i> K12 and <i>S. aureus</i> .....	91
<b>5.4. Conclusion.....</b>	<b>93</b>
<b>Chapter 6. ....</b>	<b>94</b>
<b>Flow-based dielectrophoretic biosensor for detection of bacteriophage MS2 as a foodborne virus surrogate .....</b>	<b>94</b>
<b>ABSTRACT.....</b>	<b>94</b>
<b>6.1. Introduction .....</b>	<b>95</b>

<b>6.2. Materials and methods .....</b>	<b>99</b>
6.2.1. Materials .....	99
6.2.2. Biosensor device fabrication .....	100
6.2.3. Antibody immobilization on the detector .....	101
6.2.4. Bacteriophage MS2 propagation .....	102
6.2.5. Bacteriophage MS2 qualification by plaque assay .....	103
6.2.6. Electrochemical measurement .....	103
6.2.7. Dielectrophoretic MS2 detection .....	103
6.2.8. Statistical analysis .....	105
<b>6.3. Results and discussion.....</b>	<b>105</b>
6.3.1. Characterization of SWCNTs-antibody functionalized surface and MS2 detection .	105
6.3.2. Effect of DEP concentration on change in signal response .....	109
6.3.3. Detection of bacteriophage MS2 in the continuous flow mode .....	111
<b>6.4. Conclusion.....</b>	<b>113</b>
 <b>Chapter 7. ....</b>	 <b>114</b>
<b>CONCLUSIONS AND FUTURE WORKS.....</b>	<b>114</b>
<b>7.1. Conclusions .....</b>	<b>114</b>
<b>7.2. Future works.....</b>	<b>116</b>
7.2.1. Optimization of immunocapture: Antibody selection and immobilization .....	116
7.2.1. Study on other physical effects on the particles in the electric field .....	118
7.2.3. Dielectrophoretic separation of pathogens from food sample .....	119
7.2.4. Dielectrophoretic concentration of pathogens in fluidic channel .....	119
7.2.5. Portable device for detection of multiple pathogens .....	120
 <b>REFERENCES.....</b>	 <b>121</b>

## LIST OF FIGURES

<b>Figure 2.1</b> Common biosensor components and classification (Lazcka et al., 2007; Velusamy et al., 2010).....	12
<b>Figure 2.2</b> Schematic for principle and electrochemical function of the impedimetric biosensor. (a) A transducer surface is functionalized with a polymer or self-assembled monolayer to anchor the bioreceptor elements allowing specific recognition for the analyte. The change in electron transfer resistance is monitored under the electrochemical cell with an electron mediator ( $\text{Fe}(\text{CN})_6^{3-/4-}$ ) and can be expressed as Randles equivalent circuit consisting of electrolyte solution resistance ( $R_s$ ), double-layer capacitance ( $C_{dl}$ ), electron transfer resistance ( $R_{et}$ ), and Warburg impedance ( $Z_w$ ). (b) The Nyquist plot shows the components of Randles equivalent circuit and impedance can be represented by a vector arrow with magnitude $ Z $ and frequency angle $\phi$ . (c) Impedance is proportionally changed to the analyte concentration interacting with the electrode surface. (Modified from Ahmed et al. (2014a)) .....	18
<b>Figure 2.3</b> Comparison of behaviors of charged and neutral bodies in (a) a uniform electric field, (b) a non-uniform electric field, and (c) the non-uniform electric field when alternating current is applied .....	24
<b>Figure 2.4</b> Directions of particle movement depending on the charge distribution of the medium and electric field strength near the neutral body.....	25
<b>Figure 3.1</b> A schematic of selective capture of target bacteria with functionalized microwire and a photograph of inserted the functionalized wire into the sample droplet for bacterial cell capture by dielectrophoresis .....	43
<b>Figure 3.2</b> SEM images for bare (a)-(b) and functionalized (c)-(d) microwires.....	45
<b>Figure 3.3</b> Electrical signal response enhancements by SWCNTs coatings. Means followed by the same letter do not differ significantly at $p \leq 0.05$ .....	47
<b>Figure 3.4</b> Effect of BSA on non-specific binding reduction. * and ** $\Delta R_{et}$ values from different BSA treatments were analyzed separately.....	48

<b>Figure 3.5</b> Changes of electron transfer resistance with <i>E. coli</i> K12 captured on the electrode surface of <i>E. coli</i> sensor in pure <i>E. coli</i> K12 solution. ....	49
<b>Figure 3.6</b> <i>E. coli</i> K12 attachments on the base plane (a, $\times 5.0k$ ) and the cylinder side (b, $\times 40.0k$ ) of microwire observed by SEM.....	50
<b>Figure 3.7</b> Specificity and selectivity of the <i>E. coli</i> MEI sensor for detection of <i>E. coli</i> K12 against non-target bacteria suspension and cocktail samples. Acronyms mean bacteria suspending in pure and mixed samples; EC: <i>E. coli</i> K12, SA: <i>S. aureus</i> , ST: <i>S. Typhimurium</i> , LM: <i>L. monocytogenes</i> , EC + SA: a mixture of <i>E. coli</i> K12 and <i>S. aureus</i> , EC + ST: a mixture of <i>E. coli</i> K12 and <i>S. Typhimurium</i> , and EC + LM: a mixture of <i>E. coli</i> K12 and <i>L. monocytogenes</i> .....	51
<b>Figure 3.8</b> Bacterial attachments on the surface of <i>E. coli</i> specific sensor (a) when applied to the cocktail solution ( <i>E. coli</i> K12 and <i>S. aureus</i> ) and (b) when applied to the pure <i>S. aureus</i> solution. ....	52
<b>Figure 3.9</b> Changes of electron transfer resistance with <i>S. aureus</i> captured on the electrode surface of <i>S. aureus</i> sensor in pure solution. Means with the same letter are not significantly different ( $p \leq 0.05$ ) and SEM images of <i>S. aureus</i> bacteria cells on the base plane (a, $\times 5.0k$ ) and the cylinder side (b, $\times 30.0k$ ) of the microwire .....	53
<b>Figure 3.10</b> Specificity and selectivity of <i>S. aureus</i> specific sensor against non-target bacteria and cocktail samples. Acronyms mean bacteria suspending in pure and mixed samples; EC: <i>E. coli</i> K12, SA: <i>S. aureus</i> , ST: <i>S. Typhimurium</i> , LM: <i>L. monocytogenes</i> , SA + EC: a mixture of <i>S. aureus</i> and <i>E. coli</i> K12, SA + ST: a mixture of <i>S. aureus</i> and <i>S. Typhimurium</i> , and SA + LM: a mixture of <i>S. aureus</i> and <i>L. monocytogenes</i> .....	54
<b>Figure 4.1</b> Changes in electron transfer resistance ( $\Delta R_{et}$ ) with <i>E. coli</i> K12 captured on the <i>E. coli</i> sensor; black: <i>E. coli</i> K12 contamination on the surface of spinach leaves, white: internalized contamination of <i>E. coli</i> K12 into the main vein.....	66
<b>Figure 4.2</b> Relationship between $\Delta R_{et}$ and <i>E. coli</i> K12 in the range of $10^3$ - $10^6$ CFU/mL contaminated in spinach by two inoculation methods; on the surface (black) and into the vascular tissue (white). * $\Delta R_{et}$ values of <i>E. coli</i> K12-spinach juice recovered from two inoculation methods were analyzed separately. ....	66

<b>Figure 4.3</b> Specificity test of the <i>Salmonella</i> biosensor against <i>E. coli</i> K12 in peptone water and bacteria-free peptone water. Inserted SEM images represent the surface of the <i>Salmonella</i> sensor after testing with the <i>S. Typhimurium</i> and <i>E. coli</i> K12 suspensions.....	68
<b>Figure 4.4</b> Changes in electron transfer resistance ( $\Delta R_{et}$ ) with <i>S. Typhimurium</i> captured on the <i>Salmonella</i> sensor .....	69
<b>Figure 4.5</b> Relationship between $\Delta R_{et}$ and <i>S. Typhimurium</i> in the range from $10^3$ to $10^7$ CFU/mL contaminated in spinach. ....	70
<b>Figure 4.6</b> SEM images of the <i>Salmonella</i> sensor after testing with the spinach juices in the presence of <i>S. Typhimurium</i> (a) and <i>E. coli</i> K12 (b). ....	71
<b>Figure 5.1</b> A continuous flow multi-junction sensor device. (a) Illustration of bio-nano functionalized junction (Yamada et al., 2014). (b) Conceptual design of multi-junction biosensor for multiplexed detection in a continuous flow mode (cross sectional view), (c) Individual sensor chip ready to use .....	84
<b>Figure 5.2</b> A current change profile of the continuous flow junction sensor for pure peptone water (solid) and <i>E. coli</i> K12 suspended in peptone water (dot) in Phase I (when the junction was open), Phase II (when the junction met the flow head) and Phase III (when the antigen-antibody reaction fully developed). The concentration of <i>E. coli</i> K12 suspended was $10^4$ CFU/mL.....	86
<b>Figure 5.3</b> Sensing signal enhancement of a continuous flow junction sensor vs. a stationary sensor on the basis of the equivalent current reading (75 nA): (a) Increase of the sensing sensitivity by a factor of 10 and (b) Current changes of the continuous flow sensor with <i>E. coli</i> K12 in the range of $10^2$ - $10^5$ CFU/mL.....	88
<b>Figure 5.4</b> Specificity testing for the developed sensors functionalized with anti- <i>E. coli</i> (a) and <i>S. aureus</i> (b): Microbial concentrations ranged from $10^2$ to $10^5$ CFU/mL.....	90
<b>Figure 5.5</b> Electrical signal responses of multi-junction sensors specific for <i>E. coli</i> K12 (a) and <i>S. aureus</i> (b) when mixture samples of <i>E. coli</i> K12 and <i>S. aureus</i> were used. ....	92
<b>Figure 6.1</b> A schematic of the fluidic device, which consists of the PDMS-fluidic channel (Blue), Ag electrode array for the DEP generator, and the anti-MS2 IgG immobilized on the SWCNTs coated electrode (Red). The fluid channel has 1mm of the width and 100 $\mu$ m of	

the height. The width of each strip of DEP generator electrode array was 800 $\mu\text{m}$ , and the gap between strips was 400 $\mu\text{m}$ .	101
<b>Figure 6.2</b> A concept design for a negative DEP manipulation of MS2 particles to biorecognition site in the fluidic channel. The MS2 particles randomly react with antibodies when no DEP force applied. The MS2 experience the negative DEP force, which repel from higher electric field gradient, can travel toward the bottom of the fluidic channel and then bind to the antibody immobilized on the detector electrode.	104
<b>Figure 6.3</b> Cyclic voltammograms of the detector in each modification step when the potential ranged from 1V to -1V at a scan rate of 100 mV/s in an electrolyte solution consisting of 5 mM $\text{K}_3\text{Fe}(\text{CN})_6$ , 5 mM $\text{K}_4\text{Fe}(\text{CN})_6$ , and 0.1 M KCl.	106
<b>Figure 6.4</b> Impedance spectra corresponding to each modification step on the detector electrode in the presence of 5 mM $[\text{Fe}(\text{CN})_6]^{3-/4-}$ as a redox probe.	108
<b>Figure 6.5</b> Change in current in response to captured MS2 on the detector with and without MS2 antibody on the surface of detector electrode. The electrical current responses were measured with 10 $\mu\text{L}$ of MS2 solution ( $\sim 10^{10}$ PFU/mL) on the detector in stationary mode.	109
<b>Figure 6.6</b> Effect of DEP on current change in response to captured MS2 on the detector. DEP was applied at 10 $V_{pp}$ with a frequency of 1 MHz. The current signals were obtained from the detector filled with PBS after the 1mL of MS2 solution ( $\sim 10^7$ PFU/mL) passed through the biorecognition site at the flow rate of 0.1 mL/min.	110
<b>Figure 6.7</b> Relationship between logarithmic values of change in current ( $\Delta I$ ) and concentrations of MS2 bound to the detector with DEP applied at 10 $V_{pp}$ and 1 MHz. The current was measured at 0.2 $V_{DC}$ . Averaged logarithmic $\Delta I$ values with different letters are significantly different at 95% confidence level.	112
<b>Figure 7.1</b> The conceptual design for multiplexed detection using multi-electrodes biosensor connected to a field deployable unit. The proposed biosensor system consists of microwire sensing probes for cell concentration and collection, a sample container, and the combination unit of an electric power module for dielectrophoresis, and electronic sensor interface for multiplexed microbial detection. The multiplexed design will permit	

simultaneous measurement of nine different functionalized microelectrodes. It will incorporate a bus control, frequency response analyzer, and a multiplexer to switch the analyzer between nine microelectrodes. .... 120

## LIST OF TABLES

<b>Table 1.1</b> Summary of the biosensor fabrication, detection mode, and target microorganisms studied for each technical research objective and corresponding chapter.....	5
<b>Table 3.1</b> Concentrations of each bacterium in pure and in mixed samples when <i>E. coli</i> sensor (top) and <i>S. aureus</i> sensor (bottom) were tested for specific and selective detection.....	41
<b>Table 4.1</b> Specificity test for the <i>E. coli</i> sensor against <i>S. Typhimurium</i> in the spinach leaves..	67
<b>Table 4.2</b> Specificity test for the <i>Salmonella</i> sensor against <i>E. coli</i> K12 in the spinach leaves ..	71
<b>Table 7.1</b> Summary of dynamic detection range, limit of detection, and assay time achieved for each technical research objective and corresponding chapter .....	115



## LIST OF ABBREVIATIONS

1D	One-dimensional
2D	Two-dimensional
3D	Three-dimensional
AC	Alternating current
ANOVA	Analysis of variance
AuNP	Gold nanoparticle
BSA	Bovine serum albumin
CDC	U.S. Center for Disease Control and Prevention
$C_{dl}$	Double-layer capacitance
CFU	Colony Forming Unit
CM	Clausius–Mossotti factor
CNT	Carbon nanotube
CV	Cyclic voltammetry
DEP	Dielectrophoresis
DEPIM	Dielectrophoretic impedance measurement
DMF	N-N-dimethylformamide
DNA	Deoxyribonucleic acid
EDC	1-ethyl-3-[3-dimethylaminopropyl]carbodiimide hydrochloride
E	Voltage (V)
EIS	Electrochemical impedance spectroscopy
ELISA	Enzyme-linked immunosorbent assay
$E_{pa}$	Anodic peak potential
$E_{pc}$	Cathodic peak potential
$F_{DEP}$	Dielectrophoretic force
$F_{drag}$	Hydrodynamic drag force
FESEM	Field emission scanning electron microscope
FET	Field effect transistor
HRT	Hydraulic retention time
I	Electric current (A)
IME	Interdigitated microelectrode
LOC	Lab-on-a-chip
LOD	Limit of detection
MEI	Microwire-based electrochemical immunosensor
MNP	Magnetic nanoparticle
MWCNT	Multiwalled carbon nanotube
nDEP	Negative Dielectrophoresis
NHS	N-hydroxysuccinimide

NP	Nanoparticle
PBS	Phosphate Buffer Solution
PCR	Polymerase chain reaction
pDEP	Positive Dielectrophoresis
PDMS	Polydimethylsiloxane
PEI	Polyethylenimine
PFU	Plaque Forming Unit
QD	Quantum dot
$R_{et}$	Electron transfer resistance
RNA	Ribonucleic acid
$R_s$	Electrolyte solution resistance
SEM	Scanning electron microscopy
SPR	Surface plasmon resonance
SWCNT	Single-walled carbon nanotube
TEM	Transmission electron microscope
TSA	Tryptic Soy agar
TSB	Tryptic Soy Broth
$V_{DC}$	Applied direct current voltage (V)
$V_{pp}$	Applied peak-peak volatege (V)
WHO	World Health Organization
XLD	Xylose lysine deoxycholate
Z	Impedance
Z'	Real impedance
Z''	Imaginary impedance
$Z_w$	Warburg impedance
$\Delta R_{et}$	Change in electron transfer resistance
$\Delta I$	Change in current (A)
$\epsilon_m$	Permittivity of Suspending Medium
$\epsilon_0$	Permittivity of Free Space
$\mu$ TAS	Micro total analysis system
$\sigma_m$	Conductivity of Medium
$\sigma_p$	Conductivity of Particle
$\phi$	Shift in phage
$\Omega$	Ohm
$\omega$	Angular frequency

## Chapter 1.

### INTRODUCTION

The interest in food safety has increased worldwide because it is closely related to public health issues. Food-safety hazards refer to physical, chemical, and biological contaminants in foods that can cause illness or injury to people. Biological hazards include harmful bacteria and viruses that may cause food poisoning in humans by infection or intoxication. To avoid potential health hazards in food products, food manufactures must ensure food safety to protect public health. Methods to control and prevent human foodborne infections by monitoring and pathogen detection have been established along with the development of food processing technology. Most foodborne diseases are caused by *Escherichia coli* O157:H7, *Salmonella* spp., nontyphoidal, *Listeria monocytogenes*, *Clostridium perfringens*, *Campylobacter* spp., *Staphylococcus aureus*, and *norovirus* (CDC, 2011). These disease-causing organisms can be found in various food sources such as: raw produce; undercooked meat, poultry or seafood; unpasteurized milk; dairy products; juice; or eggs and contaminated water. The rapid and precise monitoring of food products contaminated with pathogenic microorganisms before distribution to grocery stores, restaurants, and manufacturing facilities can be a solution to prevent emerging hazards from becoming real risks and causing foodborne incidences (Pedrero et al., 2009; Shriver-Lake et al., 2007).

Conventional laboratory-based methods for the identification and quantification of biological hazards in food use various techniques such as microscopy and cell cultures, biochemical assays, immunological tests, or genetic analysis (Ahmed et al., 2014a). Those methods have been successful for detecting pathogens because they are sensitive and provide

both qualitative and quantitative information on the microorganisms tested (Leonard et al., 2003; Velusamy et al., 2010). Although culturing is the most accurate, it has some disadvantages due to prolonged detection time, initial sample enrichment, and viable but non-culturable cells. Nucleic acid testing is also susceptible to high false-positive results due to its inability to distinguish between viable and dead cells (Wolffs et al., 2005). Those methods are usually laborious and time-consuming, requiring complex instruments in stationary laboratories that can only be operated by skilled personnel (Fournier et al., 2013). The limitations of conventional detection methods arouse the demands for innovative technological development to rapidly detect foodborne pathogens in food products.

Biosensor technology has emerged for the rapid detection of foodborne pathogens with sensitivity and selectivity comparable to traditional methods with the potential to fabricate compact and multiplexing devices for on-site monitoring (Zhao et al., 2014). The reaction between the analytes and the corresponding recognition molecules is caught by the biosensor's transducer element to provide measurable electrical signals (Nandakumar et al., 2008). The biosensor can be classified based on types of bio-recognition materials or mechanisms and transducer elements. The selection of the biosensor components and the fabrication of the biosensor device influence its accuracy, reliability, and analysis time, as well as its sensitivity and specificity for the sample of interest. Besides currently established biosensor platforms, the attention to nanotechnology and dielectrophoresis (DEP) has increased due to the enhancement of the detection process by incorporating them into the bioreceptor or transducer of the biosensor. Surface modification using nanomaterials have shown an advance in sensitivity and help with antibody adsorption on the electrode surface (Ezzati Nazhad Dolatabadi & De La Guardia, 2014; Rodriguez et al., 2015). Among the functional nanomaterials, carbon nanotubes (CNTs) can be

highlighted as the most attractive nanomaterial for biosensor construction due to their excellent optical and mechanical conductivity, high surface-to-volume ratio, good chemical stability, and biocompatibility (Allen et al., 2007; Kang et al., 2006; Katz & Willner, 2004; Putzbach & Ronkainen, 2013; Rodriguez et al., 2015). On the other hand, biological particles suspended in the medium can be polarized, translated, and finally, trapped at a specific position when they are subjected to a non-uniform electric field (Pohl, 1978). DEP is the translational motion imparted on an uncharged particle by the polarization effect. It has been recognized as a powerful tool in the manipulation of biological cells and integrated with the biosensing platform to address sensitivity and specificity challenges. Another suitable technique that can be applied to biosensor development is microfabrication, including lab-on-a-chip (LOC) and microfluidics. Micro-scale biosensor devices are a fast, low-cost, and high-throughput analysis method used for particle manipulation and separation in the field of biology, chemistry, and medicine (Li et al., 2014b).

In this dissertation, bacterial cells or viral particles were detected via changes in the electrical signal within the electrochemical cell by immunoreaction between the antibody and microbial antigen on the surface of the electrode, also known electrochemical immunosensing. The effects of single-walled CNTs (SWCNTs) incorporation into the bioreceptor, DEP-assisted cell attraction, and use of fluidic devices for sensitive, selective, specific, or simultaneous detection of bacteria and viruses were studied. Thus, the overall goal of this research was to develop the bio- and nano-material functionalized electrochemical immunosensors, in conjunction with DEP and/or fluidic technology, for the detection of foodborne pathogens. Specific research objectives to achieve this goal were:

*Objective 1:* Design and improve the functionalized electrochemical immunosensor for the detection of a single analyte in mixed bacterial communities

*Objective 2:* Evaluate the proposed biosensor for the detection of *E. coli* K12 and *S. Typhimurium* in real food systems, i.e. spinach leaves

*Objective 3:* Explore the simultaneous detection of *E. coli* K12 and *S. aureus* using a multi-junction biosensor in a continuous flow mode

*Objective 4:* Develop a flow-based biosensor for the detection of bacteriophage MS2 as a norovirus surrogate

Table 1.1 summarizes the biosensor fabrication, detection mode, and target microorganisms studied for each research objective and corresponding chapter. The electrochemical immunosensor was fabricated using a single microwire or microwire crossbar array for bacterial detection, and a silver electrode array for viral detection, in non-flow mode or flow mode. The surface of the electrode was functionalized with SWCNTs and specific antibodies. The immunoreaction was analyzed by measuring changes in impedance or current.

**Table 1.1** Summary of the biosensor fabrication, detection mode, and target microorganisms studied for each technical research objective and corresponding chapter

	<b>Objective 1 Chapter 3</b>	<b>Objective 2 Chapter 4</b>	<b>Objective 3 Chapter 5</b>	<b>Objective 4 Chapter 6</b>	
	Selective detection of target from non-target bacteria	Selective detection of target from non-target materials in food	Simultaneous detection of two different bacteria	Viral detection	
<b>Biosensor fabrication</b>	<b>Electrode configuration</b>	An individual microwire for each target bacteria	An individual microwire for each target bacteria	2 × 2 microwire crossbar junctions on the sensor chip	Silver electrode array for concentrator and detector, individually, embedded on fluidic channel
	<b>Bio-nanocomposites coating on electrode</b>	SWCNT functionalization/ polyclonal antibodies via avidin-biotin complex	SWCNT functionalization/ polyclonal antibodies via avidin-biotin complex	SWCNT functionalization/ polyclonal antibodies via avidin-biotin complex	SWCNT functionalization/ polyclonal antibodies via covalent bonding
<b>Detection mode</b>	<b>Electrical signals</b>	Impedance	Impedance	Current	Current
	<b>Detection mode</b>	Stationary	Stationary	Continuous flow	Continuous flow
	<b>Use of DEP</b>	DEP attraction to the microwire	DEP attraction to the microwire	-	DEP attraction to the detector
<b>Microbial sample</b>	<b>Target microorganisms</b>	<i>E. coli</i> K12 <i>S. aureus</i>	<i>E. coli</i> K12 <i>S. Typhimurium</i>	<i>E. coli</i> K12 <i>S. aureus</i>	Bacteriophage MS2
	<b>Suspension (Amount of sample used)</b>	Mixed two bacterial communities (Droplet, 10uL)	Spinach extract, in 1% peptone water (Droplet, 10uL)	1% peptone water (1 mL)	10 mM PBS (1 mL)

## **Chapter 2.**

### **LITERATURE REVIEW**

#### **2.1. Introduction**

This chapter includes research background and the significance of foodborne pathogens and their impact on public health, as well as established conventional methods to detect foodborne pathogens. Among the various detection methods, the biosensing technique for microbial analysis will be discussed. Also, emerging technologies such as nanotechnology, electrophoresis, and microfabrication in the biosensor to improve the sensor's performance will also be reviewed.

##### **2.1.1. Foodborne pathogens and illness outbreaks**

Food safety and quality are essential to sustaining life and promoting good health. However, physical, chemical, and biological hazards incorporated into the food supply chain and manufacturing facilities can threaten the production of safe and nutritious food. Chemical substances, potentially harmful bacteria, viruses, or parasites can contribute to food poisoning, causing illness or injury to people. Preventing contamination by these hazards can be accomplished by using proper food hygiene practices, as well as food safety management strategies including the hazard analysis and critical control point (HACCP) system (FDA, 1997; Stannard, 1997). While the implementation of preventive systems has greatly improved food safety, biological hazard related food poisoning ingredients are still reported. The World Health Organization (WHO) estimated that almost 1 in 10 people, approximately 600 million, in the world experience illness after eating contaminated food and 420,000 people die every year (Kirk



et al., 2015). The Centers for Disease Control and Prevention (CDC) estimated that there are about 48 million foodborne illnesses annually, the equivalent of sickening 1 in 6 Americans each year. Also, 128,000 hospitalizations and 3,000 deaths result from these illnesses annually (CDC, 2011). About 20% of foodborne illnesses, 9.4 million cases, are caused by 31 known pathogens, and it imposes over \$ 15.5 billion in economic burden due to medical costs, productivity loss, and deaths per year (Hoffmann, 2015). Foodborne illnesses caused by bacteria, fungi, parasites, or viruses are transmitted through the consumption of contaminated food or water. Most illnesses are caused by norovirus (58%), followed by nontyphoidal *Salmonella* spp. (11%), *Clostridium perfringens* (10%), *Campylobacter* spp. (9%), and *Staphylococcus aureus* (3%). The leading causes of hospitalization were nontyphoidal *Salmonella* spp. (35%), Norovirus (26%), *Campylobacter* spp. (15%), *Toxoplasma gondii* (8%), and *E. coli* (STEC) O157 (4%). The leading causes of death were nontyphoidal *Salmonella* spp. (28%), *T. gondii* (24%), *Listeria monocytogenes* (19%), norovirus (11%), and *Campylobacter* spp. (6%) (Scallan et al., 2011). Five pathogens (nontyphoidal *Salmonella* spp., *T. gondii*, *L. monocytogenes*, *Campylobacter* Spp., and norovirus) contributed to 90% of the total economic burden (Hoffmann, 2015). Foodborne disease-causing organisms have been reported in various food sources, from raw products to processed food when the handling and processing are not conducted properly. The identification and detection of potentially harmful bacteria and viruses in food products remain a critical issue, along with the preventive procedures to prevent contamination and eliminate hazards, to secure food safety for our health and minimize the economic burden.

### **2.1.2. Current detection methods**

Conventional laboratory-based methods for the identification and quantification of pathogens in food have used various techniques such as microscopy and cell culture, biochemical assays, immunological tests, or genetic analysis (Ahmed et al., 2014a). Culturing methods for detecting pathogens in food are based on the growth of viable bacteria on nutrient media. A general procedure includes nonselective enrichment, selective enrichment, selective/differential plating, and finally, morphological, biochemical, and serological confirmation (Ahmed et al., 2014b). Conventional culture methods are known to be simple, easy, adaptable, practical, and inexpensive; however, they are time-consuming and labor-intensive because of the multiple enrichment steps. It takes 2-3 days for the initial results and up to 7-10 days for confirmation (Velusamy et al., 2010). When one or more enrichment steps are required, 8-24 h may be added to the detection time (Gracias & McKillip, 2004). Besides, some bacterial species are still viable but not culturable on routine agar, and it impairs their detection by culture-based techniques (Li et al., 2014a)

Immunoassays such as enzyme-linked immunosorbent assay (ELISA) and nucleic acid-based techniques, such as polymerase chain reaction (PCR), have been used as alternative methods to reduce the assay time from days to hours (Wang & Salazar, 2016). ELISA methods rely on the specific binding of an antibody to an antigen and involve chromogenic reporters and substrates that produce some observable color change to indicate the presence of antigens. The primary antibody, usually used for capturing the antibody, is immobilized on the walls of the wells in microtiter plates, and then the antigen is added to the walls to allow them to specifically bind to the antibody. The secondary antibody, which is used as the detection antibody and conjugated with reporter enzyme, provides visual results. ELISA format is called the 'sandwich'

assay and known as the most powerful design due to its high sensitivity and stability. The specificity and the sensitivity of immunological methods depend on the binding strength of the antibody specific to its antigens, and they work well for food matrices without interfering factors such as other non-target cells, DNA, and proteins (Zhao et al., 2014). ELISA has been used to detect bacteria in food products; thermophilic *Campylobacter* spp. in turkey samples (Borck et al., 2002), *S. Typhimurium* in milk and juice (Chattopadhyay et al., 2013), *S. Typhimurium* and *E. coli* O157:H7 in milk, ground beef, and pineapple juice (Cho & Irudayaraj, 2013), and *E. coli* O157:H7 in vegetables and milk (Shen et al., 2014). The drawbacks of ELISA include its requirements for many reagents, large amounts of antibodies for further separation, and use of optical instruments. Recent advanced immunology-based methods, such as lateral flow immunoassay and immunomagnetic separation assay, are gaining attention in the area of pathogen detection as rapid, simple, and cheap (Cho et al., 2014; Karoonuthaisiri et al., 2009; Wu et al., 2014). However, this method remains a challenge with a lower limit of detection (LOD,  $10^4$ - $10^5$  CFU/mL) than other conventional culture- and nucleic acid-based ( $10^2$ - $10^3$  CFU/mL) methods. Polymerase chain reaction (PCR) is a method used for the *in vitro* enzymatic synthesis of specific DNA sequences by *Thermus aquaticus* (*Taq*) and other thermoresistant DNA polymerases (López-Campos, 2012). PCR utilizes oligonucleotide primers that are 20-30 nucleotides in length, and is performed in repeated cycles by controlling the temperature. The PCR steps include the unfolding of the DNA strand, binding primers to target DNA or RNA segments, and polymerization (Hill & Wachsmuth, 1996). PCR products are separated by gel electrophoresis and visual inspection is used to analyze the electrophoretic patterns. The specificity can be subsequently confirmed by sequencing the amplified DNA fragment (Abubakar et al., 2007). The amplification of target DNA or RNA sequences achieved with

PCR-based methods make them ideal candidates for the development of faster microbiological detection systems. The advantages of PCR include high specificity and sensitivity, as well as the rapid detection and identification of pathogenic bacteria. Because this method uses a specific DNA sequence it amplifies the target DNA by  $10^7$  fold in 2 h, which also reduces enrichment time. However, it requires trained personnel and expensive instruments, which limit their use in a practical environment. Different PCR methods used for pathogenic detection are (1) simple PCR, (2) multiplex PCR (de Freitas et al., 2010), in which several specific primer sets are combined into a single PCR assay for simultaneous amplification, (3) quantitative PCR (also called real-time PCR) (Bakthavathsalam et al., 2013; Chen et al., 2010), which can be used to continuously monitor the PCR product formation throughout the reaction, and (4) multiplex real-time PCR (Barletta et al., 2013; Garrido et al., 2013). PCR based methods are used to detect a wide range of pathogens such as *Salmonella* (Canato et al., 2011; Koyuncu et al., 2010; Soria et al., 2013), *L. monocytogenes* (Day & Basavanna, 2015; Gattuso et al., 2014), *Bacillus cereus* (Kalyan Kumar et al., 2010; Kim et al., 2000; Oliwa-Stasiak et al., 2011), *E. coli* (Fedio et al., 2011; Madic et al., 2011), *Yersinia enterocolitica* (Lambertz et al., 2008; Thisted Lambertz et al., 2000), and *Campylobacter jejuni* (Sails et al., 2003; Wang et al., 1999).

Established current detection methods have been successful for the detection of pathogens because these methods can be sensitive and give both qualitative and quantitative information on the microorganisms tested (Leonard et al., 2003; Velusamy et al., 2010). However, those methods involve relatively long assay times and require complicated equipment and a technician to operate it, which might interfere with the early identification of foodborne pathogens in food products. The demands for innovative technological developments to rapidly and directly detect foodborne pathogens are on the rise to overcome the challenges of

conventional detection methods.

## **2.2. Biosensors for detection of foodborne pathogens**

A biosensor is an analytical device, which consists of a bioreceptor and a transducer, and some biosensors include a signal processor in the unit. The biological materials on the bioreceptor, such as antibodies, bacteriophages, enzymes, cells, DNA, or RNA, recognize the corresponding analyte and this reaction generates measurable signals. The biosensor has developed as a useful tool for rapid and sensitive microbial detection. It allows for the construction of portable and straightforward equipment for fast analysis in the field and has a high potential for automation (Sharma et al., 2013). Therefore, the biosensor-based detection method can be suitable for food safety and quality assurance to ensure a timely response to possible risks in the field.

### **2.2.1. Biosensor classification**

Biosensors can be classified depending on the mechanism of the biorecognition process or the method of signal transduction as presented in Figure 2.1. The recognition molecules can be: biological materials, such as tissue, microorganisms, organelles, cell receptors, enzymes, antibodies, nucleic acid, and natural products; biologically derived materials such as recombinant antibodies and engineered proteins; or biomimics, for example, synthetic catalysts, combinatorial ligand, and imprinted polymers (Lazcka et al., 2007). The type of the biocompound determines the degree of selectivity or specificity of the biosensor. The biosensor device is divided into four groups based on the transducers: optical-based including surface plasmon resonance (SPR), Raman and Fourier transform infrared spectroscopy, and optical fibers; electrochemical-based

including amperometric, potentiometric, impedimetric, and conductometric; and mass-based including piezoelectric and magnetoelastic. The choice of biorecognition materials and the adjusted transducer depends on the properties of each sample of interest and the type of physical magnitude to be measured (Mello & Kubota, 2002).

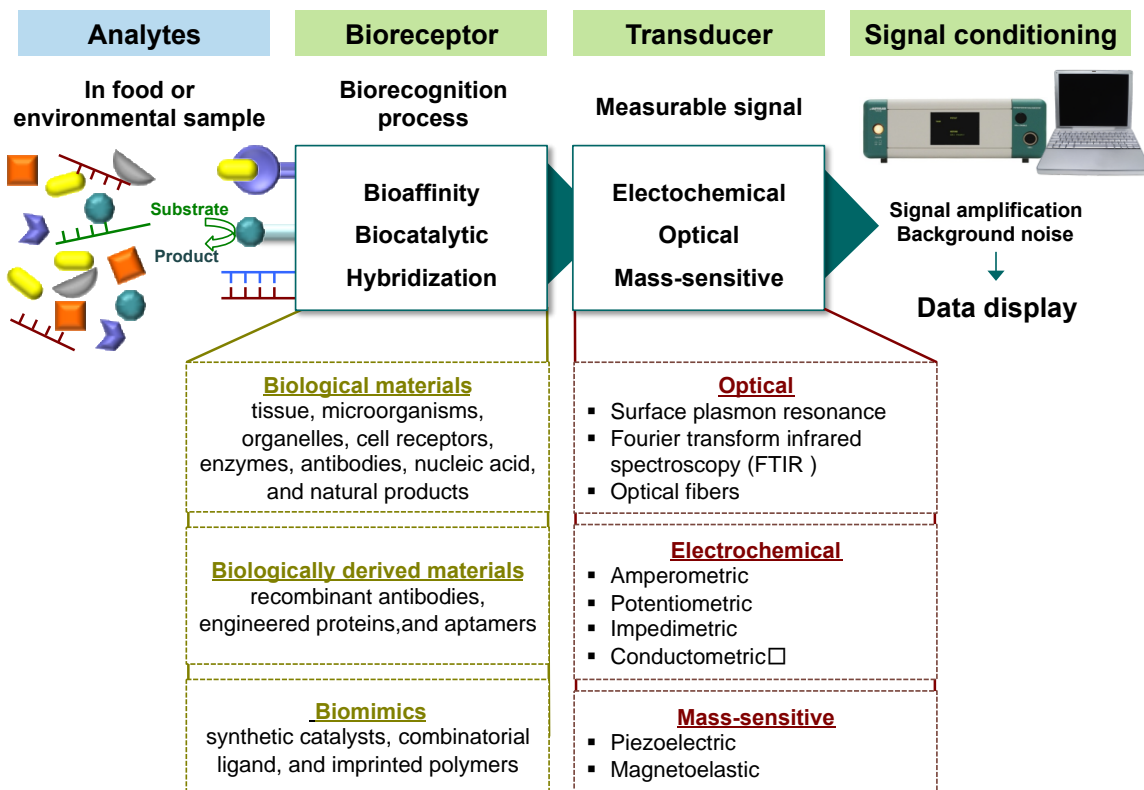


**Figure 2.1** Common biosensor components and classification (Lazcka et al., 2007; Velusamy et al., 2010)

The biorecognition processes occur by bioaffinity reaction, biocatalytic reaction, and hybridization. The affinity-based biosensors can be made using antibodies or bacteriophages. The antibodies interact with the given ligand to form a thermodynamical complex in a highly specific manner (Goode et al., 2015). In the case of electrochemical transduction, the antibody-antigen complexes act as electron transfer barriers, or electrochemically active substrates

conjugated to the antibody can generate the changes in electrical signal response. The bacteriophages are also used to detect bacteria using phage infection in which it binds to specific receptors on the surface of bacterial cells to inject their genetic material into the bacteria. Bioaffinity bioreceptors are in high demand in specific and selective detection because they allow the analysis of any compound as long as specific antibodies are available (Mello & Kubota, 2002). The biocatalytic receptors can be enzymes, whole cells, cells organelles, and plant or animal tissue slices (Davis et al., 1995). Enzyme sensors work by immobilization of the enzyme system on the transducer that can convert the reduction-oxidation reaction of the enzyme to potentiometric, amperometric, optoelectric, calorimetric, and piezoelectric signals. The oxidases are most often used to facilitate electron transfer to the working electrode in electrochemical sensors. Enzymes are commonly used to function as a label conjugated to other biological molecules because they are stable and offer high sensitivity and direct visualization (Velusamy et al., 2010). A microbial sensor is based on the detection of organic components assimilated by the microorganisms or monitoring the metabolic process occurring in a living cell (Mello & Kubota, 2002). DNA or RNA fragments and aptamers are used as hybrid receptors, and these receptors are immobilized onto a support and combined with a complementary base pair, which is an unknown nucleic acid to be identified (Mello & Kubota, 2002). Nucleic acid biosensing seems to be the most sensitive approach for detecting microorganisms and their genetic modifications.

Surface plasmon resonance (SPR) is known as a common method for pathogen detection (Rasooly, 2006). It is based on the measurement of the angle change of the reflected light when the cells bind to receptors immobilized on the transducer surface. The interaction between the target substance and the antibody results in a change in mass at the surface, which in turn causes a change in refractive index. There has been research interest in SPR sensors for foodborne

pathogen detection. SPR immunosensors for *E. coli* in spinach (Linman et al., 2010), for *E. coli* O157:H7 (Subramanian et al., 2006), for *Salmonella* Typhimurium in milk (Mazumdar et al., 2007), for feline calicivirus (Yakes et al., 2013) and norovirus-like particles (Ashiba et al., 2017) used as a norovirus surrogate, as well as an SPR DNA-based sensor for the detection of *Salmonella* (Zhang et al., 2012) have been reported.

The transducers can be further divided into label and label-free methods (Velusamy et al., 2010). The labeled methods depend on the detection of a specific label such as fluorescent dye, a secondary antibody with a reporter molecule, or an enzyme. These methods have advantages in greater sensitivity allowing for signal amplification, but the procedure involves multiple steps causing longer assay time. Label-free detection is the direct measurement of a phenomenon occurring as a biorecognition reaction on the transducer surface. It allows for rapid and simple detection, real-time monitoring, and non-destructive sensing; however, it has limited sensitivity issues.

### **2.2.2. Electrochemical immunosensor**

Electrochemical immunosensors convert the immune reaction between the antigen and the corresponding recognition molecules conjugated to the biosensor into measurable electrical signals (Nandakumar et al., 2008). Electrochemical biosensors themselves are a subclass of chemical sensors, and combine the sensitivity of electrochemical transducers with the high specificity of biological recognition processes (Ronkainen et al., 2010). They measure the change in electrical properties (current, potential, impedance, and conductance) in electrode structures as cells become entrapped or immobilized on or near the electrode (Radke & Alocilja, 2004). Electrochemical biosensors can operate well in turbid media and uses low amounts of



sample that do not require sample preparation. The reasons for their popularity are that they are label-free, simple analytical methods that have a low economic cost. However, the sensitivity and specificity are slightly limited. To overcome these issues, the functionalization of the electrode with high-affinity recognition elements has been used to bind target molecules selectively. Affinity-based bioreceptors are preferred over catalytic ones for the detection of microorganisms, due to their enhanced selectivity and specificity, as well as the lack of additional reagents required for enabling simple assays (Ahmed et al., 2014a).

### *Amperometric biosensors*

Amperometric biosensing measures the current generated by the association with a bioaffinity reaction at the surface of the working electrode, or through the oxidation/reduction catalyzed by their enzyme (Leonard et al., 2003). The sensor potential is set at a value where the analyte produces current. The applied potential serves as the driving force for the electron transfer reaction, and the current produced is a direct measure of the rate of electron transfer (Velusamy et al., 2010). Amperometry provides linear concentration dependence over a defined range. The advantages of these systems are that they are sensitive and enable fast, precise, and accurate analysis. Also, the amperometric biosensor can be small, robust, and economical; therefore, it is easily used outside the laboratory environment. An amperometric immunosensor for the detection of low concentrations of *E. coli* was developed (Carnes & Wilkins, 2005). A flow-through immunoassay was conducted to achieve the rapid detection of *E. coli* with a working range of 50-1000 cells/mL. The detection of *S.aureus* in milk, cheese, and meat samples were studied using an amperometric immunosensor modified with PEI-glutaraldehyde (Majumdar et al., 2013). Amperometric response showed a linearity in the *S. aureus* concentration range of  $10^1$  - $10^8$  CFU/mL, achieving a low detection limit of only 10 CFU/mL.

### *Potentiometric biosensors*

Potentiometric detection of microorganisms is based on the measurement of the potential of a solution generated by the specific interaction with ions between ion selective electrodes and the solution. Potentiometry is widely used in the biosensor field, but, the interest in the potentiometric detection of pathogens seems to not be high when compared to other electrochemical biosensors (Ahmed et al., 2014a).

### *Impedimetric biosensor*

An impedimetric transduction technique has also been applied to detect and quantify a variety of foodborne pathogens (Yang & Bashir, 2008). Impedance is defined as the apparent resistance in an electric circuit to the flow of alternating currents, which corresponds to the actual electrical resistance to a direct current (Wang et al., 2012). Thus, its principle is based on the changes in electrical impedance of the medium due to microbial growth or antigen-antibody reactions on the electrode. Electrochemical Impedance Spectroscopy (EIS) has been widely used for the detection of bacterial and viral antigens due to its relative ease of use and high sensitivity (Siddiqui et al., 2012). The process involves the application of a sinusoidal signal at low voltages onto an electrode (usually around 1-10 millivolts), and then the resulting current through the electrode is measured. In the presence of an electrochemical redox probe ( $[\text{Fe}(\text{CN})_6]^{3-/4-}$ ), the electron transfer rate is reduced due to the bacterial cells bound to the transducer surface, causing a decrease in electron transfer current (Figure 2.2 (a)) (Ruan et al., 2002). The ratio of applied voltage and measured current is the impedance of the electrode at the applied sinusoidal signal frequency, which is given by the equation below.

$$Z = \frac{E_t}{I_t} = \frac{E_o \sin(\omega t)}{I_o \sin(\omega t + \phi)} \quad (2.1)$$

$E_o \sin(\omega t)$  is the applied voltage,  $I_o \sin(\omega t + \phi)$  is the measured current, where  $\phi$  is the phase shift.

By repeating this procedure over a range of frequencies, impedance changes concerning the frequency are indicated as  $Z(\omega)$ . Transforming the above equation into the frequency domain with Euler's relationship allows the impedance to be expressed as a complex function given by the equation as below.

$$Z(\omega) = Z_o \exp(j\phi) = Z_o (\cos(\phi) + j\sin(\phi)) \quad (2.2)$$

Plotting the real ( $Z'$ ) and imaginary ( $Z''$ ) parts of the above equation, with the imaginary on the Y-axis and the real on the X, allows us to visualize the measured impedance in a Nyquist plot, which is one of the most popular formats for the evaluation of EIS data as shown in Figure 2.2 (b). The Nyquist plot makes it easy to compare differences in ohmic resistance, but fails to show the frequency related to the information presented explicitly. A bode plot is used for this purpose and often more desirable when data is too scattered to fit properly onto the Nyquist plot. The change in impedance in respect to a bio-functionalized electrode can be interpreted as detection, and current research and data indicate the changes are proportional to antigen concentration represented in Figure 2.2 (c) (Siddiqui et al., 2012). Impedimetric immunosensors are widely used to detect pathogenic bacteria (Dweik et al., 2012; Geng et al., 2008; Huang et al., 2010; Varshney & Li, 2007; Varshney et al., 2007) and viruses (Attar et al., 2016; Hong et al., 2015) and is a rapid, sensitive, and label-free method.

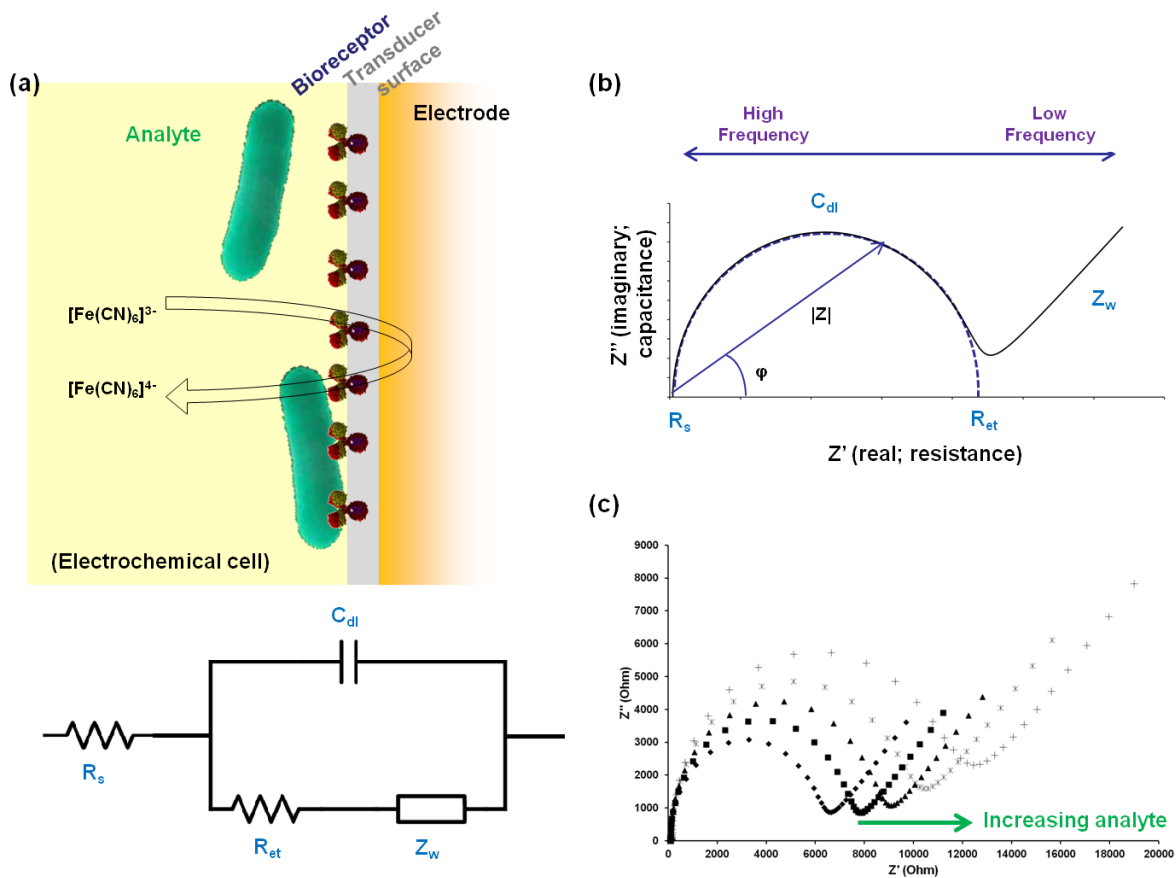


**Figure 2.2** Schematic for principle and electrochemical function of the impedimetric biosensor. (a) A transducer surface is functionalized with a polymer or self-assembled monolayer to anchor the bioreceptor elements allowing specific recognition for the analyte. The change in electron transfer resistance is monitored under the electrochemical cell with an electron mediator ( $[\text{Fe}(\text{CN})_6]^{3-/4-}$ ) and can be expressed as Randles equivalent circuit consisting of electrolyte solution resistance ( $R_s$ ), double-layer capacitance ( $C_{dl}$ ), electron transfer resistance ( $R_{et}$ ), and Warburg impedance ( $Z_w$ ). (b) The Nyquist plot shows the components of Randles equivalent circuit and impedance can be represented by a vector arrow with magnitude  $|Z|$  and frequency angle  $\phi$ . (c) Impedance is proportionally changed to the analyte concentration interacting with the electrode surface. (Modified from Ahmed et al. (2014a))

### **2.3. Advanced technologies incorporated to electrochemical immunosensors**

A wide range of new biosensor technologies are being developed to overcome the issues associated with current biosensors for microbial detection. Significant progress has been made with bioreceptors and transducing platforms by combining the recent advances in nanotechnology, dielectrophoresis, and microfabrication.

#### **2.3.1. Functionalization of the biosensor with nanomaterials**

As detection elements in diagnostic tools, nanostructures and nanomaterials have become the focus of intense research due to their unique properties related to their shape, structure, and size (1 to 100 nm) (Rodriguez et al., 2015). They can bridge the gap between the bulk and molecular levels, and lead to entirely new avenues for application, especially in electronics, optoelectronic, and biology. Nano-scale structures and materials have a high aspect ratio providing much more surface area for biomolecules to interact (Wujcik et al., 2014). It allows the reduction in instrument size and amount of sample; thereby, greater portability and a lower limit of detection can be possible (Perfzou et al., 2012). Biosensing technique improvement by nanotechnology can be divided into two categories: nanostructure platform biosensor used as the transducer for ultrasensitive detection and integration of nanomaterials into the biosensor as labels or transducer modifiers for signal enhancement.

Nanostructure transducers, such as the nano-size electrodes and nanoporous surfaces, have been used for the detection of single or low levels of molecules. Due to their unique semiconductive properties associated with the nanostructures, they are believed to be ultrasensitive in performing single molecule sensing (Wanekaya et al., 2006). TiO<sub>2</sub> nanowire bundle microelectrode based impedance immunosensor was used for the rapid and sensitive

detection of *L. monocytogenes* (Wang et al., 2008). The TiO<sub>2</sub> nanowire bundle was connected to gold microelectrodes using mask welding, and then monoclonal antibodies were immobilized on the surface of a TiO<sub>2</sub> nanowire bundle to capture specific bacteria. The immunosensor could detect *L. monocytogenes* at a concentration as low as  $4.7 \times 10^2$  CFU/ml, and the total detection time was only 50 min. Moreover, there was no significant interference observed with non-target foodborne pathogens. Nanoporous membranes modified with antibodies specific to target organisms or molecules are also used for biosensor applications. Joung et al. (2013) fabricated a nanoporous membrane based impedimetric immunosensors for the detection of *E. coli* O157:H7 in whole milk. Anti-*E. coli* antibodies were immobilized on the nanoporous membrane by hyaluronic acid. The sensor detected *E. coli* O157:H7 in whole milk with the detection limit of 83.7 CFU/ mL with 95% probability. The hyaluronic acid-functionalized nanoporous membrane-based impedimetric sensor provided an excellent platform for the electrical detection and characterization of pathogenic bacteria in whole milk samples without any sample preparation.

Nanomaterials, such as gold nanoparticles (AuNPs), magnetic nanoparticles (MNPs), quantum dots (QDs), and carbon nanotubes (CNTs) have been used in the biosensor for improved sensitivity. AuNPs were used for the immunosensing of *E. coli* O157:H7 (Lin et al., 2008). Attached AuNPs to the screen-printed carbon electrode contribute to an enhanced response current by 13.1-fold along with ferrocenedicarboxylic acid used as a mediator. *E. coli* O157:H7 was detected in the concentration range of  $10^2$  -  $10^7$  CFU/ml, with the detection limits of approximately 6 CFU/strip in phosphate buffer saline (PBS) and 50 CFU/strip in milk. Fast and sensitive detection of *L. monocytogenes* was attained using anti-*Listeria* polyclonal antibody immobilized AuNPs and anti-*Listeria* monoclonal antibody immobilized MNPs (Chen et al., 2016). The MVP-*Listeria* cell-AuNP-urease complexes were captured in the separation chip and

transported into a microfluidic detection chip. The assay could detect *Listeria* concentrations as low as  $1.6 \times 10^2$  CFU/mL within one hour. The study of a NP-enhanced impedimetric biosensor for *Salmonella enteritidis* detection was conducted by Kim (2007). The anti-*Salmonella* antibodies were immobilized on the surface of interdigitated gold electrodes and conjugated to nanoparticles to use as the impedance response enhancer. The impedimetric biosensor could detect  $10^6$  CFU/mL of *S. enteritidis* in PBS within 3 min. The additional use of nanoparticles enhanced the detection limit of the biosensor with  $10^4$  CFU/mL of *S. enteritidis* in PBS and  $10^5$  CFU/mL of cells in milk.

CNTs can be emphasized as the most attractive nanomaterial for providing excellent sensitivity and selectivity in electrochemical biosensors for the detection of pathogens (Rodriguez et al., 2015). CNTs can be described as one-dimensional (1D) cylindrical structures of graphene sheets. Single-walled CNTs (SWCNTs) are formed by a graphene layer wrapping with diameters of 0.8-5 nm, while the multiwalled CNTs (MWCNTs) are multiple rolled SWCNTs layers with a larger diameter range from 3 nm to 100 nm (Rodriguez et al., 2015). CNTs can be adsorbed or linked to an enormous amount of biomolecules by a noncovalent and/or a covalent binding for different types of transduction (Venturelli et al., 2011). The CNT-biosensors functionalized with the biocomposites have been explored for the immunosensing of various pathogens. Several studies demonstrated the electric signal amplification of SWCNTs-based biosensors for the detection of *E. coli* K12 and *S. aureus* (Yamada et al., 2014), *E. coli* O157:H7 and bacteriophage T7 (García-Aljaro et al., 2010), *Salmonella* (Jain et al., 2012), as well as single stranded DNA for the detection of *S. Typhimurium* (Weber et al., 2011). MWCNTs-based biosensors have been studied for the immunosensing of *E. coli* O157:H7 with a MWCNT-sodium alginate nanocomposite film modified screen-printed carbon electrode (Zhan

et al., 2013). The proposed immunosensor showed good sensitivity to *E. coli* O157:H7 in a concentration range from  $10^3$  to  $10^{10}$  CFU/mL and LOD of  $2.94 \times 10^2$  CFU/mL. Another MWCNTs-based electrochemical immunosensor has been developed for the multiplexed detection of *E. coli* O157:H7, *Campylobacter*, and *Salmonella* (Viswanathan et al., 2012). The immunoassay was performed with nanocrystal bioconjugates, which are immobilized with three antibodies. The result exhibited LODs of 400 cells/mL for *Salmonella* and *Campylobacter* and 800 cells/mL for *E. coli* and the feasibility of multiplexed determination of bacteria in milk samples. Liu et al. (2014) fabricated the multifunctional MWCNTs for detecting the pathogen *Vibrio alginolyticus* in fishery and environmental samples. MWCNTs could function as an immuno-, magnetic, and fluorescent sensor by the incorporation of biomolecules into CNTs. The multifunctional MWCNTs showed the potential for rapid (30 min), sensitive ( $1.0 \times 10^4$  CFU/mL), and specific detection of *Vibrio alginolyticus*. MWCNTs are also used for capturing bacterial pathogens with assistance by coating copolymer poly(propionyl ethylenimine-co-ethylenimine)-MWCNTs onto the filters (Wang et al., 2015).

### **2.3.2. Manipulation of microorganism movement by dielectrophoresis**

#### *Theory of dielectrophoresis*

Dielectrophoresis (DEP) is a phenomenon where the translational motion of a particle is caused by the polarization effects in an inhomogeneous alternating current (AC) electric field (Pohl, 1978). It is distinguished from the phenomenon known as ‘electrophoresis’ which is the motion caused by the response to free charge on a body in an electric field. The body can be electrically charged or neutral. If an objective possesses higher numbers of protons than electrons, it can be positively charged, whereas if it has a higher numbers of electrons than protons, it can



be negatively charged. On the other hand, if the protons and electrons are balanced, the object is electrically neutral. Because the charges inside of the neutral body are mobile, the neutral body can be polarized, which puts a negative charge on the side nearer the positive electrode, and a positive one on the side nearer the negative electrode.

The charged and uncharged bodies indicate the different behaviors in response to a uniform and non-uniform electric field. When the charged particle is subject to two electrodes, they migrate towards the corresponding charged plates by faradic movement. In the same field, the neutral particle would not move towards either electrode because they have an equal net force under the same electric field strength surrounding the body. In the case of a non-uniform electric field, where the electric strengths are different throughout the field, the local electric force near the two polarized regions on the neutral particle are unequal, resulting in a net translational force toward the area with a more intense field. However, the charged particle behaves the same as when under a uniform electric field, being attracted to the electrode of opposite polarity. When an alternating current electric field is applied across the electrode shown in Figure 2.3, the charged particles move up and down to the oppositely charged electrode, followed by slight vibrations around its original position at high frequency. However, the polarized neutral body does not reverse their direction although the field is reversed, no matter which electrode is charged positively or negatively.

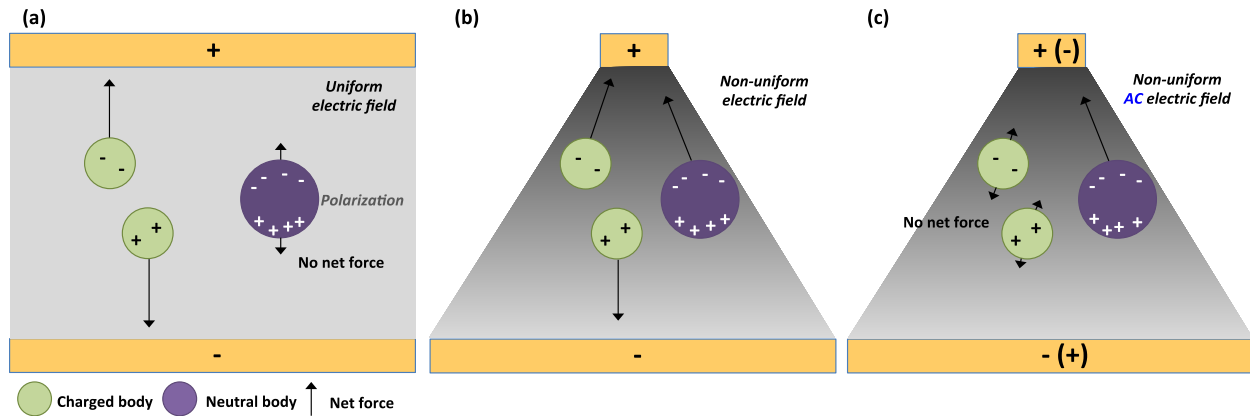


**Figure 2.3** Comparison of behaviors of charged and neutral bodies in (a) a uniform electric field, (b) a non-uniform electric field, and (c) the non-uniform electric field when alternating current is applied

The translational motion of polarized particles can be attracted to or repelled by the strongest electric field depending on the electric properties of the particles and suspending medium with applied frequency represented in Figure 2.4. When the particle is more polarizable than the medium, net dipoles are interacting with the charges on the charged plate instantly. When the top electrode is positively charged, a driving force on the negative pole side of the particle is toward the top electrode, whereas a repulsive force on the positive pole side is toward the bottom electrode. Also, if there is a higher electric field acting on the top region of this particle than on the bottom region; the electric force can also attract the particle to the top electrode. Finally, the particle has a net movement toward the maximum field gradient regions, which is called positive DEP or pDEP. The opposite situation occurs when the particle is less polarizable than the surrounding medium, and the net movement is toward the minimum field regions, which is called negative DEP or nDEP.

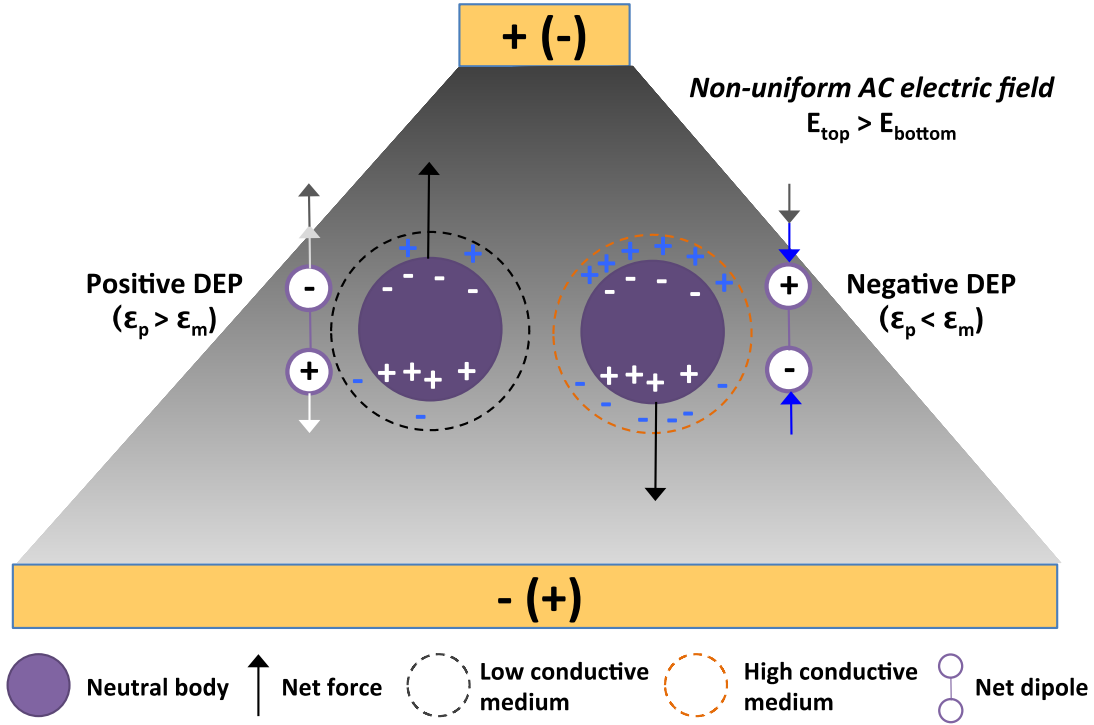


**Figure 2.4** Directions of particle movement depending on the charge distribution of the medium and electric field strength near the neutral body

The DEP force acting on an isolated spherical particle can be represented as:

$$F_{DEP} = 2\pi r^3 \epsilon_0 \epsilon_m \text{Re}[F_{CM}] \nabla |E_{rms}|^2 \quad (2.3)$$

where  $r$  is the radius of the particle,  $\epsilon_0 \epsilon_m$  are the permittivities of the free space and suspending medium, and  $E_{rms}$  is the root-mean-square local electric field, and  $\text{Re}[F_{CM}]$  is the real part of the Clausius–Mossotti (CM) factor. Therefore, the DEP force operating on the particle is proportional to the size of the particle body and the local electric field. Moreover, the movement direction of the particle can be determined by the sign of the CM factor, which depends on the relationship between the particle and the medium complex permittivity, that is,

$$F_{CM} = \frac{\epsilon_p^* - \epsilon_m^*}{\epsilon_p^* + 2\epsilon_m^*} \quad (2.4)$$

where  $\varepsilon^*$  is the dielectric complex permittivity of the particle and medium, respectively. The dielectric complex permittivity can be expressed by

$$\varepsilon^* = \varepsilon_0 \varepsilon - (j\sigma/\omega) \quad (2.5)$$

where  $j$  is  $\sqrt{-1}$ ,  $\sigma$  is the conductivity of particle or medium, and  $\omega$  is the frequency in radians ( $\omega = 2\pi f$ ). The sign of equation (2.3) is dependent on the sign of  $\text{Re}[F_{CM}]$ , equation (2.4) and (2.5). Therefore, when the conductivity of the particle is higher than that of the medium at a specific frequency, it corresponds to a larger complex permittivity of the particle than the medium. In this case,  $F_{CM}$  achieves a positive value, as does  $F_{DEP}$ . Thus, the particle experiences a positive DEP. Whereas, when the medium has a higher conductivity which increases complex permittivity, negative values of both  $F_{CM}$  and  $F_{DEP}$  are obtained, and the particle experiences a negative DEP, moving away from the high field gradient zone.

#### *Dielectric properties of bacterial cells and virus particles*

The cellular system can attain such a high polarizability because there are structured areas in the surface where ionic double layers and structural regions, like lipid membranes, act as a capacitive region. Also, the cell contains a significant portion of water and dissolved polar molecules in the intercellular region such as protein, sugar, DNA, and RNA, which can contribute to the polarization (Pohl, 1978). When the biological cell suspension is exposed to an external electric field, it is influenced by different polarization mechanisms called  $\alpha$ -,  $\beta$ -, or  $\gamma$ -dispersions (Schwan, 1994). The  $\alpha$ -dispersion is associated with the ionic characteristics of both the cytoplasm and the extracellular medium occurring in an audio frequency range between 10 Hz and a few kHz. It causes a polarization of the ionic atmosphere around the cell surface and the presence of a surface conductivity. The  $\beta$ -dispersion is due to the polarization of the cellular

membrane and proteins and other organic macromolecules from 1 kHz to several MHz, giving rise to the Maxwell-Wagner effect. The last type of dielectric response,  $\gamma$ -dispersion, is related to the polarization of water molecules and internal subcellular components at high-frequency regions of more than 10 GHz. The  $\alpha$ - and  $\beta$ -dispersions are considered to be more influential to the dielectric properties of a biological cell suspension (Di Biasio et al., 2010).

As mentioned above, the magnitude of DEP force experienced by the cells and the direction of their movements are dependent on frequency and certain properties of the cells like its size, morphology, conductivity, and permittivity. Biological cells have complex heterogeneous structures, which consist of a cell wall, cell membrane, and cytoplasm which have different conductivity and permittivity values. The conductivities of *E. coli* cells are assumed to be around 0.68 S/m,  $5 \times 10^{-8}$ S/m, and 0.19 S/m for the cell wall, plasma membrane, and cytoplasm, respectively. Besides, microbial cells have diversity of sizes ranging from a few nanometers (viruses) to microns (bacteria), and different shapes such as spherical, rod-like, or elongated. Therefore, when calculating the DEP force on a single bacterial cell or virus particle and assuming their translational motions, the complex permittivity of a cell ( $\epsilon_p^*$ ) should be replaced by the effective complex permittivity of the cell ( $\epsilon_p^*_{\text{eff}}$ ). The specific cell model should be also be considered for either single shell spherical or double-shell spheroid shape (Park et al., 2011).

#### *Dielectrophoresis application in biosensors*

DEP has been widely used to electrically control the trapping, manipulation, transportation, and separation of biological analytes within a fluid suspending medium (Gascoyne & Vykoukal, 2002). The incorporation of DEP technology into biosensors has been

studied to improve the detection of bacteria and viruses by the separation and concentration of target microbial cells from non-target analytes, as well as the enhancement of antibody capture efficiency (Yang, 2012).

Positive DEP driven bacterial cell trapping for detection has been reported for *Salmonella* and *E. coli*. *S. Typhimurium* is concentrated on the detector of the sensor chip at 100 kHz and 10 V<sub>pp</sub> for 40 min (He et al., 2013). They achieved the rapid and sensitive detection of *S. Typhimurium* in deionized water and artificially contaminated mineral water samples with LODs of 56 CFU/mL and 110 CFU/mL, respectively. *E. coli* K12 can be deposited directly on the electrode array in a droplet (1 µL) form by applying 1 MHz and 5 V<sub>pp</sub> into the electrode device (Yoo et al., 2008). Other researchers found that *E. coli* K12 displayed positive DEP behavior and was captured by the antibody-immobilized microwire at 20 V<sub>pp</sub> and 1-10 MHz. At 3 MHz, the fluorescence intensity and impedance were significantly increased due to increases in the antibody and bacterial antigen complexes (Kim et al., 2011; Lu et al., 2013). Hamada et al. (2013) utilized the combination of negative and positive DEP by using two individual electrodes which serve as a bacteria concentrator using nDEP, and as a bacteria detector using pDEP. The number of bacteria trapped on the pDEP microelectrode with an nDEP concentrator was twice as much as the microbial count obtained without nDEP. A DEP impedance measurement (DEPIM) technique has been developed for the selective detection of target bacteria (Del Moral- Zamora et al., 2015; Suehiro et al., 2003; Suehiro et al., 2006). Bacterial cells could be captured on an interdigitated microelectrode array by positive DEP in the form of pearl-chains, which are electrically connected parallel to the gap of the interdigitated electrode strips. When more bacteria cells accumulate between the adjacent electrode strips; the conductance and the capacitance are increased. Suehiro et al. (2003) found that viable *E. coli* K12 cells could be

separated from the heat sterilized nonviable cells by DEP forces dependent on bacteria viability. The viable *E. coli* K12 cells were selectively collected by positive DEP at 1 MHz. A combination of DEP and hydrodynamic drag forces have been utilized to separate *Lactobacillus* bacteria from a background of yeasts based on their different magnitudes of DEP force experienced at specific frequencies (Khoshmanesh et al., 2011). Yeast and bacterial cells were trapped at different locations on the microelectrodes at 10 MHz. At the other applied frequency, the bacteria were caught along the microelectrodes, while the yeasts were repelled from the microelectrodes, and then washed out by drag force. Yang (2009) integrated DEP with non-flow through biochip sensing platforms to enhance the immuno-capture and detection of *Salmonella*. They accomplished this by concentrating bacterial cells from the suspension in different locations on the chip surface where the antibodies were immobilized. When DEP was applied for 15 and 30 min, immuno-capture efficiencies for *Salmonella* increased from 10.4% and 17.6% to 56.0% and 64.0%, respectively.

DEP continues to be a promising tool used to manipulate, separate, and detect viruses (Hübner et al., 2007; Nakano et al., 2012; Nakano et al., 2013). Similar to the mechanism used for bacterial determination, the virus particles were dielectrophoretically trapped near the electrodes with a higher electric field zone, and the trapped particles influenced a change in impedance between the electrodes (Nakano et al., 2013). Norovirus and rotavirus were detected at 50 ng/mL and at 10 ng/mL, respectively, using the DEPIM within 100s. The researchers suggested that it would be promising for DEP to be integrated into biosensors to advance the sensitive and selective detection of foodborne pathogens.

### 2.3.3. Microfabricated biosensor devices

Micro-scale biosensing platforms have been developed for miniaturization, integration, and automation of assays in a variety of fields such as biology, chemistry, and medicine (Luka et al., 2015). Biosensor devices are usually fabricated to integrate laboratory function on a single small-scale system known as lab-on-a-chip (LOC) and micro total analysis system ( $\mu$ TAS). They require a small volume of the sample to reduce time for reaction and detection. Also, microsystems are cost-effective due to the use of fewer reagents and the lower cost of fabrication for small-sized devices versus commercial devices. The faster response and lower fabrication costs can contribute to the high-throughput analysis and the mass production of disposable biosensor chips. The compactness, portability, sensitivity, and parallelization make microfabricated biosensors beneficial for various applications (Li et al., 2014b).

Electrochemical immunosensor devices can be fabricated by screen printing, photolithography, thin-film deposition, etching, electroplating, soft lithography, and substrate bonding techniques, with metals or electroconductive polymers as the electrodes and electrode supporting materials (Zhang et al., 2000). A biosensor for *E. coli* detection was developed based on microelectromechanical systems, heterobifunctional crosslinkers, and immobilized antibodies by Radke and Alocilja (2004). The biosensor was fabricated from (100) silicon with a 2  $\mu$ m layer of thermal oxide as an insulating layer, and 9.6 mm<sup>2</sup> of the active sensing area consisted of two interdigitated gold electrode arrays. They reported that the biosensor could distinguish between different cell concentrations between 10<sup>5</sup> to 10<sup>7</sup> CFU/ mL in a pure culture within 5 min of detection time. They also applied the microelectrode array biosensor for the detection of *E. coli* O157:H7 and were able to achieve a detection limit as low as 10<sup>4</sup> CFU/mL (Radke & Alocilja, 2005).



### *Flow-based biosensor*

Flow-based detection methods such as flow-injection, sequential injection, and microfluidic systems increase the potential for assay automation (Fintschenko & Wilson, 1998; Gubitz et al., 2001) and the ratio of immobilized surface area to sample volume, offering increased bioreceptor molecule and analyte interaction (Abdel-Hamid et al., 1999). It is possible to monitor the assay process and detect the signal changes at a non-equilibrium state, where the degree of reaction is not maximized (Hartwell & Grudpan, 2010). Therefore, the assay time can be considerably shortened. In addition, a larger volume of the sample fluid can be transported to the micro-scale active sensing site using fluidic techniques. An efficient detection of *Salmonella* using microfluidic impedance based sensing was accomplished (Dastider et al., 2015). The microfluidic biosensor provides an increase in sensitivity by up to 10-fold and amplified the impedance response by 2-2.9 times compared to the non-microfluidic biosensor. A flow-injection amperometric immunofiltration assay system was reported to detect *E. coli* and *Salmonella* concentrations as low as 50 cells/mL for both bacteria with an overall assay time of 35 min (Abdel-Hamid et al., 1999).

### *Microelectrode configurations for inducing the DEP to the biosensor*

The separation and accumulation of biological micro- and nano-particles were achieved using the microdevice and DEP techniques (Dürr et al., 2003; Kentsch et al., 2003). For more efficient DEP integration into the biosensor system, the electrode array can be constructed as two-dimensional (2D) or three-dimensional structures (3D). 2D planar electrodes are commonly patterned as polynomial or interdigitated arrays on the bottom of the sensing site. They were developed for various DEP-based biosensing applications due to its easy fabrication and

miniaturized system. Interdigitated microelectrodes (IME) have received significant attention in the area of impedimetric immunosensing for *E. coli* O157:H7 (Ghosh Dastider et al., 2012; Yang et al., 2004) and *S. Typhimurium* (Dastider et al., 2015; Yang, 2009). The IME consist of a pair of microband array electrodes that mesh with each other. These two sets of electrodes can act as a two-electrode system in impedance microbiology. However, using the 2D structure for some practical applications can be problematic for the efficiency of the microsystem. Because the electric field gradient decreases as the distance from the electrodes increases, only the motion of particles near the surface of the electrode can be directed. 3D electrodes, including those patterned on both the top and bottom surface of the microchannel, extruded from the microchannel bottom, then pattered on the channel sidewalls, can increase the region where the practical DEP effect is taking place, allowing for increased microsystem efficiency (Li et al., 2014b). A top and bottom electrode configuration for DEP generation was used to capture *E. coli* K12 cells from fresh produce (Kim et al., 2011) and orange juice (Lu & Jun, 2012). The gold microwire, 25  $\mu\text{m}$  in diameter, was used as a probe and was functionalized with monoclonal *E. coli* antibodies on the surface of the microwire.

## **2.4. Conclusion**

The advances in biosensor technology for the detection of foodborne pathogens has been geared towards fast, simple, and sensitive methodologies with inexpensive and easy to operate devices. The performance of the biosensor depends on the design and construction of its bioreceptors on the transducer surface and the transducer's properties. It could be further enhanced by integrating nanotechnology, electrophoresis, and micro-detection systems. The ideal parameters and standards for microbial detection seem to be based on sensitivity, since it can

detect a single bacteria in a reasonably small sample volume (1-100mL) or bacterial cell concentrations less than  $10^3$  CFU/mL; specificity, since it can distinguish different species or serotypes of bacteria and separate bacteria from complex sample matrices; and speed, since the assay can be completed within 5-10 min for a single test (Ivnitski et al., 1999; Xu et al., 2017). Also, compact size, minimal sample processing, real-time monitoring, and multiplex detection in a single run are becoming critical features for prospective biosensor development.

### Chapter 3.

## Selective detection of *Escherichia coli* K12 and *Staphylococcus aureus* in mixed bacterial communities using a functionalized electrochemical immunosensor with dielectrophoretic concentration

### ABSTRACT

An electrochemical immunosensor has been developed for rapid detection and identification of potentially harmful bacteria in food and environmental samples. Because the antibody-antigen reactions on the sensor generate sensible shifts in the electrical signal that provide qualitative and quantitative results, it is important to fabricate sensitive and stable bioreceptors on the sensing platform. The purpose of this study was to fabricate a biosensing device for selective detection of *Escherichia coli* and *Staphylococcus aureus* in microbial cocktail samples using single walled carbon nanotubes (SWCNTs)-layered microwire and dielectrophoresis (DEP)-based cell concentration. A gold-coated tungsten microwire was functionalized by coating polyethylenimine, SWCNTs suspension, streptavidin, biotinylated antibodies and then bovine serum albumin (BSA) solutions. Double-layered SWCNTs and 5% of BSA solution were the optimized conditions for enhanced signal enhancement and non-specific binding barrier. The selective capture of *E. coli* K12 or *S. aureus* cells was achieved when the electric field was generated at a frequency of 3 MHz and 20 V<sub>pp</sub>. A linear trend in the change in the electron transfer resistance was observed as *E. coli* concentrations increased from  $5.32 \times 10^2$  to  $1.30 \times 10^8$  CFU/mL ( $R^2 = 0.976$ ). The *S. aureus* biosensor fabricated by replacing antibodies layer with the anti-*S. aureus* antibodies also showed an increase in the resistances with the concentrations of *S. aureus* ( $8.90 \times 10^2$  -  $3.45 \times 10^7$  CFU/mL) at the correlation,  $R^2 = 0.983$ .

Both sensors were able to detect targeted bacteria cells without interfering with other bacteria in mixed suspensions. *Salmonella* Typhimurium and *Listeria monocytogenes* were used to evaluate the specificity of the sensors. The functionalization process developed for the microwire-based electrochemical immunosensors (MEI sensors) is expected to contribute to sensitive and selective detection of other harmful microorganisms in food and environmental industries.

### **Highlights**

- Functionalization process contributes to signal enhancement and cell binding specificity.
- Changes in electrical signal were proportional to bacterial concentrations.
- The biosensors could detect *E. coli* and *S. aureus* as low as  $10^3$  CFU/mL within 10 mins.
- Selective captures of targeted bacteria were achieved in mixed bacteria suspensions.

### 3.1. Introduction

Microbial detection assay for the complex samples such as food, water, or soil remains challenge tasks including sample purification, discrimination of target analytes, and low-level bacteria detection. Food and environmental samples have the assortment of various components such as organic and inorganic particles, biochemical compounds, and background microflora that can interfering with accurate sensing assessments (Stevens & Jaykus, 2004; Wang & Salazar, 2016). A culture-based method has been successful for identification of the pathogens in the samples. Selective and differential media can provide both qualitative and quantitative information of microorganisms tested (Leonard et al., 2003). The culture-based method is relatively sensitive with a limit of detection of 10-100 CFU/mL and has high-level specificity. However, It takes about 24 to 72 hours to obtain the results due to extra enrichment and incubation steps (Zhao et al., 2014). Culture-independent methods like polymerase chain reaction (PCR) need less assay time about 1-3 hours with high sensitivity (LOD: < 100 CFU/mL). However, these require the complex instruments in stationary laboratories that can be operated by skilled personnel only (Yamada et al., 2016).

A novel bioaffinity and electrochemical impedance-based biosensor has been developed for rapid and simple detection and identification of target microorganisms in the sample with high level sensitivity and specificity. It can measure the change in electrical properties of electrode structures as cells become entrapped or immobilized on or near the electrode (Radke & Alocilja, 2004). An electrochemical impedance spectroscopy (EIS) is a widely used technique for probing bioaffinity binding or biocatalytic reaction at the surface of electrodes (Tully et al., 2008) and shows the electrical responses of an electrochemical cell to sinusoidal voltage signals as a function of frequency. It enables a direct measurement to occur during the biochemical

reaction on a transducer surface without secondary antibodies, enzymes, or fluorescence labels for optical identification of analytes. Although the electrochemical detection has several advantages such as low cost, the ability to work with turbid samples, and easy miniaturization, the sensing sensitivity and selectivity are slightly limited (Velusamy et al., 2010). However, immobilization of high recognition elements such as enzymes, antibodies, bacteriophages, single-stranded DNA, or RNA can enhance the selectivity and specificity of the electrochemical biosensors (Ahmed et al., 2014a). EIS coupled with immunology-based technique has been used for rapid detection and qualification of foodborne pathogens (Joung et al., 2013; Lu et al., 2013). Lu et al. (2013) reported the anti-*E. coli* antibodies immobilized microwire sensor was able to detect and enumerate *E. coli* K12 cells in suspension as low as  $10^3$  CFU/mL. The EIS technique was proven to be an alternative to fluorescence microscopy. Another research group fabricated the nanoporous membrane-based impedimetric immunosensor for label-free detection of pathogenic *E. coli* O157: H7 in whole milk (Joung et al., 2013). The detection limit was as low as 83.7 CFU/mL with 95% probability.

In the bioaffinity and electrochemical impedance-based biosensor, the key challenge is to fabricate sensitive and stable bioreceptors on the sensing platform, although the antibody-antigen reactions generate sensible shifts in the electrical signal that provide qualitative and quantitative results. The signal can be improved by incorporation of nanomaterials to the biosensor (Jain et al., 2012). Among various nanomaterials, carbon nanotubes (CNTs) have become promising materials for the advanced electrochemical biosensor due to their unique properties (Putzbach & Ronkainen, 2013; Weber et al., 2011). CNTs offer advantages of a large surface-volume ratio (Jain et al., 2012; Maroto et al., 2007), and a fast electron transfer rate (Kim et al., 2013; Weber et al., 2011; Yamada et al., 2014). Their high surface area to weight ratio allows for more bio-

recognition materials loaded on the CNT structure. When targeted biomolecules bind to recognition materials immobilized on the CNTs, electric signals are significantly changed. Jain and others found that the current density was amplified by immobilization of SWCNTs on the electrode surface (Jain et al., 2012). Yamada and others reported that the network of SWCNTs on the bio-nano combinational junction sensor enhanced the signal response by seven-fold. The SWCNTs modulated with PEI and biomolecules could enhance the signals upon binding with *E. coli* cells (Yamada et al., 2014).

Combining electrochemical immunosensor with dielectrophoresis (DEP) can be one of the strategies to reduce the detection time and enhance sensitivity (Hamada et al., 2013; Suehiro et al., 2006). DEP uses the effect of electrical polarization of particles under the influence of non-uniform electric fields to induce a translational motion (Castillo-Fernandez et al., 2015). The particle can be polarized under inhomogeneous AC electric field and show two behaviors moving toward, called as positive DEP, or repelling from, called as negative DEP, the maximum electric field. The direction of polarized particles movement depends on the properties of the particle, on the strength and frequency of the applied field, and on the conductivity of the supporting medium (Pohl, 1978). DEP has been studied to electrically control trapping (Fernández-Morales et al., 2008; Kim et al., 2011), manipulation (Hamada et al., 2013; He et al., 2013), and separation (Jaemin et al., 2008; Patel et al., 2012) of charged particles.

In this study, it is hypothesized that the impedimetric immunosensor assisted with positive DEP could rapidly and selectively detect specific bacteria in the presence of non-specific bacteria and SWCNTs layered on the surface of the biosensor can amplify electrical detection signals when target bacteria bind to corresponding antibodies immobilized on it. The effects of functionalization process on the sensor's sensitivity and specificity for detection of *E.*



*coli* K12 in pure and mixed samples were investigated. In addition, the application of the biosensor concept to detect *S. aureus* was explored.

## **3.2. Materials and methods**

### **3.2.1. Materials and instruments**

7% gold plated tungsten wire with a diameter of 50  $\mu\text{m}$  was manufactured from ESPI metals (Ashland, OR). Polydimethylsiloxane (PDMS; Sylgard 184 silicone elastomer curing agent and base) was ordered through Dow Corning (Midland, MI). SWCNTs (SWNT PD1.5L) were manufactured from NanoLab, Inc. (Waltham, MA). Polyethylenimine (PEI, branched, average  $M_w \sim 25,000$ ), N, N-dimethylformamide (DMF), Streptavidin from *Streptomyces avidinii* and bovine serum albumin (BSA; #A3294) were purchased from Sigma Aldrich (St. Louis, MO). Biotinylated polyclonal antibodies specific to *E. coli* (from rabbit, #PA1-73031) and *S. aureus* (from rabbit, #PA1-73174), and OXOID MacConkey agar were supplied from Thermo Fisher Scientific (Waltham, MA). BD Bacto™ peptone, BD BBL™ tryptic soy broth (TSB), BD Difco™ plate count agar, 95% alcohol, and phosphate buffered saline (PBS) were purchased from VWR (West Chester, PA). Petrifilm™ Staph Express Count plates based on Baird-Parker medium and Petrifilm™ Environmental Listeria Plates were obtained from 3M Food Safety (St. Paul, MN). Platinum wire with a diameter of 0.5 mm and Ag/AgCl reference electrode for constructing the electrochemical cell were supplied from CH Instruments, Inc. (Austin, TX) and VWR (West Chester, PA), respectively.

SWCNTs were dispersed in DMF using a digital sonifier (450, Branson, Danbury, CT). PEI, lyophilized streptavidin and BSA were dissolved in distilled water. Both antibodies were 10-fold diluted in PBS. Electrolyte solution used for EIS measurement was prepared by

dissolving 5 mM  $K_3Fe(CN)_6$  and 5 mM  $K_4Fe(CN)_6$  in 0.1 M KCl solution (# 244023, # P3289, and # P9541, Sigma-Aldrich Co., Saint Louis, MO).

An automated XYZ stage and stepping motor (Franklin Mechanical & Control Inc., Gilroy, CA) controlled by the COSMOS program (Velmex, Inc., Bloomfield, NY) was used to manipulate the microwire position during SWCNTs and antibodies coating and bacteria detection. DEP field was generated using a function generator (3220A, Agilent Technologies, Santa Clare, CA). Electrochemical impedances were measured using a frequency response analyzer ( $\mu$ Autolab III/FRA2 potentiostat/galvanostat, Metrohm Autolab USA Inc., Riverview, FL) equipped with NOVA software version 1.6.

### **3.2.2. Microbial preparation**

Frozen stock cultures of *E. coli* K12, *S. aureus*, *Salmonella* Typhimurium (ATCC 14028), *Listeria monocytogenes* (F2365) were provided from the Food Microbiology Lab, University of Hawaii. Each 100  $\mu$ L of bacterium stock was inoculated in 10mL of TSB twice and incubated at 35°C for 24 h. For pure bacterial solutions, cultured bacteria were serially diluted in the 0.1% peptone water. Mixed microbial communities were prepared by transferring 100  $\mu$ L of target bacteria solution ( $10^3$  CFU/mL) into 900  $\mu$ L of non-target bacterial dilutions with a concentration of approximately  $10^4$  CFU/mL. The concentrations of the stock cultures were obtained using plate counting methods before and after the experiments. MacConkey agar, 3M petrifilm Staph express count plate, Xylose lysine deoxycholate agar, and 3M petrifilm Listeria plate were used for enumeration of *E. coil* K12, *S. aureus*, *S. Typhimurium*, and *L. monocytogenes* in the cocktail sample, respectively. The concentrations of each bacterium in pure and mixed samples were summarized in Table 3.1.

**Table 3.1** Concentrations of each bacterium in pure and in mixed samples when *E. coli* sensor (top) and *S. aureus* sensor (bottom) were tested for specific and selective detection

Bacteria	Concentration	In pure sample (CFU/mL)	
		Target	Non-target
<i>E. coli</i> K12		$8.53 \times 10^3$	
<i>S. aureus</i>			$1.41 \times 10^4$
<i>S. Typhimurium</i>			$1.60 \times 10^4$
<i>L. monocytogenes</i>			$3.40 \times 10^4$

Bacteria	Concentration	In mixed sample (CFU/mL)	
		Target	Non-target
<i>E. coli</i> K12+ <i>S. aureus</i>		$1.67 \times 10^4$	$9.76 \times 10^4$
<i>E. coli</i> K12+ <i>S. Typhimurium</i>		$1.15 \times 10^4$	$3.30 \times 10^3$
<i>E. coli</i> K12+ <i>L. monocytogenes</i>		$1.90 \times 10^4$	$9.00 \times 10^2$

Bacteria	Concentration	In pure sample (CFU/mL)	
		Target	Non-target
<i>E. coli</i> K12			$1.96 \times 10^4$
<i>S. aureus</i>		$2.39 \times 10^4$	
<i>S. Typhimurium</i>			$3.70 \times 10^4$
<i>L. monocytogenes</i>			$1.59 \times 10^4$

Bacteria	Concentration	In mixed sample (CFU/mL)	
		Target	Non-target
<i>S. aureus</i> + <i>E. coli</i> K12		$5.65 \times 10^4$	$2.33 \times 10^4$
<i>S. aureus</i> + <i>S. Typhimurium</i>		$6.08 \times 10^3$	$9.08 \times 10^3$
<i>S. aureus</i> + <i>L. monocytogenes</i>		$9.83 \times 10^3$	$2.20 \times 10^4$

### 3.2.3. Functionalization of microwire surface

The microwires were cut into 25 mm in length and washed by distilled water and 70% alcohol using the digital sonifier for 5 min each. The sanitized wire was functionalized with multi-layers of PEI, SWCNTs, streptavidin, antibodies, and BSA. The first layer on the entire surface of microwire was coated with 1% polyethylenimine and baked in a furnace at 175 °C for 1 h, followed by allowing SWCNTs incorporation to PEI networks using 0.01% SWCNTs dispersion. The end of PEI-SWCNTs coated microwire was immersed in 5  $\mu$ L of streptavidin droplet on the PDMS supporting layer for 5 min, then being withdrawn. In the same way, the droplets of antibodies and BSA were used to coat the microwire sequentially. These dipping and retracting processes were repeated twice per each coating. Functionalized microwires (Figure 3.1) were stored at refrigerator before use for detection.

### 3.2.4. Bacterial cell capture by dielectrophoresis

A droplet of bacterial sample (10  $\mu$ L) was placed in a hemispheric concave (3 mm in diameter) on a gold plate as a bottom electrode. The microwire was dipped in the droplet at a velocity of 50 mm/min until the distance between the microwire tip and bottom electrode was as close as 1 mm. DEP was applied at 3 MHz and 20  $V_{pp}$  for 2 min (Figure 3.1) thereafter the microwire was withdrawn at a speed of 5 mm/min for impedance measurement.

Pure *E. coli* K12 and *S. aureus* stock dilutions from  $10^3$  to  $10^8$  CFU/mL were used to test the sensor's sensitivity. The specificity and selectivity of the microwire-based electrochemical immunosensor (MEI sensor) for detection of *E. coli* K12 was evaluated against pure non-target bacteria (*S. aureus*, *S. Typhimurium*, and *L. monocytogenes*) and mixtures of two different bacteria (*E. coli* K12 and *S. aureus*, *E. coli* K12 and *S. Typhimurium*, or *E. coli* K12 and *L.*

*Monocytogenes*). In the same manner, pure *E. coli* K12, *S. Typhimurium*, and *L. monocytogenes* solutions and their cocktail samples mixed with *S. aureus* were used to test the specificity and selectivity of the *S. aureus* MEI sensor

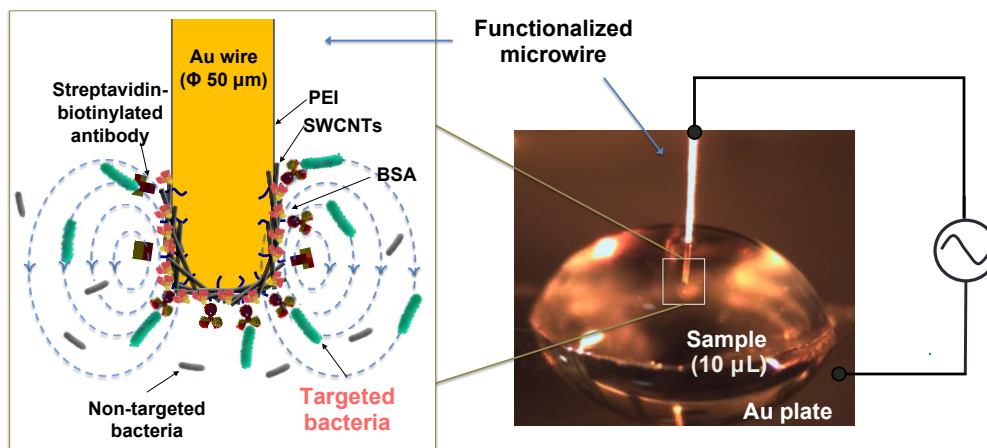


**Figure 3.1** A schematic of selective capture of target bacteria with functionalized microwire and a photograph of inserted the functionalized wire into the sample droplet for bacterial cell capture by dielectrophoresis

### 3.2.5. Impedance measurement

Electrochemical impedance measurements were carried out within a frequency range of 0.1 - 100 kHz at a set potential of 200 mV and the amplitude of 10 mV. An electrochemical cell was three-electrode configuration consisting of microwire for electrochemical immunosensor as a working electrode, platinum wire served as the counter electrode, and Ag/AgCl in 3 M KCl reference electrode. Experimental data were displayed by Nyquist plots. The Nyquist plots were fitted by the built-in analytical tool in the NOVA software, and then electron transfer resistance ( $R_{et}$ ) for the redox reaction at the electrode-film interface was obtained from the equivalent circuit model as Figure 2.2. The changes of electron transfer resistance ( $\Delta R_{et}$ ) by target binding events were calculated as follows:

$$\Delta R_{et} = R_{et}(\text{antibody-bacteria}) - R_{et}(\text{antibody}) \quad (3.1)$$

### **3.2.6. Data analysis**

Each serially diluted concentration of *E. coli* K12 and *S. aureus* was tested in triplicate. The mean and standard deviations of  $\Delta R_{et}$  were calculated for the dilutions, the cocktails, and the control. The differences between the means were analyzed based on Duncan's multiple range tests using a single factor analysis of variance (ANOVA) offered by Statistical Analysis Software (SAS version 9.4, SAS Institute Inc., Cary, NC) at 95% confidence level ( $p \leq 0.05$ ).

### **3.2.7. FESEM visualization and validation**

Field Emission Scanning Electron Microscope (FESEM, Pacific Biosciences Research Center, University of Hawaii, Model: Hitachi S-4800) was used to visualize and validate the surface of functionalized wire and *E. coli* K12 and *S. aureus* cells captured on the sensing wire. Each microwire obtained after functionalization process and capture the bacteria was put into 1 mL microtubes, submerged in glutaraldehyde/cacodylate fixative for 1 h, and washed in 0.1 M cacodylate buffer twice. 1% osmium tetroxide in cacodylate buffer was used for post-fixation for 30 mins. The buffer in each container was replaced by graded ethanol series (30%, 50%, 70%, 85%, 95% and 100%) to dehydrate bacterial cell. The treated microwires were attached to carbon tapes on aluminum stubs and were coated with a thin gold/palladium layer using a Hummer 6.2 sputter coater for 45 seconds.

## **3.3. Results and discussion**

### **3.3.1. Surface morphology of bare and functionalized microwires**

SEM images of the bare wire right after sanitization show cracks and valley forms with highly irregularity (Figure 3.2 (a) and (b)). However, a functionalized microwire has the smooth

surface with well-developed SWCNTs network as shown in Figure 3.2 (c) and (d). When the bare wire was tested as a sensor, bacteria cells were stacked up along the cracks by capillary attraction. Also, undesired materials, which may interfere with electrical signal responses, could be loaded on the sensor during the DEP concentration and impedance measurement. The first dip-coat of PEI seems to improve the surface structure by filling the gaps as well as modifying the surface charge for further SWCNTs coating step. Therefore, it appears to be important to initiate the first even and smooth coating layer to minimize the false positive results occurring from impurities and to promote the appropriate layer assembling.

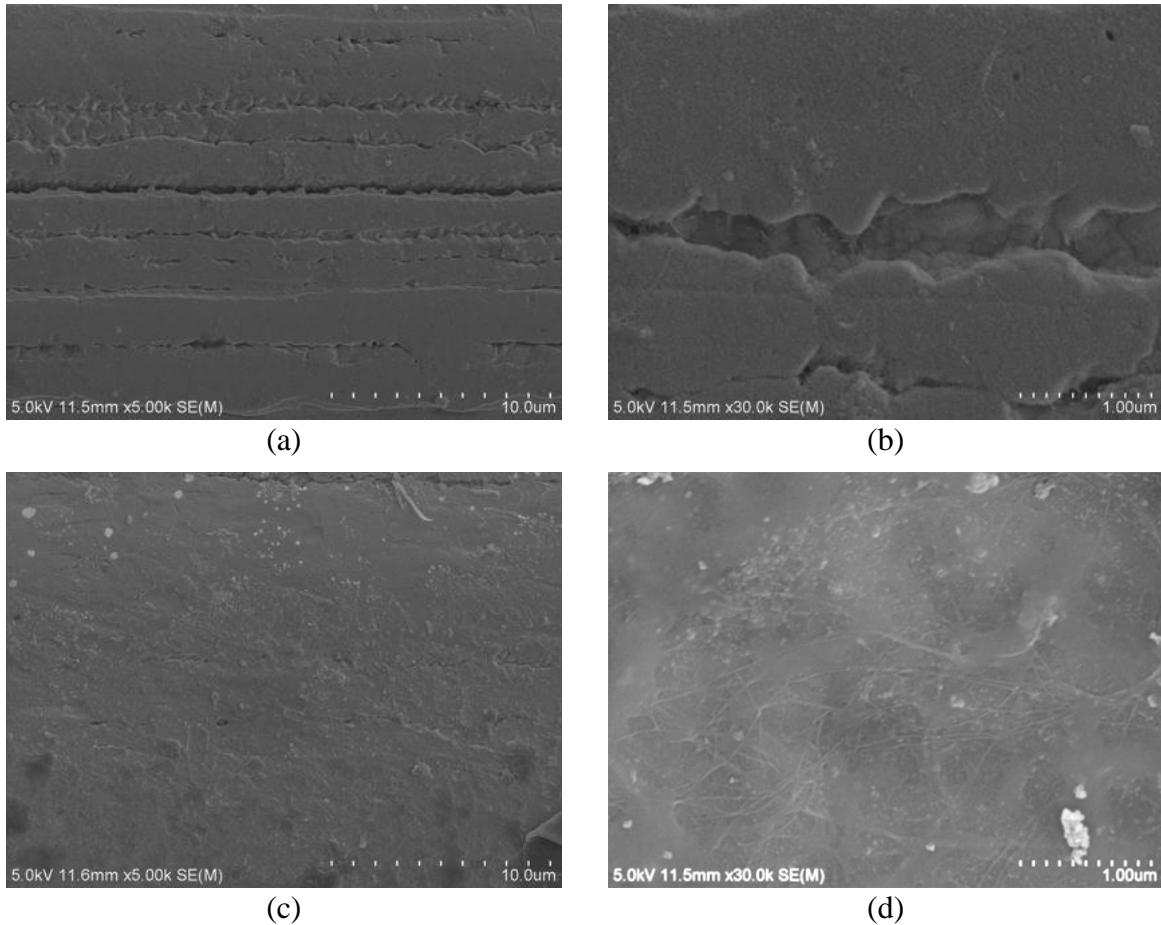


**Figure 3.2** SEM images for bare (a)-(b) and functionalized (c)-(d) microwires

### 3.3.2. Effect of SWCNTs coating on signal enhancement

Figure 3.3 shows the change in electric transfer resistance by the antibody-bacteria reaction was increased by coating the SWCNTs on the microwire. Double-layered SWCNTs on the sensor provided the signal enhancement compared to the sensor without SWCNTs. For instance, the  $\Delta R_{et}$  was  $288 \pm 107 \Omega$  when functionalized microwire except the SWCNTs layer was applied to detect the *E. coli* K12 at a concentration of  $10^7$  CFU/mL. On the other hand, the values of  $\Delta R_{et}$  for single and double-layered SWCNTs sensors were  $1687 \pm 118 \Omega$  and  $3213 \pm 748 \Omega$  for the equivalent concentrations of *E. coli* K12, respectively. The magnitudes of  $\Delta R_{et}$  were increased by six-fold for single-layered SWCNTs sensor and eleven-fold for double-layered SWCNTs sensor comparing to the sensor without SWCNTs. However, the resistance change was decreased after the second coat.

The phenomenon of increase in electric signal response can be explained that a large effective electrode surface area by SWCNTs coating serves as an active binding site of antibodies permitting more antibody-bacteria complexes on the electrode surface. The modified SWCNTs-electrodes were observed the significant increase in current density and the magnitude of changes in current by binding analyte to antibody (Jain et al., 2012; Weber et al., 2011; Yamada et al., 2014). However, more than double-coated SWCNTs causes the aggregation of SWCNTs and the excess of SWCNTs was released from the electrode surface. This phenomenon might cause the formation of uneven layer, consequently, the place where SWCNTs are more intense than other position can block the electron transfer to the electrode surface (Gomes-Filho et al., 2013).



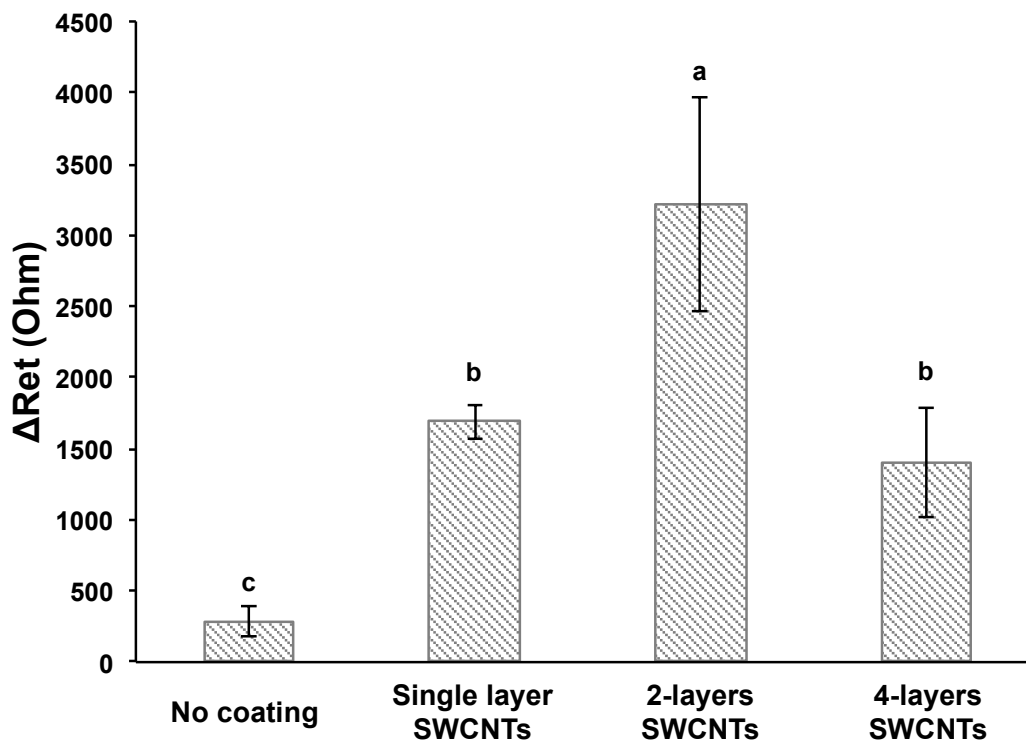


**Figure 3.3** Electrical signal response enhancements by SWCNTs coatings. Means followed by the same letter do not differ significantly at  $p \leq 0.05$

### 3.3.3. Effect of BSA solution on blocking the non-specific binding

The response signal from cells attached to the non-functionalized sensing area was reduced down to 58.4% by the use of 2% BSA solution. However, the *E. coli* sensor coated with 2% BSA does not provide the significant signal differences to discriminate *E. coli* from non-target bacteria (*S. aureus*) and bacteria-free sample (0.1% peptone water). When the microwire treated with 5% BSA solution, there were significant differences in  $\Delta R_{et}$  between targets, non-target bacteria, and bacteria-free sample shown in Figure 3.4. Bacterial cells can be bound to immobilized antibodies via the bioaffinity reaction but it may also be attached to the non-functionalized area. The latter can be target bacteria or non-target bacteria. In either case, it affects sensor's accuracy and sensitivity. These non-specific binding can be minimized by filling

the unoccupied sites with a blocking agent. BSA is widely used for non-specific binding blocker with 0.1-3% of solutions (Punbusayakul et al., 2013; Tlili et al., 2006). Unlike the common practices for BSA treatment on the sensor, i.e. placing the BSA droplet on the sensing surface or immersing the biosensor into BSA solution for several minutes to hours, BSA was coated as an outer layer by dipping for 5 min in this study. Therefore, the microwire might be required more concentrated BSA solution to saturate the non-functionalized area for a shorter incubation period. BSA treatment can also allow stabilization of biomolecules bound to the surface. The amplified electron transfer resistance change with 5% BSA treated microwire might result from enhanced bacteria attachment reacting with stably anchored antibody molecules.

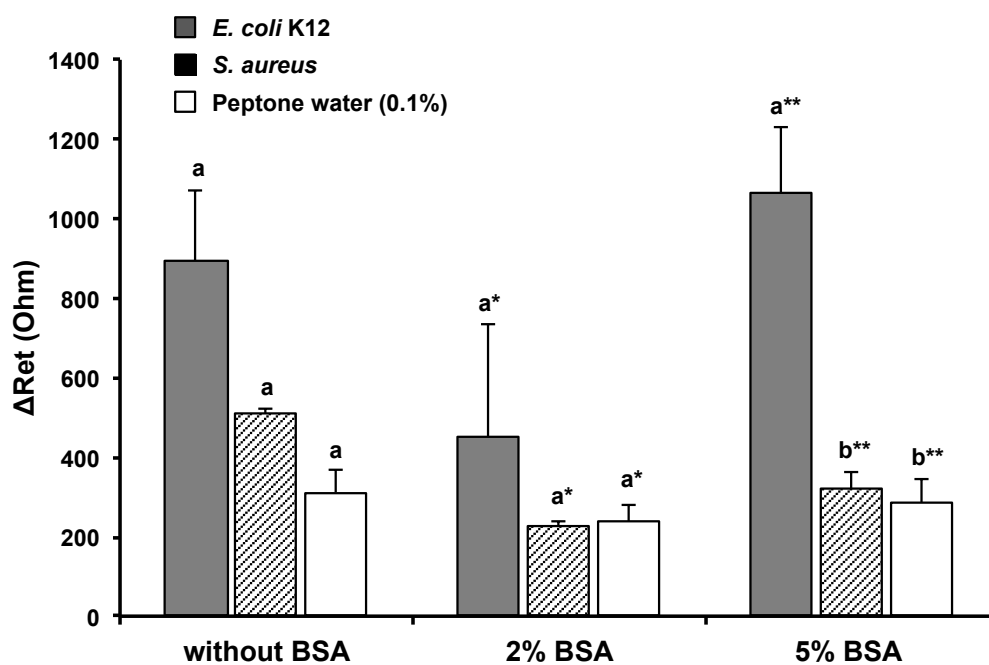


**Figure 3.4** Effect of BSA on non-specific binding reduction. \* and \*\*  $\Delta R_{et}$  values from different BSA treatments were analyzed separately.

Means followed by the same letter do not differ significantly at  $p \leq 0.05$ .

### 3.3.4. Detection of *E. coli* K12 in pure and mixed solution

The linear regression for detection of pure *E. coli* K12 samples was observed in the range from  $5.32 \times 10^2$  to  $1.30 \times 10^8$  CFU/mL (Figure 3.5). Since 10  $\mu$ L of sample loaded could not verify the presence of bacteria cells below the concentration of  $10^2$  CFU/mL, the  $\Delta R_{et}$  values were not significant difference between the bacteria-free solution and lower concentration of bacteria presenting sample than  $10^2$  CFU/mL. Based on the statistical similarity analysis, the limit of detection for the *E. coli* specific microwire sensor was  $8.21 \times 10^2$  CFU/mL with a detection time of 10 min including both cell concentration and signal measurement. SEM images present captured *E. coli* K12 on the functionalized surface of microwire (Figure 3.6).

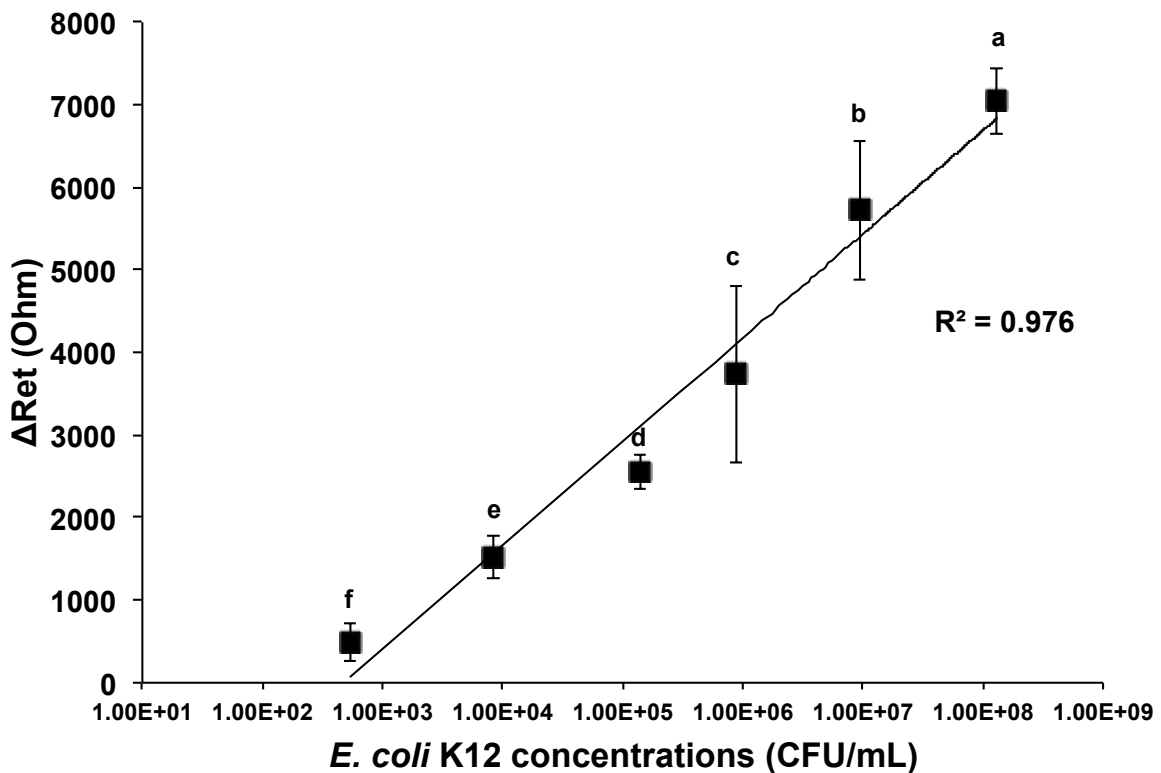


**Figure 3.5** Changes of electron transfer resistance with *E. coli* K12 captured on the electrode surface of *E. coli* sensor in pure *E. coli* K12 solution.

Means with the same letter are not significantly different ( $p \leq 0.05$ ).

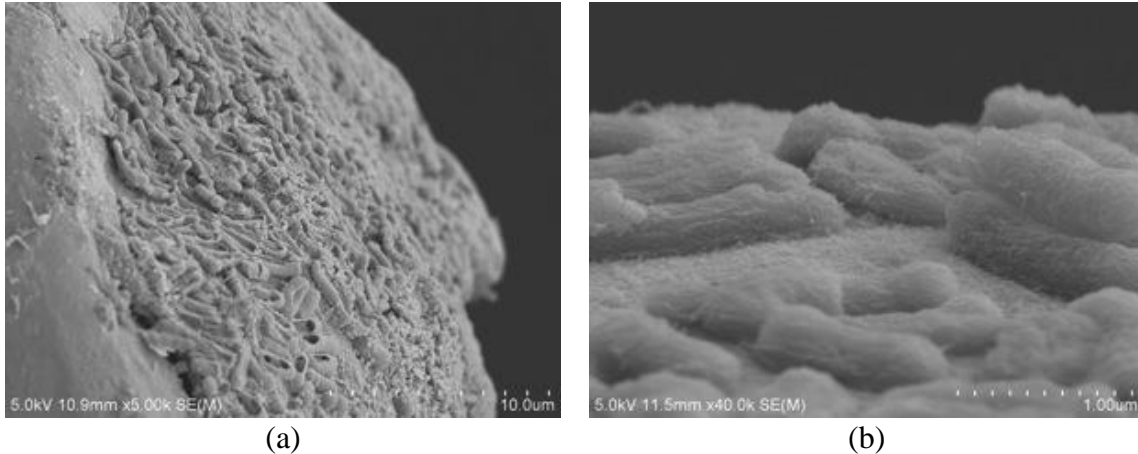


**Figure 3.6** *E. coli* K12 attachments on the base plane (a,  $\times 5.0k$ ) and the cylinder side (b,  $\times 40.0k$ ) of microwire observed by SEM

When pure *S. aureus*, *S. Typhimurium*, and *L. monocytogenes* were applied to the sensor functionalized with anti-*E. coli* antibodies, the  $\Delta R_{et}$  varied from 400-645  $\Omega$  (Figure 3.7). In comparison, the  $\Delta R_{et}$  of  $1629 \pm 295 \Omega$  was measured with pure *E. coli* K12 sample for the same concentration. Also, there were no significant differences in  $\Delta R_{et}$  values between pure and cocktail samples for the comparable amount of *E. coli* K12 cells. The values for mixed samples with *S. aureus*, *S. Typhimurium*, and *L. monocytogenes* were  $1696 \pm 390 \Omega$ ,  $1702 \pm 207 \Omega$ , and  $1553 \pm 117 \Omega$ , respectively. Most of bacteria attached to the surface of the *E. coli* sensor were observed as *E. coli* K12 cells after the sensor was tested with the mixture of *E. coli* K12 and *S. aureus* showing in Figure 3.8 (a). However, the surface of microwire remains clear, which means no bacteria capture under DEP when the sensor was dipped into the pure *S.aureus* solution (Figure 3.8 (b)).

These electrical signal response results agreed with Jain and other's study reporting that the decreased current density and increased impedance were observed due to the formation of antibody-antigen (*Salmonella*) complexes on the glassy carbon electrode immobilized with SWCNTs (Jain et al., 2012). Antibody-bacteria complexes attached to the surface and insulating

properties of the cell walls of the bacteria are blocked the electron transfer within electrochemical cell resulting in an increased electron transfer resistance (Jain et al., 2012; Ruan et al., 2002).

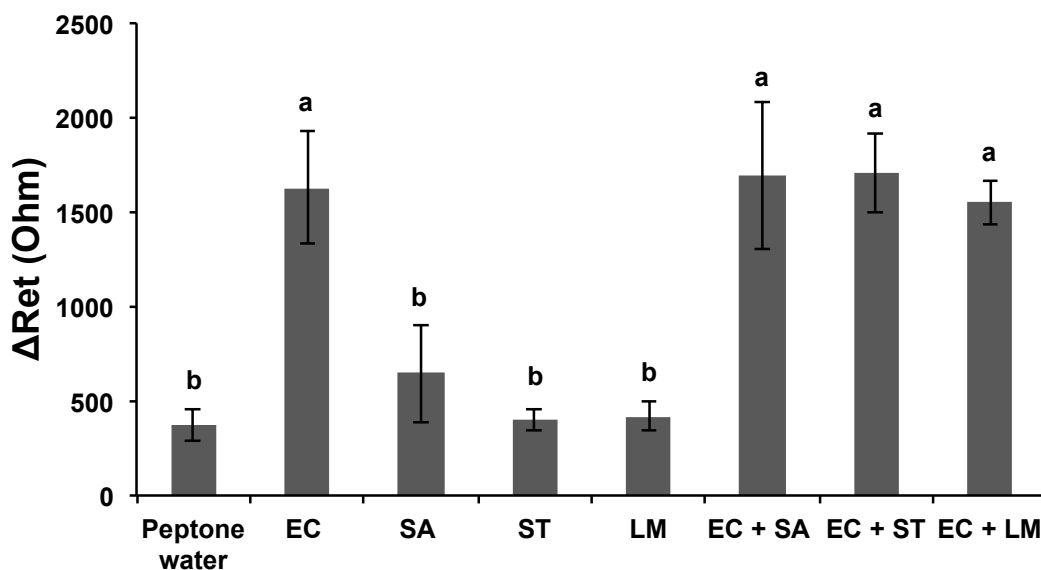


**Figure 3.7** Specificity and selectivity of the *E. coli* MEI sensor for detection of *E. coli* K12 against non-target bacteria suspension and cocktail samples. Acronyms mean bacteria suspending in pure and mixed samples; EC: *E. coli* K12, SA: *S. aureus*, ST: *S. Typhimurium*, LM: *L. monocytogenes*, EC + SA: a mixture of *E. coli* K12 and *S. aureus*, EC + ST: a mixture of *E. coli* K12 and *S. Typhimurium*, and EC + LM: a mixture of *E. coli* K12 and *L. monocytogenes*. Means with the same letter are not significantly different ( $p \leq 0.05$ ).

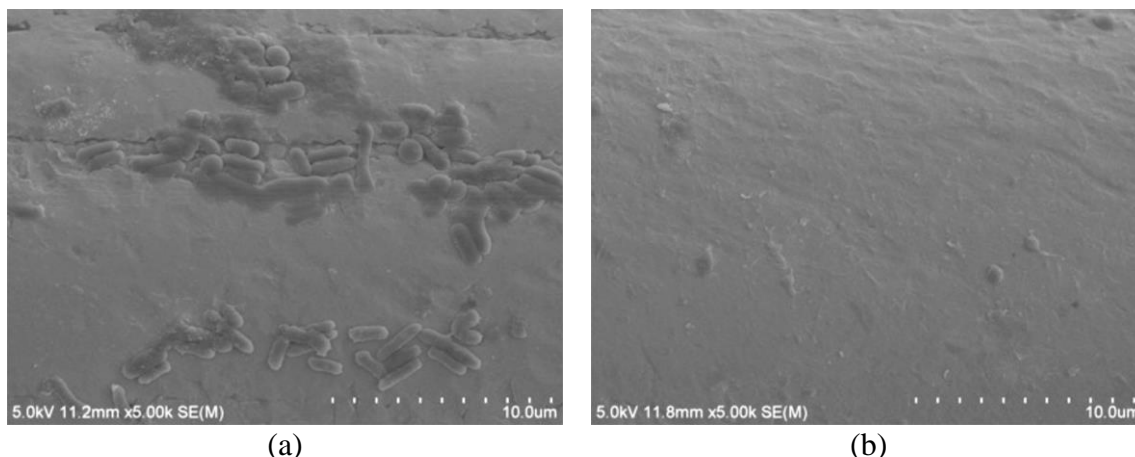


**Figure 3.8** Bacterial attachments on the surface of *E. coli* specific sensor (a) when applied to the cocktail solution (*E. coli* K12 and *S. aureus*) and (b) when applied to the pure *S. aureus* solution.

### 3.3.5. Application of developed MEI sensor for detection of *S. aureus* in pure and mixed solution

Anti-*E. coli* antibody layer was replaced with anti-*S. aureus* antibody layer to fabricate the MEI sensor for detection of *S. aureus*. Figure 3.9 shows a similar pattern that was obtained from *E. coli* sensor. The  $\Delta R_{et}$  was increased as *S. aureus* concentration increased from  $8.90 \times 10^2$  to  $3.45 \times 10^7$  CFU/mL with a  $R^2$  value of 0.983. The attachment of *S. aureus* cells on the microwire surface could be validated in the SEM images. The specificity of the *S. aureus* sensor was also demonstrated using non-target bacteria, *E. coli* K12, *S. Typhimurium*, and *L. monocytogenes* (Figure 3.10). The  $\Delta R_{et}$  values of non-target bacteria were  $373 \pm 220 \Omega$ ,  $440 \pm 88 \Omega$ , and  $389 \pm 30 \Omega$ . However, the magnitudes of  $\Delta R_{et}$  estimated from microbial cocktail samples mixed with *S. aureus* were not statistically different. The highest  $\Delta R_{et}$  of  $1365 \pm 164 \Omega$  indicated the highest amount of *S. aureus* cells ( $5.65 \times 10^4$  CFU/mL) in a mixture with *E. coli* K12 whereas the lowest value of  $\Delta R_{et}$ ,  $1133 \pm 115 \Omega$  estimated *S. aureus* concentrations about  $6.08 \times 10^3$  CFU/mL in a mixed suspension with *S. Typhimurium*.

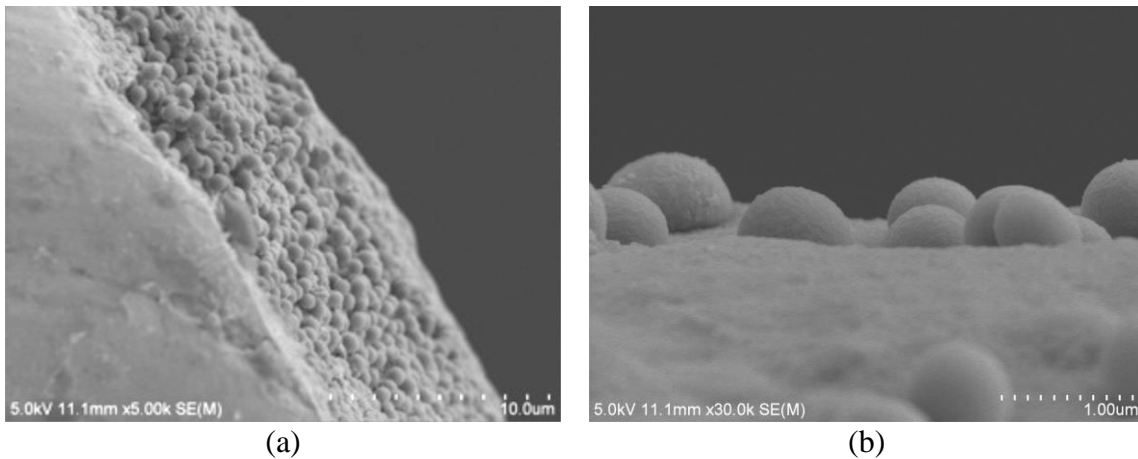
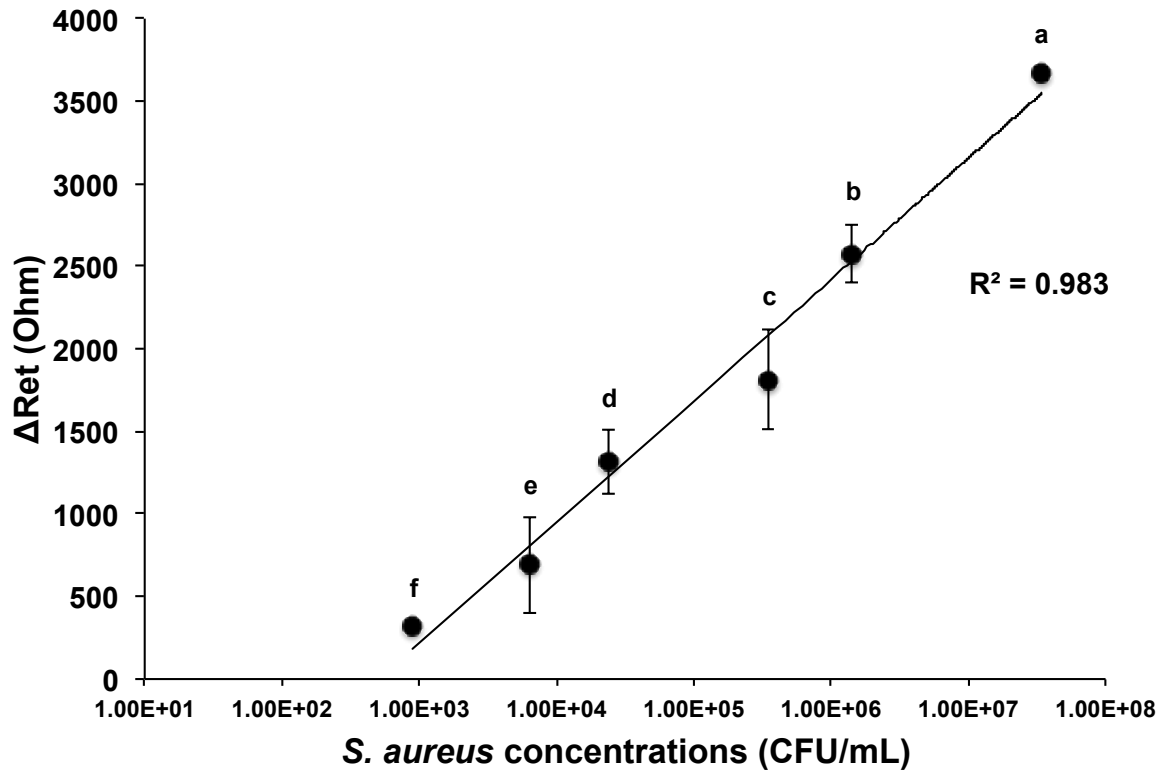


**Figure 3.9** Changes of electron transfer resistance with *S. aureus* captured on the electrode surface of *S. aureus* sensor in pure solution. Means with the same letter are not significantly different ( $p \leq 0.05$ ) and SEM images of *S. aureus* bacteria cells on the base plane (a,  $\times 5.0k$ ) and the cylinder side (b,  $\times 30.0k$ ) of the microwire

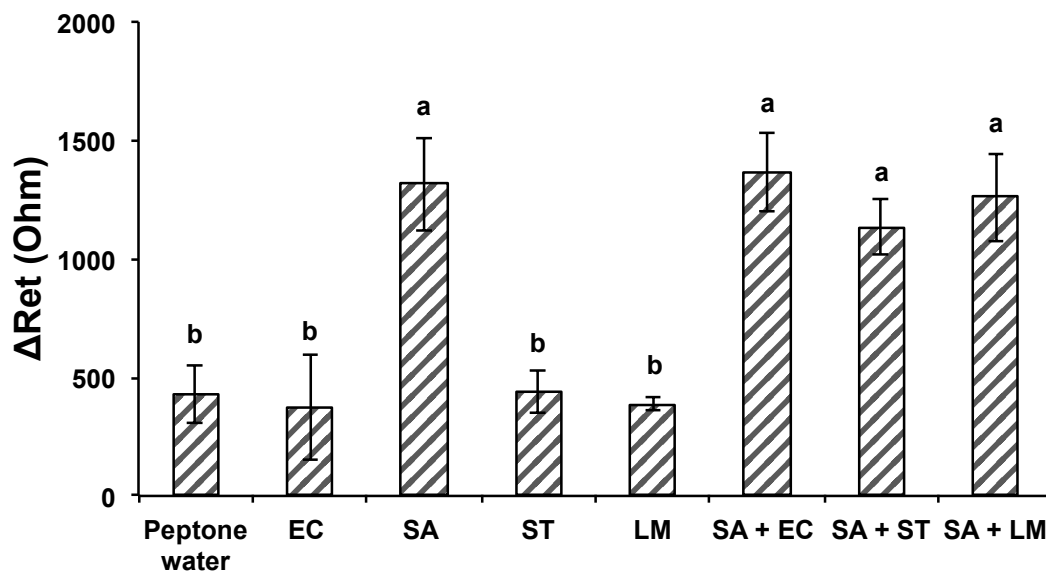


**Figure 3.10** Specificity and selectivity of *S. aureus* specific sensor against non-target bacteria and cocktail samples. Acronyms mean bacteria suspending in pure and mixed samples; EC: *E. coli* K12, SA: *S. aureus*, ST: *S. Typhimurium*, LM: *L. monocytogenes*, SA + EC: a mixture of *S. aureus* and *E. coli* K12, SA + ST: a mixture of *S. aureus* and *S. Typhimurium*, and SA + LM: a mixture of *S. aureus* and *L. monocytogenes*.

Means with the same letter are not significantly different ( $p \leq 0.05$ ).

These findings demonstrated that microwire sensors for bacterial detection could be fabricated by simply changing the antibodies specific to anticipated analytes. It was proven that functionalization procedure and bio-nanomaterial layers used in this study could make stable bioreceptor platforms on the MEI sensor to selectively detect the bacteria. The developed sensor can be widely utilized for detecting a wide range of microorganisms by immobilizing with specific antibodies on the sensor.



### **3.4. Conclusion**

The MEI sensor functionalized with double-layered SWCNTs and 5% BSA solution provided sensitive and specific detection of target bacteria. We achieved rapid (within 10 min) and sensitive detection of *E. coli* K12 and *S. aureus* (limit of detection:  $10^3$  CFU/mL) in pure bacterial samples. The developed MEI sensor shows a potential for selective detection of target bacteria in mixed bacterial communities. It can be used for microbial analysis of complex samples in food and environmental industries.

## Chapter 4.

### **Microwire-based electrochemical immunosensing technique combined with dielectrophoresis for rapid detection of *Escherichia coli* K12 and *Salmonella* Typhimurium in baby spinach**

#### **ABSTRACT**

As the number of foodborne illnesses linked to the consumption of fresh produce increases, a fast and accurate technique for detecting pathogens in fresh produce is urgently needed. A microwire-based electrochemical immunosensing device (MEI sensor) coupled with dielectrophoresis (DEP) was developed for rapid and simple detection of *Escherichia coli* K12 and *Salmonella* Typhimurium in a baby spinach leaf. The microwire was functionalized with polyethylenimine, single walled carbon nanotubes, streptavidin, biotinylated antibodies and then bovine serum albumin on the tip surface. Two different MEI sensors to individually detect *E. coli* K12 and *S. Typhimurium* were fabricated by immobilizing antibodies specific for each bacterium. The homogenate of bacteria infected spinach leaves and its dilutions were subjected to an AC electric field at 3 MHz and 20 V<sub>pp</sub> for 2 min to capture the bacterial cells. Changes in the electron transfer resistance by antigen-antibody reactions were measured. The estimated electrical resistance changes demonstrated a linear correlation with the bacterial concentrations determined by plate counting method with an R<sup>2</sup> value of 0.972 and 0.942 for *E. coli* K12 and *S. Typhimurium*, respectively. The *E. coli* sensor was able to achieve a detection limit of 10<sup>3</sup> CFU/g for *E. coli* K12 concentrations and the *Salmonella* sensor detected *S. Typhimurium* with a detection limit of approximately 10<sup>4</sup> CFU/g. The average detection time was 10 min with the cell concentration stage prior to signal measurement included. The *E. coli* and *Salmonella* sensors

demonstrated specificity toward their target bacteria within a sample containing spinach debris and non-target bacteria. These results suggest that the MEI sensor with DEP-assisted cell trapping has the potential to achieve fast and simple detection of various microorganisms in complex matrices.

### **Highlights**

- Rapid and sensitive bacterial detection in food with simple preparation was achieved.
- The developed *E. coli* specific biosensor can detect *E. coli* K12 as sensitive as  $10^3$  CFU/spinach (g).
- The biosensor platform shows potential for detection of other pathogens with modification.
- *S. Typhimurium* in spinach was detected as low as  $10^4$  CFU/g with the *Salmonella* specific sensor.

#### 4.1. Introduction

Although food quality control programs have been established, increased consumption, larger scale production, and greater distribution of minimally processed food products have contributed to an increase in the number of illness outbreaks (Scallan et al., 2011). According to the Centers for Disease Control and Prevention report, they estimate roughly one in six Americans get sick from contaminated food per year (CDC, 2011). About 46 % of outbreaks associated with foodborne illnesses are related to produce. The primary pathogenic bacteria responsible for recent produce related foodborne illness include *Salmonella* reading and *Salmonella* Abony in alfalfa sprouts (2016), *L. monocytogenes* in packaged salads (2016), *Salmonella* Poona in cucumbers (2015), *E. coli* O157:H7 in ready-to-eat salads (2013), and *E. coli* O157:H7 in spinach and spring mix (CDC, 2017). Since produce products are highly perishable and primarily consumed raw, a fast and accurate technique for the detection of potentially harmful microorganisms can be a possible solution to preventing emerging hazards and outbreaks.

A wide range of technologies for the identification and verification of microorganisms in food samples have been established. Conventionally, culture-based methods have been successful in detecting pathogens within ready-to-eat foods and fresh produce. However, other methods are more acceptable over cultural-based methods due to advantages regarding accuracy, sensitivity and assay time (Law et al., 2014). Biosensor-based microbial detection methods in particular has significant advantages over other methods due to its fast analysis times, which typically range within a couple of minutes. This attribute makes this method a suitable candidate for food quality assurance application in ensuring timely responses to possible foodborne risks (Pedrero et al., 2009).

Biosensors are analytical devices composed of bioreceptor and transducer, some biosensors are equipped with a signal processor built into the unit. The biological materials on the bioreceptor, for example, immobilized antibodies; recognize and bind with their corresponding antigens, this event contributes to generating measurable electrical signals (Sharma et al., 2013). An electrochemical immunosensor has been developed for rapid and simple detection and identification of target analytes in test samples with high sensitivity and specificity. The biosensor analyzes the change in electrical properties of electrode structures as cells are entrapped on or associated with the electrode (Sadik et al., 2009; Yang & Bashir, 2008). The immunocaptured bacterial cells on the surface of working electrode prevent the electron transfer between a counter electrode and the working electrode in the electrolyte solution accordingly, resulting in measurable changes in the electron transfer resistance.

Microbial detection using biosensor technology can reduce or eliminate cultural enrichment steps required prior to measurement. However, complications treating complex samples, such as food, water, soil, or biological sample, can make attaining accurate result difficult. Food matrices have various components including inorganic particles, biochemical compounds, indigenous microflora, and organic ingredients, which can interfere with downstream analysis and detection (Wang & Salazar, 2016). Also, internal components, enzymes, or antimicrobial compounds can be released during the preparation of the food samples, which can also become obstacles for assay (Wang & Salazar, 2016). Therefore, separation and concentration of bacterial cell from food system becomes necessary to enhance the efficiency of biosensors for practical use (Stevens & Jaykus, 2004).

The biorecognition process in the compound matrix can be improved by dielectrophoresis (DEP), which can be used to electrically manipulate bacterial cells in a suspension toward a

specific region of a non-uniform AC electric field. Depending on the electric properties of the particle interacting with the surrounding medium and the frequency applied to the electric field, the direction of the particle movement can be toward the regions of strong electric field gradient (positive DEP behavior, pDEP) or towards the weak electric field gradient (negative DEP behavior, nDEP) (Pohl, 1978). DEP-assisted immunocapture has demonstrated bacterial cells can be concentrated near a sensor surface with pDEP conditions and in combination with selective targeting of bacteria with immobilized antibodies on the surface of a sensor, immunocapture efficiency can be enhanced (Lu & Jun, 2012; Yang, 2009). In a food matrix, it is expected that electrochemical immunosensors are capable of detecting target bacteria with improved sensitivity by using DEP assisted bacterial cells concentration.

In the previous study, the change in electron transfer resistance was determined by detecting *E. coli* K12 and *S. aureus* within pure and mixed culture solutions using a microwire-based electrochemical immunosensing device (MEI sensor) coupled with DEP. The electron transfer resistances within these studies demonstrated direct dependence with the number of viable cells in the pure culture solution, and the sensor achieved selective detection of target bacteria in mixed bacteria solution. Therefore, the objective of this study was to investigate the potential of the developed MEI sensor with DEP cell attraction for real food application.

## **4.2. Materials and methods**

### **4.2.1. Bacterial cultures preparation**

The bacteria used in this study were *E. coli* K12 and *Salmonella* Typhimurium obtained from the Food Microbiology Lab, University of Hawaii. Each bacterium was grown in tryptic soy broth at  $37 \pm 1^\circ\text{C}$  for 24 h. The viable counts were determined by microbial plate count

method on MacConkey agar and Xylose lysine deoxycholate (XLD) agar. The initial concentrations of *E. coli* K12 and *S. Typhimurium* in culture were  $1.43 \pm 0.28 \times 10^9$  CFU/mL and  $9.42 \pm 2.21 \times 10^8$  CFU/mL respectively. The cultures were used for inoculating spinach leaves artificially.

#### **4.2.2. Inoculation of *E. coli* K12 and *S. Typhimurium* into spinach leaves**

Bacteria contaminated spinach leaves were prepared by applying *E. coli* K12 or *S. Typhimurium* culture on the surface of the leaf (Linman et al., 2010) or by injecting *E. coli* K12 into the vascular tissue (Kim et al., 2011). Baby spinach leaves were purchased from local grocery stores in Honolulu and were rinsed in 70% alcohol for 2 min and distilled water for 5 min. Ten grams of washed spinach leaves were transferred into a sterile Whirl-Pak sample bag (Nasco, Fort Atkinson, WI) and inoculated with two mL of each bacterial strain by pipetting on the surfaces of leaves to achieve approximately  $10^8$  CFU/g. For internalized contamination, two mL of *E. coli* K12 culture were injected into each of the leafy main vein with syringe. The inoculated leaves were dried at room temperature for 3 h. After drying, the contaminated spinach leaves were homogenized with 90 mL of sterile 0.1% peptone water using a stomacher (Stomacher 400 Circulator; Seward Inc., Bohemia, NY) at 260 rpm for 2 min. Then the spinach juice was used as the test sample and was serially diluted in 0.1% peptone water from  $10^1$  to  $10^7$  folds for sensitivity evaluation. The number of viable cells in the spinach juice was determined by plate counting method on MacConkey and XLD agar. The number of viable *E. coli* K12 cells in the spinach was counted and varying from  $6.50 \times 10^8$  to  $1.25 \times 10^9$  CFU/g. The viable *S. Typhimurium* cell counts recovered from the spinach were determined between  $1.03 \times 10^8$  and  $2.02 \times 10^8$  CFU/g.

#### 4.2.3. Functionalization of microwire surface

The MEI sensors were prepared by the previous procedure (refer to 3.2.3). A gold-plated tungsten microwire (50  $\mu\text{m}$  in diameter and 25 mm in length) was cleaned with distilled water and 70% alcohol for 5 min each under sonication. The microwire was coated with 1% polyethylenimine (PEI, branched, average Mw  $\sim$  25,000, Sigma Aldrich, St. Louis, MO) and 0.01% single carbon nanotubes dispersion (SWNT PD1.5L, NanoLab. Inc., Waltham, MA). Streptavidin (from *Streptomyces avidinii*, Sigma Aldrich, St. Louis, MO) and biotinylated polyclonal antibodies were immobilized on the surface of the microwire sequentially. Two different MEI sensors, *E. coli* sensor and *Salmonella* sensor, were fabricated using antibodies specific for *E. coli* serotype O/K (from rabbit, #PA1-73031, Thermo Fisher Scientific, Waltham, MA) and for *Salmonella* species (from rabbit, #PA1-73022, Thermo Fisher Scientific, Waltham, MA) to individually detect *E. coli* K12 and *S. Typhimurium* in the sample. 5% bovine serum albumin solution (BSA, #A3294, Sigma Aldrich, St. Louis, MO) was applied to the outer layer to minimize non-specific binding.

#### 4.2.4. Detection of *E. coli* K12 and *S. Typhimurium* in contaminated spinach leaves

The Functionalized MEI sensor was attached to an automated XYZ stage (Franklin Mechanical & Control Inc., Gilroy, CA) and connected to an electrical wire. The MEI sensor was lowered into 10  $\mu\text{L}$  of a sample droplet placed on a gold plate, the gap between the end of the microwire and the surface of the plate was approximately 1 mm. DEP was introduced into the sample droplet at 3 MHz and 20  $V_{pp}$  for 2 min using a function generator (3220A, Agilent Technologies, Santa Clare, CA) to manipulate bacteria cells toward the MEI sensor. The MEI



sensor was retracted from the sample solution at a velocity of 5 mm/min and transferred to an electrochemical cell for impedance measurement.

#### **4.2.5. Impedance measurement**

Electrochemical impedance was measured using a frequency response analyzer ( $\mu$ Autolab III/FRA2, Metrohm Autolab USA Inc., Riverview, FL) with a frequency range from 0.1 to 100 kHz at a DC offset of 200 mV and AC amplitude of 10 mV. The electrochemical cell consisted of microwire as a working electrode, a platinum wire as a counter electrode, and an Ag/AgCl reference electrode immersed in electrolyte solution (5 mM  $K_3Fe(CN)_6/K_4Fe(CN)_6$  (1:1) aqueous solution with 0.1 M KCl). When the microwire was placed in the cell, experimental data was collected for 5 min. and analyzed by NOVA software version 1.6.

Electron transfer resistance ( $R_{et}$ ) for the redox reaction at the MEI sensor boundary was obtained from an equivalent circuit fitting model with mixed kinetic and charge-transfer kinetics included (Lu et al., 2013). Changes in the electron transfer resistance ( $\Delta R_{et}$ ) by antigen-antibody reactions were calculated by equation 3.1, which compares the  $R_{et}$  values of the single MEI sensor before ( $R_{et}$  (antibody)) and after the capture the bacterial cells ( $R_{et}$  (antibody-bacteria)). Due to the small amount (10  $\mu$ L) of sample solution loaded on the sensor device, the MEI sensor biosensor detected the bacterial cells at 1/1000 levels of total population in spinach sample (g). Therefore,  $\Delta R_{et}$  values were plotted versus bacterial cell counts in sample volume (10  $\mu$ L) used for detection or estimated bacterial concentrations per gram of spinach leaf.

#### **4.2.6. Data analysis**

Data was collected in a minimum of triplicates from separate spinach sample preparation for each individual run. The mean and standard deviations of  $\Delta R_{et}$  was calculated for the serial dilutions of prepared spinach juices. The differences between the means were analyzed based on Duncan's multiple range tests using a single factor analysis of variance (ANOVA) offered by Statistical Analysis Software (SAS version 9.4, SAS Institute Inc., Cary, NC) at 95% confidence level ( $p \leq 0.05$ ). The independent sample t-test was conducted using SPSS statistics 20.0 at 95% confidence level to compare the  $\Delta R_{et}$  means from the target and non-target bacteria detection results with target specific sensor.

#### **4.2.7. FESEM visualization**

Attached bacterial cells on the surface of the MEI sensors were observed using a Field Emission Scanning Electron Microscope (FESEM, Pacific Biosciences Research Center, University of Hawaii, Model: Hitachi S-4800) at an acceleration voltage of 5 kV. Before loading the samples into the FESEM, the microwire was treated with glutaraldehyde/cacodylate fixative, 1% osmium tetroxide in cacodylate buffer, and ethanol series (from 30% to 100%) for fixation and dehydration of microbial cells. The treated microwires were mounted on aluminum stub with carbon tape and coated with a gold/palladium for 45 seconds using a Hummer 6.2 sputter coater.

### 4.3. Results

#### 4.3.1. Detection of *E. coli* K12 in spinach leaves using the *E. coli* specific sensor

Figure 4.1 shows a distribution in changes of electron transfer resistance with *E. coli* K12 captured on the *E. coli* sensor. As the *E. coli* K12 concentration in loading sample solution increased from 1 to  $10^4$  CFUs, the  $\Delta R_{et}$  values increased. However as the concentration continued towards  $10^4$  CFU/sample vol. a drop in  $\Delta R_{et}$  was observed. At low concentrations of *E. coli* K12 no observable change in  $\Delta R_{et}$  was recorded. The results from the detection of *E. coli* K12 in the internally contaminated sample (white squares, Figure 4.2) matched the results of sample prepared by surface contamination. Figure 4.2 indicates the calibration curves for  $\Delta R_{et}$  versus *E. coli* K12 counts contaminated in spinach samples by two inoculation methods. A linear relationship was observed between  $\Delta R_{et}$  and *E. coli* K12 concentrations from  $8.33 \times 10^2$  to  $7.97 \times 10^5$  CFU/g for the surface contamination method ( $R^2 = 0.972$ ) and  $1.05 \times 10^3$  to  $8.83 \times 10^5$  CFU/g for internalized method into the main vein of leaves ( $R^2 = 0.989$ ). In the low concentrations of *E. coli* K12, roughly  $10^3$  CFU/g, the  $\Delta R_{et}$  values obtained from both injection methods showed no significant difference. The  $\Delta R_{et}$  of the surface inoculation sample was  $388 \pm 219 \Omega$  and the value of the inoculated sample through the vein was  $392 \pm 212 \Omega$ . This similarity in trend of  $\Delta R_{et}$  was also shown in  $10^4$  CFU/g concentration of the *E. coli* K12. However, a growing difference between the two  $\Delta R_{et}$  values at in the two spinach samples was observed as the bacterial cell concentration increased.

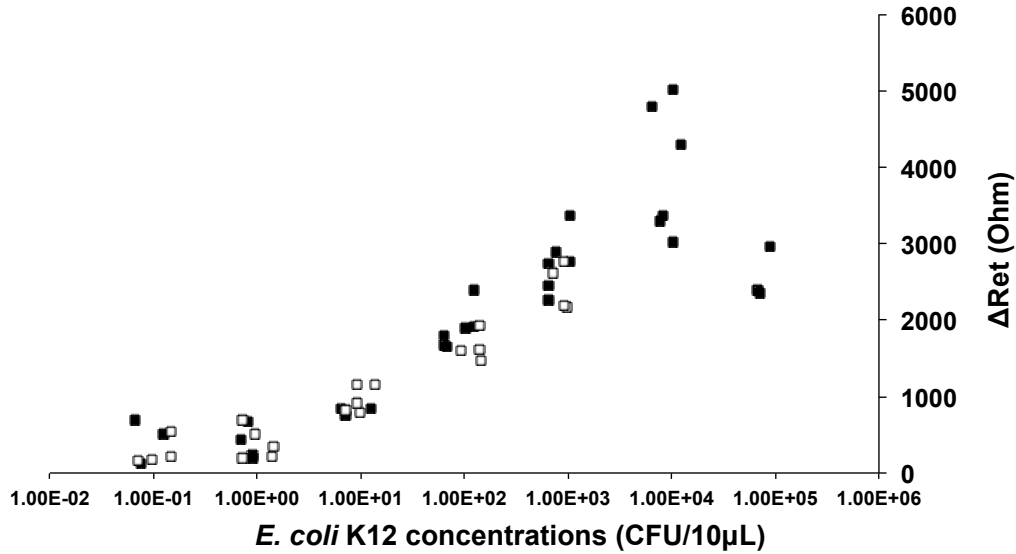


**Figure 4.1** Changes in electron transfer resistance ( $\Delta R_{et}$ ) with *E. coli* K12 captured on the *E. coli* sensor; black: *E. coli* K12 contamination on the surface of spinach leaves, white: internalized contamination of *E. coli* K12 into the main vein.

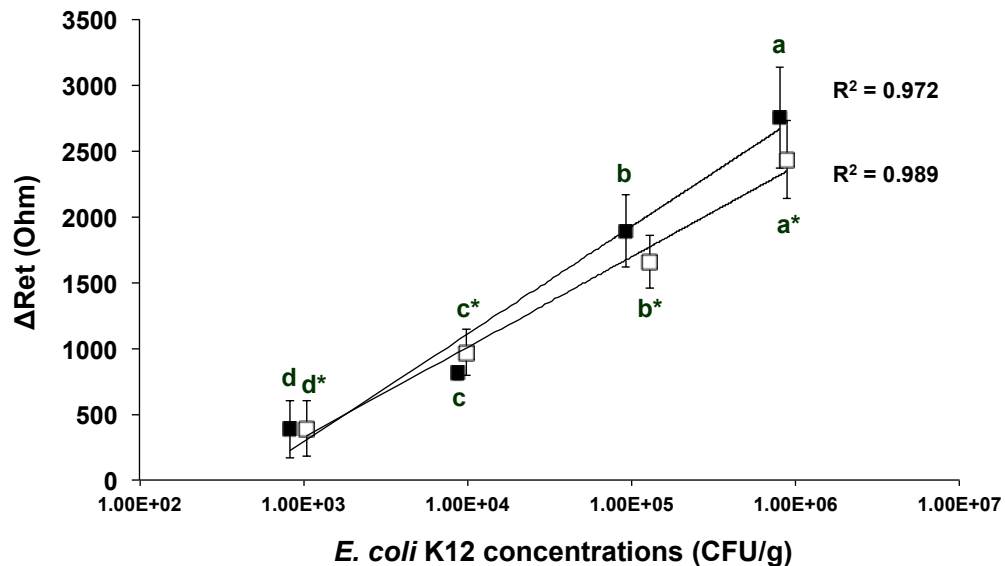


**Figure 4.2** Relationship between  $\Delta R_{et}$  and *E. coli* K12 in the range of  $10^3$ - $10^6$  CFU/mL contaminated in spinach by two inoculation methods; on the surface (black) and into the vascular tissue (white). \* $\Delta R_{et}$  values of *E. coli* K12-spinach juice recovered from two inoculation methods were analyzed separately.

Average signal changes with different superscripts are significantly different at 95% confidence level (probability < 0.05).

The specificity of the *E. coli* sensor was investigated with the presence of *S. Typhimurium* in the spinach leaves via the surface application method. A comparison of the  $\Delta R_{et}$  values resulting from target bacteria and non-target bacteria detections at high and low concentrations is shown in Table 4.1. There is a significant difference in  $\Delta R_{et}$  means between *E. coli* K12 and *S. Typhimurium* captures using the *E. coli* sensor at high concentrations and low concentrations of both bacteria ( $p < 0.05$ ). The averages of  $\Delta R_{et}$  for *E. coli* K12 inoculated samples with high and low concentrations were larger than the average  $\Delta R_{et}$  for *S. Typhimurium* contained samples.

**Table 4.1** Specificity test for the *E. coli* sensor against *S. Typhimurium* in the spinach leaves

	Bacterial concentration (CFU/g)		$\Delta R_{et}$ ( $\Omega$ )	t	p
<i>E. coli</i> K12	High	$9.25 \times 10^6$	$3968 \pm 845^a$	10.145	< 0.001
<i>S. Typhimurium</i>	(7 log)	$1.87 \times 10^7$	$450 \pm 60^b$		
<i>E. coli</i> K12	Low	$8.30 \times 10^3$	$810 \pm 52^{a*}$	20.982	< 0.001
<i>S. Typhimurium</i>	(4 log)	$1.93 \times 10^4$	$143 \pm 33^{b*}$		

Average  $\Delta R_{et}$  with different letters are significantly different at 95% confidence level. \*  $\Delta R_{et}$  values obtained from high- and low-concentration of bacteria in samples were analyzed separately.

#### 4.3.2. Specificity test of the *Salmonella* specific sensor against *E. coli* K12 in buffer

The MEI sensor functionalized with anti-*Salmonella* antibody was fabricated to examine the suitability for detection of *Salmonella* subspecies in spinach leaves. Before the *Salmonella* sensor was applied to capture the microbial cells in *S. Typhimurium* inoculated spinach sample, the specificity of the biosensor against *E. coli* K12 in peptone water was evaluated. The  $\Delta R_{et}$  by *S. Typhimurium* attachment on the *Salmonella* sensor ranged from 1.59 to 2.64 k $\Omega$  (Figure 4.3). The concentration of *S. Typhimurium* in the peptone solution was  $7.65 \times 10^7$  CFU/mL. In

comparison, approximately  $393 \pm 201 \Omega$  and  $170 \pm 101 \Omega$  of  $\Delta R_{et}$  was calculated with comparable concentration of *E. coli* K12 ( $1.66 \times 10^8$  CFU/mL) and bacteria-free peptone solutions, respectively. There was a significant difference between *S. Typhimurium* and controls. SEM micrograph show *S. Typhimurium* cells to be present on the surface of the *Salmonella* sensor but no microbial cells were observed on the sensor surface when the diluted *E. coli* K12 culture was used.

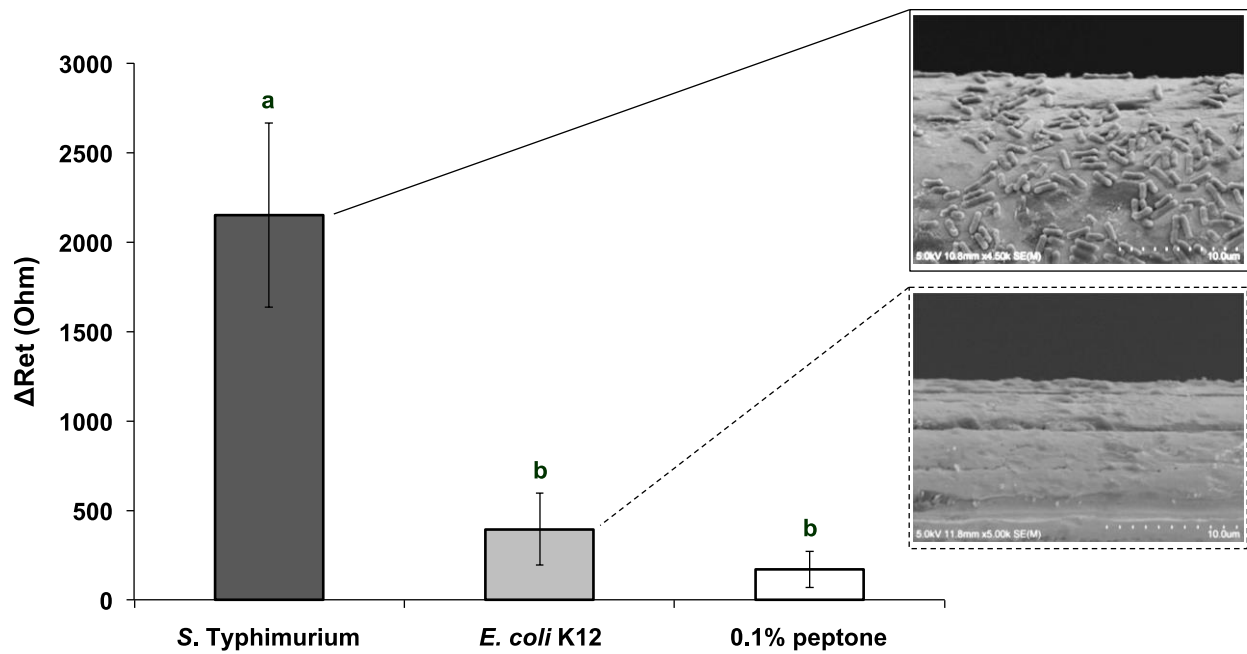


**Figure 4.3** Specificity test of the *Salmonella* biosensor against *E. coli* K12 in peptone water and bacteria-free peptone water. Inserted SEM images represent the surface of the *Salmonella* sensor after testing with the *S. Typhimurium* and *E. coli* K12 suspensions.

Average  $\Delta R_{et}$  with different letters are significantly different at 95% confidence level.

### 4.3.3. Detection of *S. Typhimurium* in spinach leaves using the *Salmonella* specific sensor

The changes in electron transfer resistance increased as the *S. Typhimurium* concentrations increased within the range of 1.03 CFU/10  $\mu$ L to  $2.02 \times 10^5$  CFU/10  $\mu$ L as seen in Figure 4.4. The collected  $\Delta R_{et}$  values ranged from 260 to 2750  $\Omega$ . The differences between  $\Delta R_{et}$  means of *S. Typhimurium* suspensions at concentrations less than 10 CFUs were not significant, as was the case with the detecting the *E. coli* K12 using the *E. coli* sensor. A linear relationship was observed between  $\Delta R_{et}$  and *S. Typhimurium* concentrations from  $1.43 \times 10^3$  to  $1.67 \times 10^7$  CFU/g with a  $R^2$  value of 0.942 (Figure 4.5).

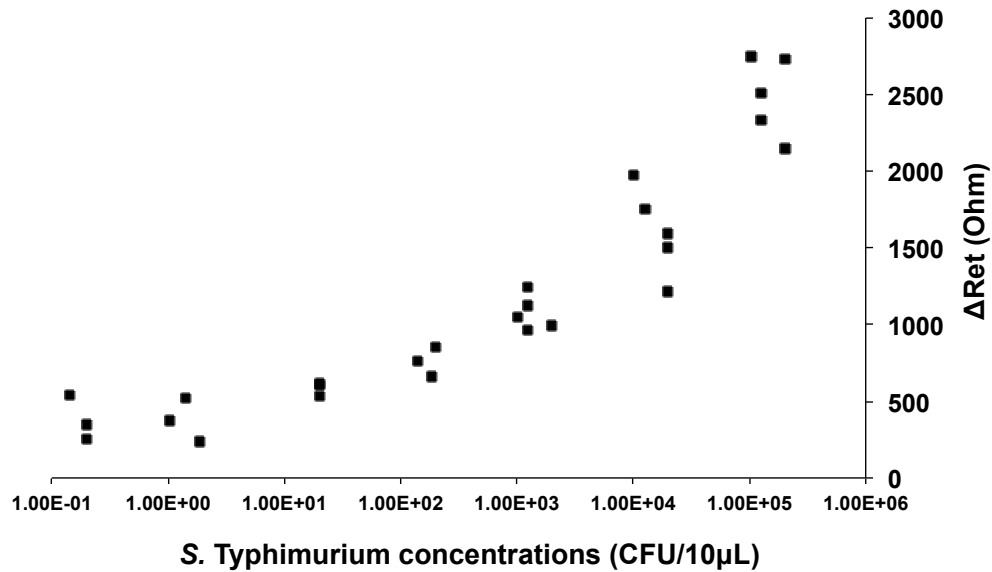


**Figure 4.4** Changes in electron transfer resistance ( $\Delta R_{et}$ ) with *S. Typhimurium* captured on the *Salmonella* sensor

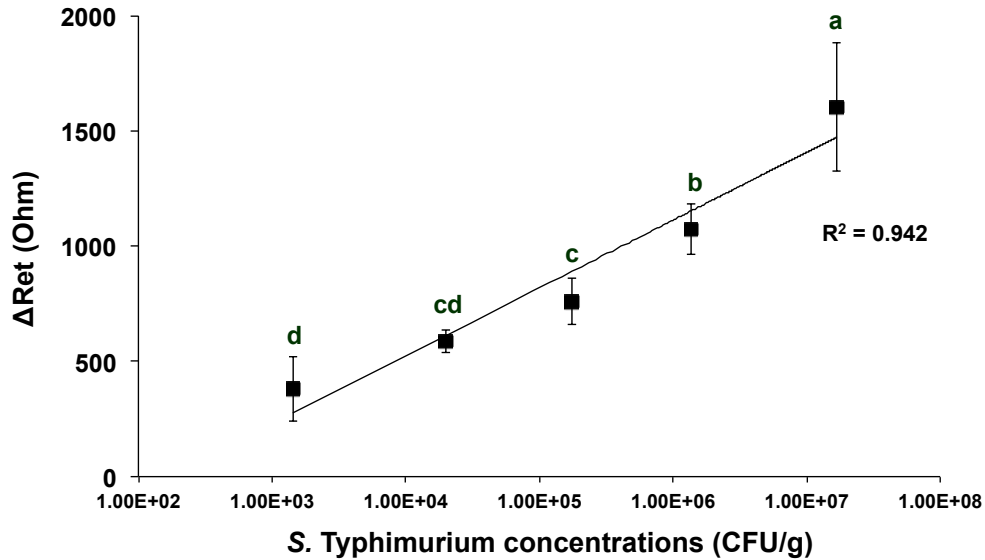


**Figure 4.5** Relationship between  $\Delta R_{et}$  and *S. Typhimurium* in the range from  $10^3$  to  $10^7$  CFU/mL contaminated in spinach.

Average signal changes with different superscripts are significantly different at 95% confidence level (probability < 0.05).

A specificity test for the *Salmonella* sensor against *E. coli* K12 in the spinach leaves was performed. Table 4.2 summarizes the results of the viable bacterial counts in the samples,  $\Delta R_{et}$  values obtained from each sample, and t-test results. At bacteria populations of 8 log CFU/mL and 4 log CFU/mL,  $\Delta R_{et}$  of the *Salmonella* sensor was observed to be higher when tested with *S. Typhimurium* compared to *E. coli* K12. T-test comparisons show a significant difference in mean  $\Delta R_{et}$  between *E. coli* K12 and *S. Typhimurium* using the *Salmonella* sensor ( $p < 0.05$ ). In the SEM image (Figure 4.6 (a)), it was observed that *S. Typhimurium* cells were captured on the surface of the *Salmonella* sensor. This implies that *E. coli* K12 cells rarely attached to the surface of the *Salmonella* sensor.



**Table 4.2** Specificity test for the *Salmonella* sensor against *E. coli* K12 in the spinach leaves

		Bacterial concentration (CFU/g)	$\Delta R_{et}$ ( $\Omega$ )	t	p
<i>S. Typhimurium</i>	High	$1.52 \times 10^8$	$2494 \pm 258^a$	18.523	< 0.001
<i>E. coli</i> K12	(8 log)	$2.01 \times 10^8$	$315 \pm 121^b$		
<i>S. Typhimurium</i>	Low	$2.02 \times 10^4$	$587 \pm 49^{a*}$	3.958	0.017
<i>E. coli</i> K12	(4 log)	$1.62 \times 10^4$	$190 \pm 166^{b*}$		

Average  $\Delta R_{et}$  with different letters are significantly different at 95% confidence level. \*  $\Delta R_{et}$  values obtained from high- and low-concentration of bacteria in samples were analyzed separately.

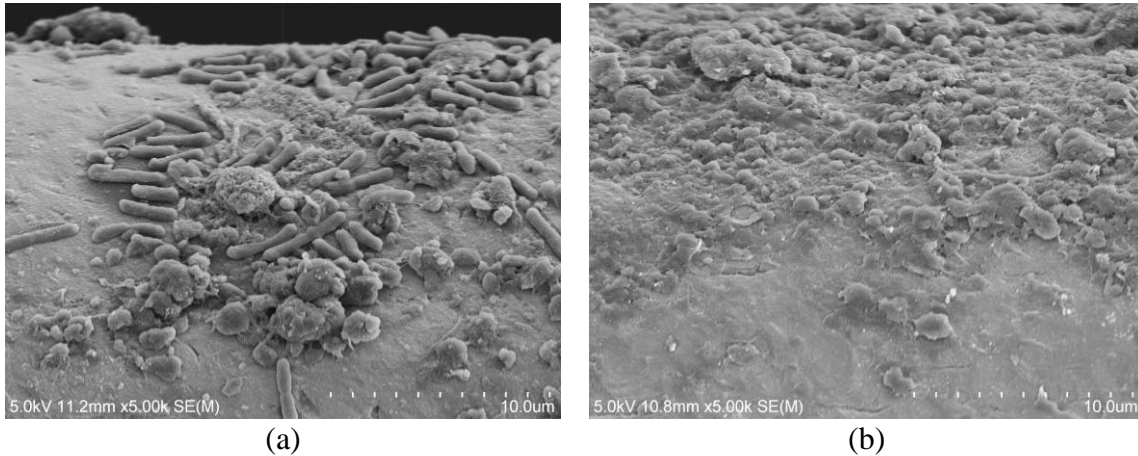


**Figure 4.6** SEM images of the *Salmonella* sensor after testing with the spinach juices in the presence of *S. Typhimurium* (a) and *E. coli* K12 (b).

#### 4.4. Discussion

Biosensors for bacterial detection are required to meet properties regarding sensitivity, specificity, detection time, size, consistency, stability, sample processing, and operator requirement (Ivnitski et al., 1999; Xu et al., 2017). As a result, biosensors should be sensitive enough to detect target bacteria at concentrations as low as  $10^3$  CFU/mL. In addition, biosensors should be able to distinguish specific target strain from other serotypes in the same or different

species within 5-10 min of assay time. Portability, durability, ease of use, and simple test procedure are also key requirements for an ideal biosensor. In this study, some of those properties of the newly developed MEI sensor were discussed for detection of *E. coli* K12 and *S. Typhimurium* in the food system.

#### **4.4.1. Sensitivity of the *E. coli* and the *Salmonella* sensors**

The *E. coli* sensor and the *Salmonella* sensor demonstrated a linear relationship between  $\Delta R_{et}$  and bacterial concentrations, implying a measurable effect of antibody-bacteria complexes on the electrical signal changes exist. The limit of detection (LOD) for the *E. coli* sensors was determined as  $8.33 \times 10^2$  CFU/g. The *Salmonella* sensor was able to detect the *S. Typhimurium* with a LOD of approximately  $2.02 \times 10^4$  CFU/g. In low concentration ranges of bacteria, the magnitude of  $\Delta R_{et}$  was not significantly different. Since the 10  $\mu$ L of sample solution was estimated having bacterial cells less than 1 CFU, the MEI sensors seemed to recognize the sample as the bacteria-free solution. The total detection time for a single analysis was measured to be 10 minutes with the inclusion of the bacterial cell concentrating stages with DEP and the electrical signal collection process. There are several prior studies regarding detection of *E. coli* or *S. Typhimurium* in spinach sample using biosensing methods. Linman et al. (2010) reported the detection of *E. coli* in the buffer and spinach leaves by surface plasmon resonance spectroscopy with a tetramethylbenzidine-based enzymatic signal enhancement method. They achieved an LOD of  $10^3$  CFU/mL in PBS buffer and  $10^4$  CFU/mL in spinach extracts in a few hours. Yazgan et al. (2014) studied electrochemical detection of *E. coli* K12 inoculated on the surface of spinach leaves using a gold electrode immobilized with modified mannose ligands. The LOD of their biosensor for *E. coli* was  $6.25 \times 10^2$  CFU/mL with the detection time of 10

min for *E. coli*-ligand saturation. Detection of *S. Typhimurium* on spinach leaves using an E2 phase-based magnetoelastic biosensor was also reported, and the LODs were determined at 2.17 and 1.94 log CFU/spinach for adaxial and abaxial surface, respectively (Park et al., 2013). The results described above indicate that the MEI sensors have similar or better detection limits and faster assay time than other sensors.

#### **4.4.2. Specificity of the *E. coli* and the *Salmonella* sensors**

Specificity tests for both *E. coli* and *Salmonella* sensors indicated that target bacterial cells were successfully immunoreacted on the surface resulting in electrical response changes. Non-target bacteria produced  $\Delta R_{et}$  values that were much lower than the values yielded by target bacteria in the similar bacteria concentrations. These results are in agreement with studies regarding impedimetric immunosensor specific for *E. coli* O157:H7 and *S. Typhimurium* against pure cultures of *E. coli* K12, *Listeria monocytogenes*, or *Staphylococcus aureus* (Xu et al., 2016). Additionally, results from array-based immunosensor for specific detection of *S. Typhimurium* against *E. coli* or *Campylobacter jejuni* (Taitt et al., 2004) are also in agreement. On the other hand, when the *E. coli* specific sensor was tested with *S. Typhimurium* inoculated spinach sample at 7 logs CFU/g; the electron transfer resistance changed by a magnitude of  $450 \pm 60 \Omega$ , this is noticeably higher than the value of  $385 \pm 219 \Omega$  at the LOD of the *E. coli* sensor. This finding might be due to cross-reactivity of the antibodies used in the MEI sensors. According to the supplier, the polyclonal *E. coli* antibodies immobilized on the *E. coli* sensor recognize O and K antigens of *E. coli* and cross-react with related *Enterobacteriaceae*. The signal response of the *E. coli* sensor against *S. Typhimurium* in the sample might be from the non-specific binding of some *S. Typhimurium* cells on the sensor. The *Salmonella* sensor was functionalized with

polyclonal *Salmonella* antibodies that react with *S. Enteritidis*, *S. Typhimurium*, and *S. Heidelberg* (O and H antigens). The *Salmonella* sensor showed the lower  $\Delta R_{et}$  value of  $315 \pm 120 \Omega$  in high populations of *E. coli* K12 vs.  $\Delta R_{et}$  of  $587 \pm 49 \Omega$  at the LOD of the sensor. Therefore, the  $\Delta R_{et}$  obtained from the sample with *E. coli* contaminant could exhibit less variance when compared to the *S. Typhimurium* contaminant. This implies that the MEI sensors might react with non-target bacteria if they exist at high enough levels (The type of immobilized antibodies on the sensor will also play a major role in determining cross-reactivity). Which ultimately indicates that the cross-reactivity of the antibodies between the serotypes used in the sensor could also affect the specificity of the sensor.

#### **4.4.3. Application of developed biosensing for detection of other bacteria species**

*Salmonella* specific sensor was fabricated; the compatibility of the bio-nanocomposite on the sensor surface and the assay procedure for detection of *S. Typhimurium* within a buffer and food system was evaluated. Although the *Salmonella* sensor shows high specificity toward *S. Typhimurium* in peptone water and spinach juice, it demonstrated less sensitivity when in comparison with the *E. coli* sensor. The bio-nanocomposite surface functionalized with *Salmonella* subspecies antibodies may be enough to fulfill specificity requirement of the sensor, however, *Salmonella* cell concentrating via DEP has not been optimized. The cause for the different levels of detectable bacteria concentrations for each sensor is not yet fully understood, but the differences in DEP conditions for the cell trapping may be responsible. DEP forces acting on a bacterial cell depends on its size, electrical properties and the electrical properties the suspension medium (i.e., The permittivities and the conductivities of the particles and the medium, and the frequency of the applied electrical field (Pohl, 1978)). Within the same medium

and electric field, the different sizes and electrical properties of *E. coli* K12 and *S. Typhimurium* cells could influence DEP forces causing alteration of cell movement and immunoreaction on the sensor. The applied voltage and frequency of the electric field in this study was optimized for detection of *E. coli* K12 (Kim et al., 2011), as a result the high detection limits observed with *E. coli* K12 with the *E. coli* specific sensor could be a direct results of efficient DEP application. The DEP condition optimized for *E. coli* K12 should theoretically exhibit similar pDEP behavior for *S. Typhimurium*, however its application has not been proven to provide optimal analyte detection efficiency. Therefore, application studies on the detection of other bacteria species require not only replacement of appropriate biorecognition molecules but also a slight modification of DEP protocol to obtain optimal capture efficiency.

#### **4.4.4. Detection of bacteria in food sample**

Food samples are more complex than peptone buffer solution. Inhibitory compounds associated with the food matrix such as the inorganic particles, released enzymes, and indigenous microflora can cause errors in analysis and detection by altering the conductivity of the medium and increasing the probability of non-specific binding (Bhunja, 2014; Wang & Salazar, 2016). Spinach juice is an example assay after homogenization, but other food samples with different compositions may require additional pre-treatments such as filtration, centrifugation, or reconstitution. These additional steps increase the sample preparation time but can normalize the loading sample condition, making it possible to use biosensing techniques for the same target microorganism in various foodstuffs.

#### 4.5. Conclusion

MEI sensor combined with DEP based cell concentration, achieved LODs of  $10^3$  CFU/g for *E. coli* K12 and  $10^4$  CFU/g for *S. Typhimurium* in spinach leaves. The newly developed MEI sensors requires only 10 min for a single analysis of a prepared sample via a two-steps procedure of bacterial cell capture and electrical signal measurement. Food sample processing is simple, requiring only homogenization, but some foodstuffs may need additional processes (e.g. centrifugation and resuspension) to enhance the detection efficiency. Both of the *E. coli* and *Salmonella* specific sensors with DEP based cell concentration showed a potential for selective detection of target bacteria in a samples containing suspended spinach flakes and non-target bacteria. The newly developed MEI sensor and test procedures can be applied for fast and simple analysis of other microorganisms in complex matrices such as food, environmental and biological samples.

## Chapter 5.

### **Simultaneous detection of *Escherichia coli* K12 and *Staphylococcus aureus* using a continuous flow multi-junction biosensor**

#### **ABSTRACT**

Rapid detection and identification of potentially harmful bacteria is ideal for food manufacturers to prevent foodborne illness outbreaks. Continuous monitoring method of foodborne pathogens levels and trends in food gives real-time results. Therefore, the objectives of this study were to fabricate and characterize the continuous flow multi-junction biosensor for simultaneous detection of *Escherichia coli* K12 and *Staphylococcus aureus*. Junction biosensors were fabricated using gold plated tungsten wires coated with polyethylenimine and single walled carbon nanotubes. Each junction was functionalized with streptavidin and biotinylated antibodies specific to *E. coli* K12 and *S. aureus*. Then, single or 2 biosensors for each targeted analyte were connected to tubing, perpendicular to the flow direction. Pure serial diluted samples of *E. coli* K12 and *S. aureus* and microbial cocktail samples were continuously pumped at a 0.0167 mL/s into the detection zone. Changes in the electric current by biorecognition reactions between antibody and antigens were calculated. The developed junction sensor coupled with the fluidic channel showed the enhancement of the electric signal responses for detection of *E. coli* K12, compared to the stationary sensor. A linear regression was observed for both the *E. coli* and *S. aureus* functionalized array sensors in the detection range of  $10^2$  to  $10^5$  CFU/mL. Multiplexed detection of bacteria at the sensing levels as low as  $10^2$  CFU/mL for *E. coli* K12 and *S. aureus* was achieved within 2 min. Therefore; the continuous flow multi-junction biosensor shows potential for rapid and continuous multiplexed detection of foodborne pathogens.

## 5.1. Introduction

Rapid identification and detection of bacterial pathogens in food is urgently needed to ensure food safety. Centers of Disease Control and Prevention estimated annual number of domestically acquired, 47.8 million foodborne illnesses, 128,000 hospitalizations, and 3,000 deaths due to 31 pathogens and unspecified agents transmitted through food. Most of these diseases are caused by known foodborne pathogens such as *Escherichia coli* O157:H7, *Salmonella* (nontyphoidal), *Listeria monocytogenes*, *Clostridium perfringens*, *Campylobacter spp.*, *Staphylococcus aureus*, and *norovirus* (CDC, 2011). Rapid identification of pathogenic bacteria contaminated in food products before distribution to grocery stores, restaurants and manufacturing facilities is a solution to reduce the number of foodborne illnesses (Shriver-Lake et al., 2007). A range of the number of pathogenic bacteria ingested that can cause infection is from 1 to  $10^7$  cells depending on the species, their serotype, age and health of host and the type of contaminated food consumed (Kothary & Babu, 2001). The infection dose of pathogenic *E. coli* groups is ranging from  $10^7$  to  $10^{10}$  cells; however, *E. coli* O157:H7, an enterohemorrhagic *E. coli* serotype, causes the illness with very low number of cells, in the range of 10 to 100 cells (Croxen et al., 2013). *S. aureus* population exceed  $10^5$  organisms/g in food can create one  $\mu\text{g}$  of toxin causing food poisoning (Evenson et al., 1988). Therefore, a limit of detection for pathogens in food should be less than the infective dose. The powerful analytic methods with sensitive and reliable for detecting pathogens at pre-infectious levels in foods are required to prevent the widespread outbreaks of disease.

Conventional methods based on colony counting, immunoassay, and nucleic acid amplification, remain highly reliable and have been successful for detecting bacterial pathogens (Leonard et al., 2003; Velusamy et al., 2010). However, current detection techniques rely on



specific microbiological and biochemical identification. In addition, these methods require long assay time, labors and initial enrichment steps to detect pathogens with low concentration in food (Leonard et al., 2003).

Biosensors have emerged as useful tools for pathogen detection, especially, electrochemical biosensors have the advantages of high sensitivity, rapidity, low cost and amenability of micro-fabrication (Sadik et al., 2009). The electrochemical biosensor has been studied with the immune reaction between the analyte and the corresponding recognitions molecules. The antigen-antibody complexes are formed on the biosensor's transducer to create measurable electrical signals. The detection process based on label-free electrochemical impedance spectroscopy was demonstrated to reliably detect pre-infectious levels of *Salmonella* Typhimurium at 500 CFU/mL with a detection time of 6 min, including 5 min for data acquisition and 1 min for analysis (Nandakumar et al., 2008).

Incorporation of nanomaterial to sensor platform, in particular single walled carbon nanotubes (SWCNTs)-based sensors is a promising detection alternative due to SWCNT's bio and size compatibility, structural flexibility, and electrical conductivity for enhancing the sensor's performance (Allen et al., 2007; Kang et al., 2006; Katz & Willner, 2004). The SWCNTs incorporated the biosensor have been used as field-effect transistors (FETs), which changes the electrical conductance by binding of analyte molecules to recognition molecule (Trojanowicz, 2006). García-Aljaro et al. (2010) developed the carbon nanotubes-based immunosensors for detection of *E. coli* O157:H7 and the bacteriophage T7. The detection limit and response time were  $10^3$  CFU/ mL with 60 min for *E. coli* O157:H7 detection and  $10^3$  PFU/ mL within 5 min for bacteriophage. The biosensor exhibited the selectivity against *E. coli* K12 and MS bacteriophage. Bio-nano combinational junction sensor with functionalized SWCNTs

has shown the potential for high-performance biosensing to detect foodborne pathogens (Yamada et al., 2016; Yamada et al., 2014). The junction sensor works to convert bioaffinity binding between target bacteria cell and antibodies into measurable electrical current signals (Fig. 5.1 (a)). The researchers achieved rapid (within 2 min), sensitive and selective detection of *E. coli* K12 and *S. aureus* (limit of detection:  $10^2$  CFU/ mL) in pure and cocktail bacterial samples. The combination of CNTs and specific antibodies provided excellent sensitivity and selectivity in electrochemical biosensors for detection of pathogens.

Although most biosensors exhibited high sensitivity with a fast detection time, they tended to work for small sample volumes. The volume of bacterial solution ranged from a droplet about 5  $\mu$ L to 100  $\mu$ L (Lu et al., 2013; Nandakumar et al., 2008; Yamada et al., 2014). The sample volume for detection of bacterial cells could limit adequate quantitative microbial analysis because it does not represent the whole population. It should entail a pre-enrichment step to concentrate low numbers of pathogens, resulting in an increase in the detection time. Continuous system is able to detect the pathogens with large volume of samples as well as it can be monitored food safety in real-time (Hartwell & Grudpan, 2010; Kim & Park, 2003) for food processing applications that involve continuous flow food products. In addition, flow-based detection techniques such as flow-injection, sequential injection and microfluidic system increase the potential for assay automation (Fintschenko & Wilson, 1998; Gubitz et al., 2001) and the ratio of immobilized surface area to sample volume, offering increased antibody-antigen encounter (Abdel-Hamid et al., 1999). However, most studies for flow-based biosensor have been done in microfluidic channel. Also, rapid and multiplexed detection method for commercial use in flow condition was hardly studied. Therefore, the objectives of this study were to fabricate

the continuous flow multi-junction biosensor for continuous detection of two different bacteria and to evaluate the sensing performances in a microfluidic channel.

## **5.2. Materials and methods**

### **5.2.1. Junction sensor fabrication**

The methods for individual sensor fabrication consisted of microwires coating, junction assembly, and antibody immobilization and were followed Yamada et al.'s procedure (Yamada et al., 2014). 7% gold plated tungsten wire (50  $\mu\text{m}$  in diameter, ESPI Metals, Ashland, OR) was washed by sonication in distilled water, followed by 70% alcohol for 5 min each and dried in a furnace at 175°C for 10 min. The sanitized microwires coated with 1% polyethylenimine (PEI) and then single walled carbon nanotubes (SWCNTs; SWNT PD1.5L, NanoLab, Inc., Waltham, MA) dispersed in N,N-dimethylformamide (DMF; Sigma Aldrich, St. Louis, MO) by dipping and withdrawing method using XYZ stage and stepping motor (Franklin Mechanical & Control Inc., Gilroy, CA) at a withdrawal velocity of 100  $\mu\text{m}/\text{s}$ . For sensor chip fabrication, copper clad printed circuit board (1.5 mm thick, McMaster-Carr, Santa Fe Springs, CA) were cut into small pieces (26 x 26 mm<sup>2</sup>) and drilled a hole the center with 10 mm in diameter for fluidic channel. Then, they were etched to form electrode connector pads at the four sides of the circuit board. The hole was filled with polydimethylsiloxane (PDMS; Sylgard 184 silicone elastomer curing agent and base, Dow Corning, Midland, MI). PDMS layer was used as a support during antibodies immobilization at the junction and detection of bacteria in a stationary mode, but was removed after functionalized process for continuous flow testing. PEI-SWCNT coated wires were orthogonally soldered to the connector pads on the circuit board to form a single crossbar array with two wires or multi-junction array with four wires. Mica sheets (McMaster-Carr, Santa

Fe Springs, CA) were placed to create the gap between wires at the junction. Two 100 g weights were used to adjust the tension of the wire during soldering to withstand flow pressure. Each junction was functionalized with 5  $\mu$ L of streptavidin (from *Streptomyces avidinii*, Sigma Aldrich, St. Louis, MO) for 5 min and then the droplet of streptavidin was removed. Subsequently, 5  $\mu$ L of biotinylated polyclonal antibodies specific for *E. coli* (from rabbit, #PA1-73031, Thermo Fisher Scientific, Waltham, MA) and *S. aureus* (from rabbit, #PA1-73174, Thermo Fisher Scientific, Waltham, MA) antibodies was applied to junctions for another 5 min. Each biosensor chip was prepared for each targeted analyte. Functionalized bio-nano junction sensor was dried and stored at refrigerator before use for cell detection.

### **5.2.2. Microbial preparation**

Frozen stock cultures of *E. coli* K12 and *S. aureus* were obtained from the Food Microbiology Lab, University of Hawaii. 100  $\mu$ L of each stock was inoculated separately in 10 mL of tryptic soy broth (BBL™ Trypticase™ soy broth, BD diagnostic systems, Franklin Lakes, NJ) and incubated for 24 h at 35°C. Three milliliters aliquots of cultured bacteria was put into conical tube and centrifuged at 8,000 rpm for 10 min. After the supernatant was removed, the pellets were washed with phosphate buffer saline at twice and with distilled water by centrifuging at 6,000 rpm for 5 min per each washing step. The resulting pellets were suspended in 30 mL of sterilized 0.1 % peptone water (Bacto™ Peptone, BD diagnostic systems, Franklin Lakes, NJ) by autoclave. Then, bacteria suspension was serially diluted in the peptone water to obtain varying concentrations of each organism for target sensing experiments. For microbial cocktail sample, individual resulting pellets from both bacterial cultures using same procedure above were added to the peptone water at once and serially diluted to prepare 10-fold sample

cocktail dilutions. Standard plate counting method on plate count agar (Difco™ Plate count agar, BD diagnostic systems, Franklin Lakes, NJ) was used to determine the initial concentrations of *E. coli* and *S. aureus* stock cultures. The initial concentrations of *E. coli* and *S. aureus* in culture were  $2.0 \times 10^9$  CFU/mL and  $2.1 \times 10^9$  CFU/mL, respectively. All experiments were conducted in a certified Biosafety Level II laboratory.

### **5.2.3. Continuous flow detection**

The fabricated biosensors for detection of bacteria were placed in fluidic channel perpendicular to the flow direction (Figure 5.1 (b)) and fixed by two acrylic boards with fasteners. Stepping tubing connectors (4.7 mm to 9.5 mm in diameter, Bel-art product, Pequannock, NJ) were embedded onto the center of acrylic boards (Figure 5.1 (c)). Two silicone gaskets (1.6 mm thick, McMaster-Carr, Santa Fe Springs, CA) were used to prevent liquid from leaking. Pure serial diluted samples or microbial cocktail sample was continuously pumped into the detection zone with a syringe pump (KDS 100, KD Scientific Inc., Holliston, MA) at a flow rate of 0.0167 mL/s. The bacterial suspension was filling the upward tube (4 mm in diameter) with a 30° angle. The biosensors were connected to multiplexing circuit, which was composed of a power source to generate 1 V<sub>DC</sub>, a switch and a picoammeter (6485, Keithley, Cleveland, Ohio, USA) to measure the current at the 4 junctions in real-time. The electric current readings were collected for 1 min when 1 mL of the injected sample solution fully reacted with the sensing junction. Then the valid data set was selected when the readings reached the steady state. To compare the sensor characteristics between the continuous flow and stationary junction sensors, 10 µL of 1 of serial diluted *E. coli* solutions ( $10^4$  CFU/mL) was applied to the junction for 1 min to permit full antibody-antigen reactions (Yamada et al., 2014). Then, the junction was rinsed

with distilled water for elimination of nonspecific binding *E. coli*, and the current value was measured in the existence of 1 droplet of 10  $\mu$ L of distilled water.

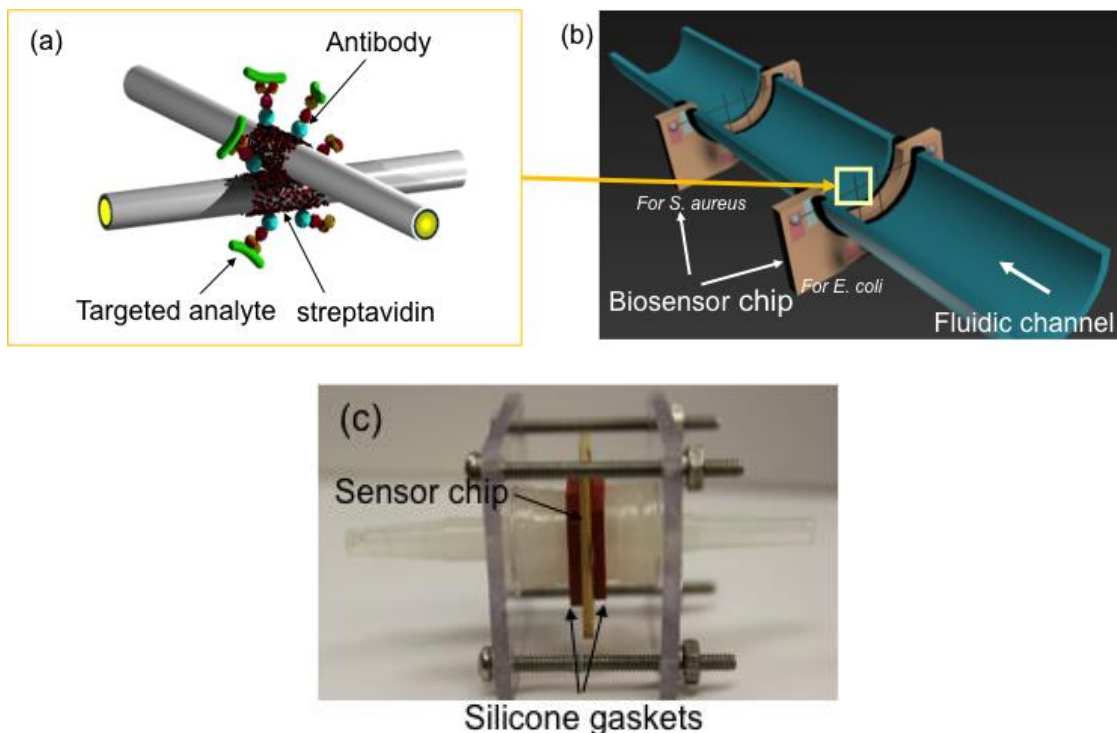


**Figure 5.1** A continuous flow multi-junction sensor device. (a) Illustration of bio-nano functionalized junction (Yamada et al., 2014). (b) Conceptual design of multi-junction biosensor for multiplexed detection in a continuous flow mode (cross sectional view), (c) Individual sensor chip ready to use

#### 5.2.4. Sensitivity and selectivity test

The sensitivity of the multi-junction sensor was evaluated using pure serially diluted *E. coli* and *S. aureus* cultures with the concentrations of  $10^2$ - $10^5$  CFU/mL. Single anti- *E. coli* functionalized multi-junction sensor chip was installed in the fluidic channel and tested for specific with  $10^2$ - $10^5$  CFU/mL of *S. aureus* solutions. The selectivity test for anti-*S. aureus* functionalized sensor was conducted in presence of pure *E. coli* K12 solutions. Two biosensors

for each targeted analyte were placed inside the channel to evaluate the multiplexed sensing to simultaneously detect *E. coli* and *S. aureus*. Mixed cultures of *E. coli* and *S. aureus* were applied to sensing area and current values were measured. Sterile 0.1% peptone water was used as negative controls

### 5.2.5. Data analysis

The current values measured at each of four junctions were averaged to obtain a representative current ( $I$ ) measurement for one sensor chip. The  $\Delta I$  signal response was determined by calculating the difference between the electrical current output of the negative control ( $I_{\text{antibody}}$ ), and that of the sample ( $I_{\text{antibody-bacteria}}$ ), as given by

$$\Delta I = | I_{\text{(antibody-bacteria)}} - I_{\text{(antibody)}} | \quad (5.1)$$

Statistical analysis was conducted based on the Duncan's multiple range tests using a single factor analysis of variance (ANOVA) offered by Statistical Analysis Software (SAS version 9.4, SAS Institute Inc., Cary, NC). The bacterial concentration dependence of the biosensor responses was statistically different at 95 % confidence level ( $p \leq 0.05$ )

## 5.3. Results and discussion

### 5.3.1. Detection *E. coli* K12 with a single junction sensor in a continuous flow mode

A Single junction biosensor was evaluated for continuous flow detection of *E. coli* K12 in a microfluidic channel. Before the flow head of the microbial solution reached the junction, there was no electric signal change because the gap between the microwires was open. An electrical signal response was obtained when the solution filled the junction zone. The signal amplitude decreased as the solution passed through the channel; eventually, the observed current

values were at equilibrium after 1 min measurement (Figure 5.2). The reaction time required for signal stabilization was consistent with our former study at the batch-sensing mode (Yamada and others 2014).

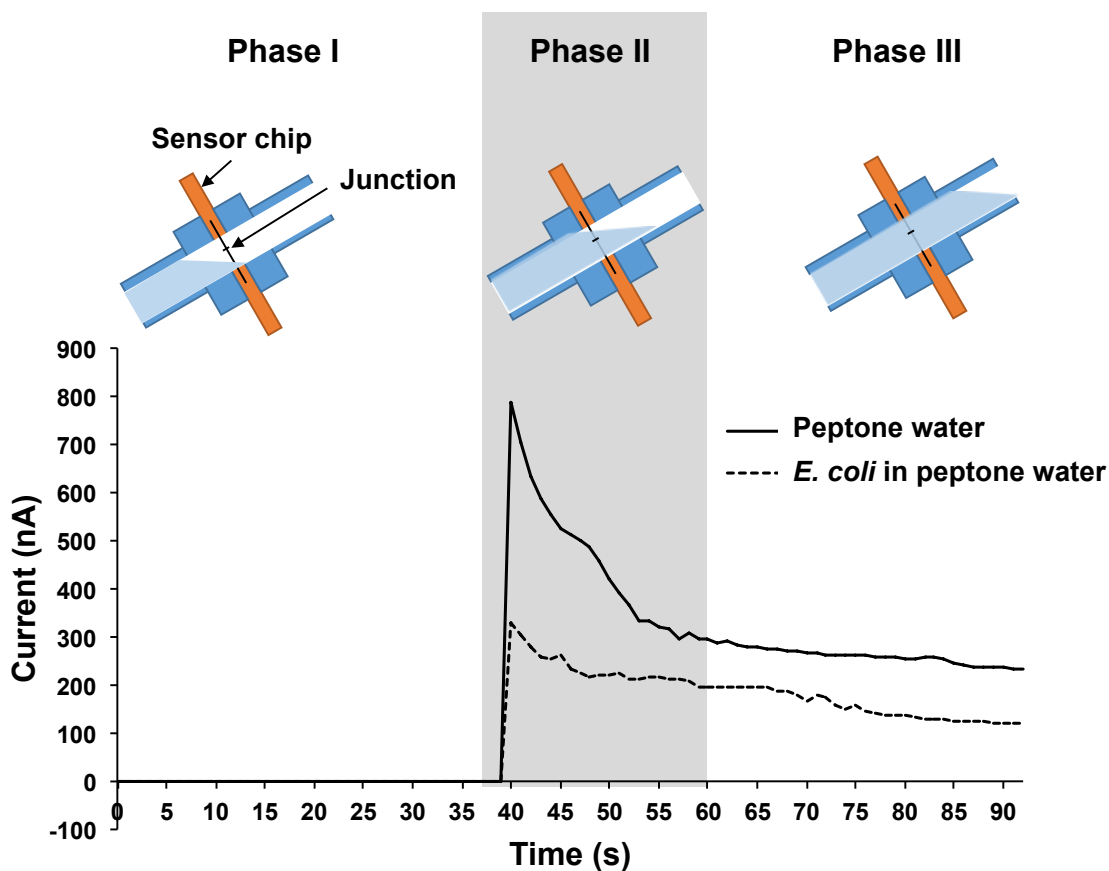


**Figure 5.2** A current change profile of the continuous flow junction sensor for pure peptone water (solid) and *E. coli* K12 suspended in peptone water (dot) in Phase I (when the junction was open), Phase II (when the junction met the flow head) and Phase III (when the antigen-antibody reaction fully developed). The concentration of *E. coli* K12 suspended was  $10^4$  CFU/mL.

The performance of the continuous flow junction biosensor was compared with the stationary junction biosensor equipped with one sample-holding platform (Figure 5.3(a)). Since different volumes of bacterial solutions were used, bacterial cell counts applied at the junctions



in both detection modes were estimated by Lu et al. (2013) equation. The change in the current was 75.1 nA when *E. coli* suspension with 3 log CFU cell counts was applied to the stationary junction sensor. However, the continuous flow junction sensor in the fluidic channel required only 2 log CFU cell counts to obtain the equivalent magnitude (75.5 nA). It is noted that bacterial loads needed for equivalent current outcomes were reduced by a factor of 10 when the continuous flow sensor was used. The continuous flow-sensing mode appears to reduce the likely steric hindrance between analytes (*E. coli* cells) and transducer (functionalized junction) by allowing bacterial cells to continuously flow over the surface of microwire immobilized with antibodies. A linear trend for the current changes was observed as *E. coli* concentration increased from  $10^2$  to  $10^5$  CFU/mL ( $R^2 = 0.988$ ) and was consistent with the trend observed in the stationary junction sensor (Yamada et al., 2014). Therefore, the signal enhancement and the limit of detection (LOD) as  $10^2$  CFU/mL for *E. coli* cells were achieved using the developed junction biosensor in a continuous flow mode.

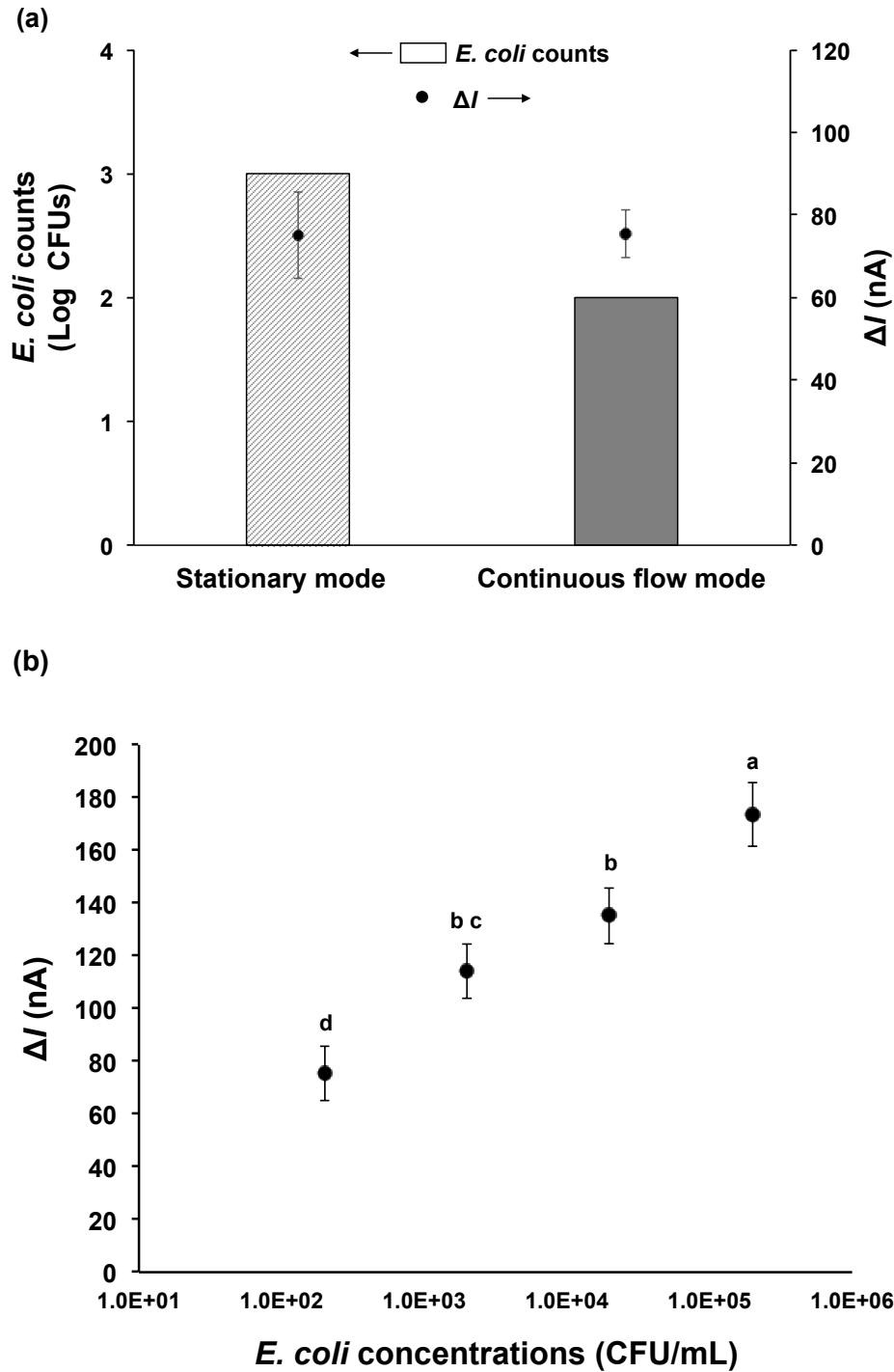


**Figure 5.3** Sensing signal enhancement of a continuous flow junction sensor vs. a stationary sensor on the basis of the equivalent current reading (75 nA): (a) Increase of the sensing sensitivity by a factor of 10 and (b) Current changes of the continuous flow sensor with *E. coli* K12 in the range of  $10^2$ - $10^5$  CFU/mL

### 5.3.2. Sensitivity and selectivity of multi-junction sensors

Electrical signal responses in multi-junction sensors targeted for each microorganism were shown in Fig. 5.4 (a) and (b). When *E. coli* suspension was flowed in channel, sensor functionalized with anti-*E. coli* was responded with a linear trend ( $R^2 = 0.994$ ) in current change values as the *E. coli* concentrations increase in range of  $10^2$ - $10^5$  CFU/mL. The  $\Delta I$  values were calculated from 246.2 nA to 493.2 nA. However, current changes in anti-*S. aureus* functionalized sensor against *E. coli* were shown between 17.8 nA to 29.7 nA, which might be attributed to background noise and nonspecific binding of *E. coli* on the junction. The sensitivity and selectivity tests of the sensor functionalized with anti-*S. aureus* were conducted using the *S. aureus* suspension flow. The anti-*S. aureus* multi-junction sensor demonstrated a linear relationship ( $R^2 = 0.978$ ) between the  $\Delta I$  value and concentrations of *S. aureus* suspension in the range of  $10^2$  to  $10^5$  CFU/mL. The  $\Delta I$  value obtained from the anti-*S. aureus* junction sensor ranged from 86.1 to 240.8 nA, whereas the  $\Delta I$  value obtained from the anti-*E. coli* sensor in the presence of interfering *S. aureus* was as low as 12.5 to 34.1 nA. Therefore, the detection limits of both anti-*E. coli* anti-*S. aureus* junction sensors were as low as  $10^2$  CFU/mL and the sensing selectivity were fully validated. The positive false results from the selectivity tests could imply that interfering non-target bacteria might latch onto the nonspecific region of the sensing junction. However, the signals were as low as 20 to 30 nA and there were no significant sensing differences for various concentrations of interfering bacteria. The magnitudes of  $\Delta I$  values observed in the multi-junction sensor were greater than those from the single junction. The  $\Delta I$  values in the single junction for detection of *E. coli* were between 75.5 and 173.5 nA, one-third of the values obtained from the multi-junction sensor. The reason might be due to enhanced

sensing areas and accordingly more frequent antigen–antibody binding reactions permitted in the multi-junction sensor.

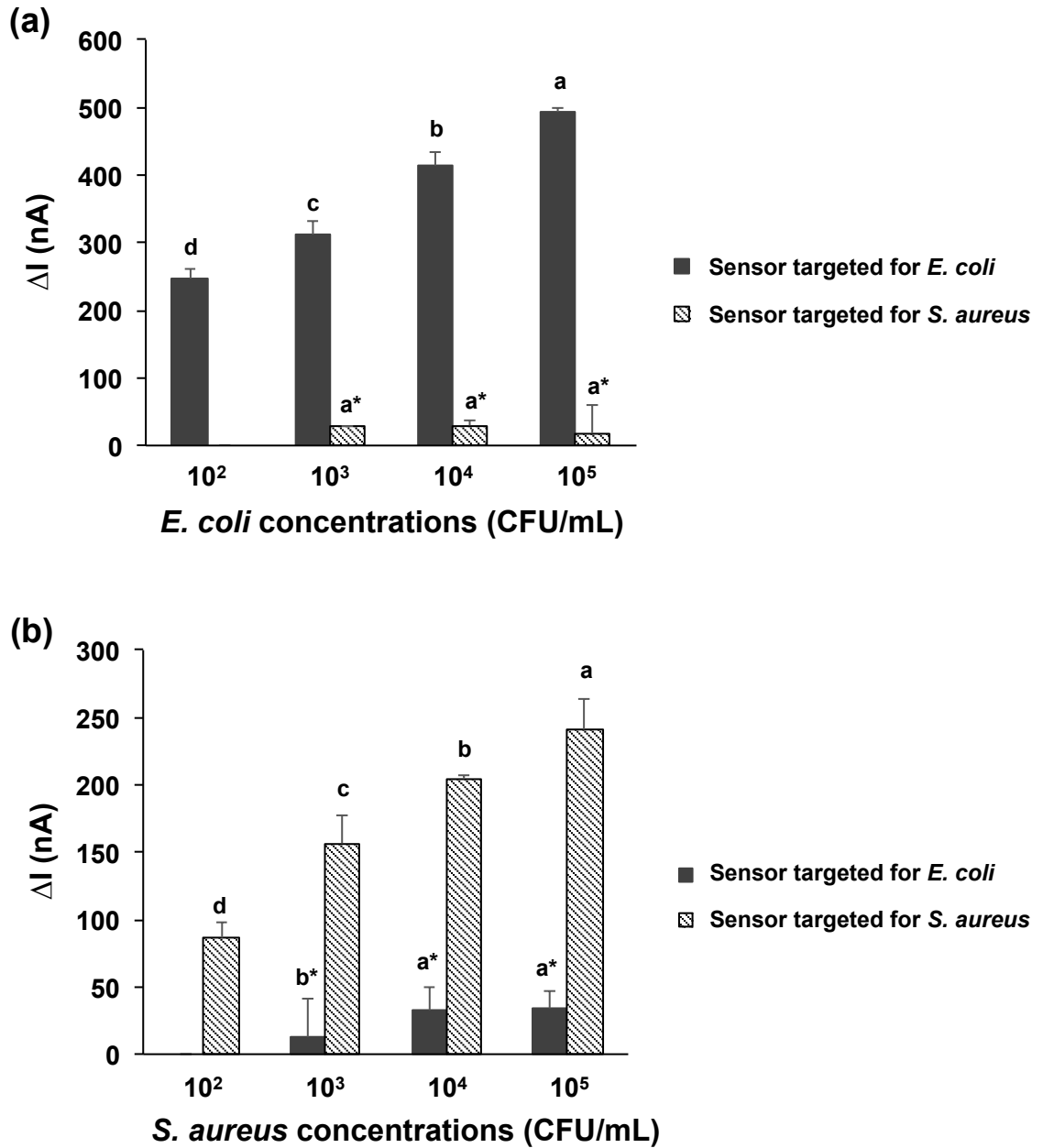


**Figure 5.4** Specificity testing for the developed sensors functionalized with anti- *E. coli* (a) and *S. aureus* (b): Microbial concentrations ranged from  $10^2$  to  $10^5$  CFU/mL.

### 5.3.3. Simultaneous detection of *E. coli* K12 and *S. aureus*

The cocktail samples in the presence of *E. coli* and *S. aureus* at the equal concentrations were used to investigate the response of the multi-junction sensor for simultaneous bacteria detection. Figure 5.5 (a) and (b) shows the  $\Delta I$  values obtained from the sensors targeted for *E. coli* and *S. aureus* in the cocktail solutions. Both bacteria were equally (1:1 mixing ratio) mixed at the concentrations ranging from  $10^2$  to  $10^5$ . The  $\Delta I$  values increased as the concentrations of microorganisms increased due to more analytes landed on the bio-nano modified surface. Both sensors showed similar measurement trends with a linearity between  $\Delta I$  and bacterial concentration ( $R^2$  values of 0.932 and 0.988 for *E. coli* and *S. aureus*, respectively). However, the magnitudes of current responses obtained from mixed bacterial samples were higher than those from pure samples. The anti-*E. coli* functionalized sensor responded the change in current with 413.5 nA to pure solution but calculated 438.1 nA current difference for mixed solution at cell concentrations of  $10^4$  CFU/mL. This phenomenon observed for anti-*S. aureus* functionalized sensor that the electrical signal was 204.3 nA in pure *S. aureus* suspension, but the signal was changed to 431.1 nA in presence of *E. coli* at the concentrations of  $10^4$  CFU/mL for both analytes. These signal shifts might be due to the attachment of nonspecific binding bacteria at the sensor surface. The developed continuous flow biosensors showed a great potential for single step multiplexed detection of bacteria.

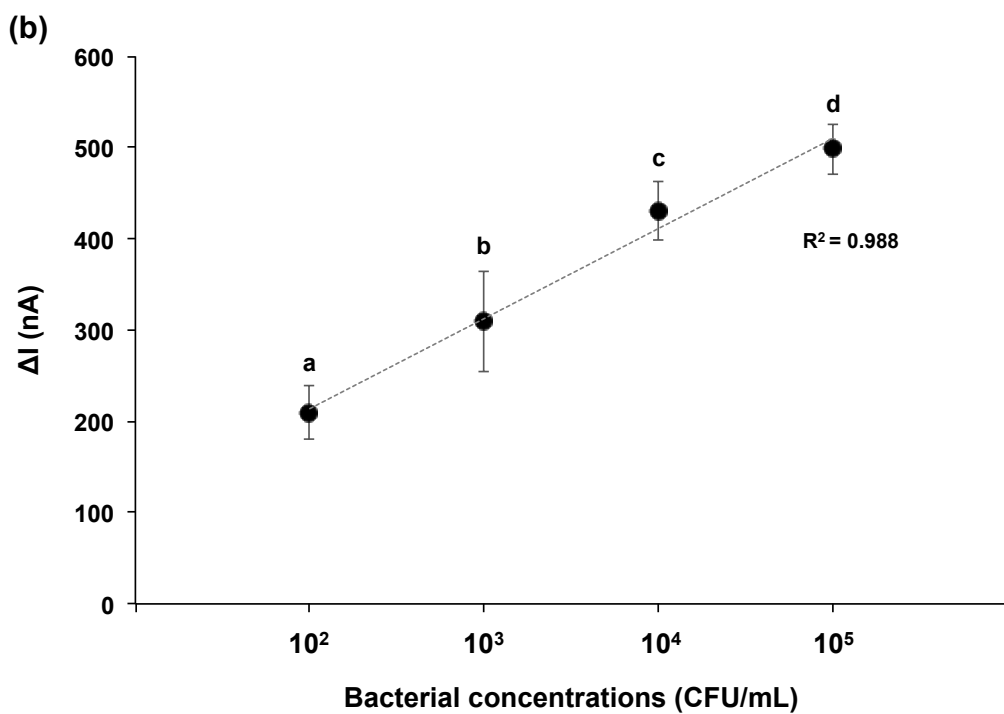
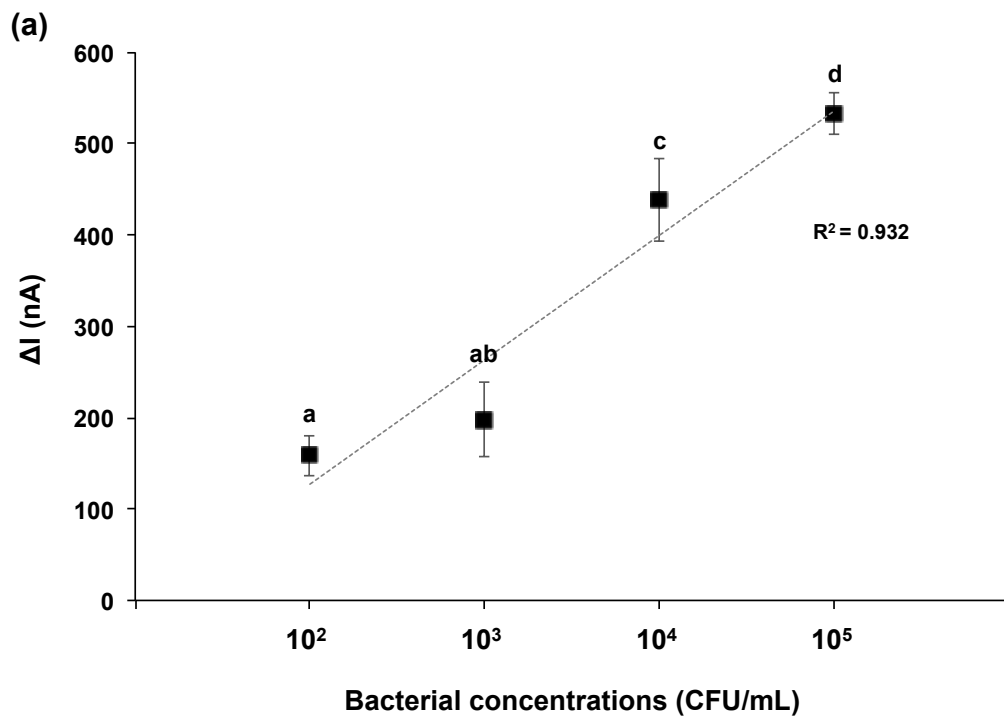


**Figure 5.5** Electrical signal responses of multi-junction sensors specific for *E. coli* K12 (a) and *S. aureus* (b) when mixture samples of *E. coli* K12 and *S. aureus* were used.

#### 5.4. Conclusion

The limits of detection for pure and mixed microbial samples were achieved in range of  $10^2$  to  $10^5$  CFU/mL with a detection time of 2 min. The developed sensing device provided sensitive and selective detection of *E. coli* K12, and *S. aureus* with a flow rate at 1 mL/min. The continuous flow multi-junction platform showed a potential for rapid and multiplexed detection of different pathogens with large volume (minimum 1 mL) in comparison to the stationary junction sensor (10  $\mu$ L). This sensing method can be applied for food safety and quality testing with advantageous rapidity and portability. The sensor was tested for liquid samples in this study but it could be applied for bacterial detection in solid samples including semi-solid or colloid if followed by pretreatment steps, that is dilution and filtration of large particles. Future study will include the establishment of minimum preparation methods for real food samples. The sensor performance will be enhanced by application of electric field; for example, dielectrophoresis (DEP) force to enable viable cells to concentrate toward the junctions, and development of durable and reusable multi-junction chips in the future.

## Chapter 6.

### **Flow-based dielectrophoretic biosensor for detection of bacteriophage MS2 as a foodborne virus surrogate**

#### **ABSTRACT**

A flow-based dielectrophoretic biosensor was designed as a proof-of-concept for detection of foodborne pathogenic viruses and tested using bacteriophage MS2 as a norovirus surrogate. The flow-based MS2 sensor has two main components: a detector and a concentrator. The detector is functionalized with polyethylenimine (PEI), single-walled carbon nanotubes (SWCNTs), anti-MS2 IgG, and bovine serum albumin (BSA). The concentrator is an interdigitated electrode array designed to impart DEP effects to manipulate viral particles toward the detector. The fluidic channel and the electrode-supporting layer are made of polydimethylsiloxane (PDMS) layers. The detector is positioned at the end of the fluidic channel and is supplied with an electrical current for purpose of measurement. Serially diluted MS2 suspensions were continuously injected into the fluidic channel at a 0.1mL/min. A cyclic voltammogram indicated current measurements regarding PEI-SWCNTs electrodes increased when in comparison with PEI film surface electrodes. In addition, a drop in the current measurements after antibody immobilization and MS2 capture was observed with the developed electrodes. Antibody immobilization on the biorecognition site provided higher current changes with the antibody-MS2 complexes vs. the assays without antibodies. The electric field applied to the fluidic channel at 10 V<sub>pp</sub> and 1 MHz, contributed to increase of current changes in response to MS2 bound on the detector. The change in current signals presented dependence to the concentrations of MS2 in the sample solution.



## 6.1. Introduction

Concerns pertaining to food safety have emerged worldwide due to its close relation with human safety and health (Neethirajan et al., 2017). Among food safety hazards, harmful bacteria and viruses cause food poisoning in human by infection or intoxication. Viruses are considered, as one of the most infectious pathogens in food industry due to their greater resistance to treatment and the smaller doses required causing infection. According to the U.S Center for Disease Control and Prevention, most foodborne illnesses are caused by viruses (59%) followed by bacteria (39%), and by parasites (2%). An estimated annual 9.4 million U.S acquired foodborne illnesses are due to 31 known pathogens (Scallan et al., 2011). Pathogenic viruses responsible for foodborne illness are norovirus, hepatitis A and E, rotavirus, sapovirus, and astrovirus. Noroviruses are responsible for 58% of viral gastroenteritis, winter diarrhea, and acute non-bacteria gastroenteritis. They are also responsible for approximately 15,000 cases of hospitalizations and 150 deaths within the United States annually (Scallan et al., 2011). The cost of foodborne norovirus is estimated to be \$ 2.3 billion per year due to deaths, non-hospitalized cases, and hospitalizations in the United States (Hoffmann, 2015). Infection by norovirus is possible even with virus concentrations smaller than 100 copies/mL. It is difficult to prevent noroviruses from contaminating water or foods due to their environmental stability. Noroviruses have been reported to survive up to 10 ppm chlorine, freezing conditions, and temperature of 60 °C (Patel et al., 2009). The potential biological threats to our health and economy emphasize the significance of developing new pathogen monitoring and detection methods.

Pathogenic viruses are transmittable through a variety of routes, including contact with an infected person, contaminated food, water, or surface. Many efforts have been made by food regulatory agencies and manufacturers to minimize the risks for foodborne illnesses, for

example, practicing proper hand hygiene, washing and processing fruits, vegetables and shellfish thoroughly, and cleaning the contaminated surfaces (FDA, 1997; Stannard, 1997). However, the occurrence of virus related contamination is still alarmingly prevalent as described above. Currently there are no detection and identification practices for viral hazards prior to the consumption and use of contaminated water or foods. Most diagnostic tests are only made after an outbreak has occurred. If norovirus can be preemptively identified, the infection can be blocked from spreading in public place (Hong et al., 2015).

Viral detection in a sample has challenges because the viruses are naturally small in size, particles range within 10-100 nm and cannot be seen with a standard light microscope. As a result, virus identification usually requires a specific host cell for replication and identification (Caygill et al., 2010). Current detection or diagnosis methods for viruses are made with observation of viral particles in solution using transmission electron microscope (TEM); with measurement of virus infectivity through the plaque assay and tissue culture infective dose assay (TCID<sub>50</sub>); or with assessment of viral protein antigens or gene expressions through hemagglutination assay, single radial immunodiffusion (SRID), enzyme-linked immunosorbent assay (ELISA), and polymerase chain reaction (PCR) (Cheng et al., 2009; Pankaj, 2013). Some tests such as TEM and the plaque assay have been widely used as standard methods for determining the quantity of virus for many decades, but they are time and labor intensive, as well as prone to show high variability in the results due to operator error. More modern methods such as ELISA and PCR are faster and give more precise and reproducible data than traditional methods (Pankaj, 2013). The highest sensitivity for virus detection is achieved with PCR based assays for detection of amplified viral DNA and RNA (Rabenau et al., 2003). However, these techniques required multiple pretreatment steps causing long assay time of up to 24 hours, in

addition specialized equipment and technical expertise makes the assay based detection expensive and non-field-deployable (Bally et al., 2013).

Biosensor technologies have been proposed to be a more accurate and faster alternative in viral detection, with less complicated sample preparation steps (Cheng et al., 2009). Electrochemical biosensors detect changes by the biological recognition events such as viral antigens binding to specific antibodies placed on the bioreceptor, which can be converted into a quantitative amperometric, potentiometric, or impedimetric signal (Caygill et al., 2010). These sensors can be used to detect and enumerate intact virus, viral proteins, and nucleic acids but the strategy for direct detection of whole virus particles has the advantages of operational simplicity and cost-effectiveness in viral diagnostics (Cheng et al., 2009). Hong et al. (2015) developed a sensitive (35 copies/mL), selective (98%), and rapid (1h) electrochemical biosensor for detection of noroviruses. The proposed electrochemical biosensor is designed around a nanostructured gold electrode conjugated with concanavalin A. The oxidation of alkaline phosphatase labeled secondary antibody generates current at the electrode that is proportional to the amount of norovirus bound to the sensor surface. An electrochemical immunosensor lab-on-chip immobilized with five-types of hepatitis (A, B, C, D, and E) virus antibodies was developed for the simultaneous detection of five-type hepatitis virus antigen with a one-step capture format (Tang et al., 2010). The detection is based on the potential change by the antigen and antibody reaction at each detection site. The sensor array can detect most analytes lower than 1.0 ng/mL within 5 min. A label-free electrochemical immunosensor has been shown to detect rotaviruses using gold sononanoparticles immobilized with antibodies (Attar et al., 2016). The detection process of the rotavirus involved measurements of electron transfer resistance at electrode surface, which showed a relationship between measured impedance changes and various

rotavirus loads in the range of 4.6 to  $4.6 \times 10^4$  PFU/mL. Attar et al. determined a detection limit of 2.3 PFU/mL with a total assay time of 55 min was possible using their developed biosensor.

Recent advances in microfabrication and nanotechnology have contributed to the miniaturization and automation of biosensor devices with improved sensitivity. Dielectrophoretic (DEP) microdevices has generated growing interest for bioparticle manipulation and separation over the past decade (Li et al., 2014b). Bioparticles such as DNA, proteins, bacteria, viruses, mammalian, and yeast cells can travel toward a specific position when subjected to DEP forces. DEP application in selective analysis of biological samples is possible because particle movement caused by DEP forces are dependent upon on particle structure, morphology, and electrical properties. In addition, DEP forces are further manipulatable by regulating the applied electric field strength, frequency, and electrical conductivity of the suspending medium. The spatial electric field gradients required for DEP effects can be generated by a number of configuration and structure regarding electrodes design and placement within a fluidic channel or sample vessel. Better electric field distribution and control of particle motion can be achieved with modern microfabrication techniques when constructing microelectrode arrays and microfluidic channel (Li et al., 2014b). Nanomaterials have begun to play an important role in biosensor design for viral diagnostics. Nanomaterials, such as graphene, carbon nanotubes, quantum dots, and metal nanoparticles, can be used for isolation and capture of target viral particles from a sample and also can be used to enhance a desired measurement signal (Neethirajan et al., 2017).

The detection and separation studies of infectious norovirus remain a challenge due to lack of an in vitro cell culture systems or small animal models (Duizer et al., 2004). Therefore, some viral surrogates have been used to model the infectious nature of norovirus in a sample

(Bae & Schwab, 2008; Bozkurt et al., 2014; Chung et al., 2015; Yakes et al., 2013). The F-specific bacteriophage MS2 has frequently been used as a surrogate for human enteric virus studies concerning compounds for disinfecting surfaces in investigating environmental transport and fate (Dawson et al., 2005; O'Connell et al., 2006). Bacteriophage MS2 has similar composition, morphology, size, and site of replication to human norovirus, making it an attractive substitute for food safety studies. Like noroviruses, MS2 is adapted to the intestinal tract, it is an icosahedral, positive sense single-stranded RNA virus, and in the same size range at 26 nm in diameter. Also, it has the similar electrical charge and characteristics to norovirus; thus it is used as a model within virus DEP application studies.

In this study, a flow-based dielectrophoretic biosensor was designed and fabricated as the proof-of-concept for rapid and direct detection of norovirus in a sample. Bacteriophage MS2 was used as the norovirus surrogate to evaluate the proposed sensor's performance. The biosensor device consisted of a detector, which is coated with single-walled carbon nanotubes (SWCNTs) immobilized with antibodies, and a concentrator. An interdigitated electrode array for DEP manipulation of viral particles toward the detector was also fabricated. Both components were embedded into supporting materials with electrical connections.

## **6.2. Materials and methods**

### **6.2.1. Materials**

Polydimethylsiloxane (PDMS; Sylgard 184 silicone elastomer curing agent and base) was ordered through Dow Corning (Midland, MI). MG Conductive silver epoxy (# 8331) was purchased from Vetco Electronics (Bellevue, WA). Carboxylic acid functionalized SWCNTs (SWNT PD1.5L COOH) was manufactured from NanoLab, Inc. (Waltham, MA).

Polyethylenimine (PEI, branched, average Mw ~ 25,000), N, N-dimethylformamide (DMF), MES (#M-3671) and bovine serum albumin (BSA; #A3294) were purchased from Sigma Aldrich (St. Louis, MO). 1-ethyl-3-[3-dimethylaminopropyl]carbodiimide hydrochloride (EDC, #22980) and *N*-hydroxysuccinimide (NHS, # 24500) were supplied from Thermo Fisher Scientific (Waltham, MA). Polyclonal antibody rabbit anti-MS2 IgG was provided from Tetracore Inc. (Gaithersburg, MD). BBL™ tryptic soy broth (TSB), agar powder, and phosphate buffered saline (PBS) tablets were purchased from VWR (West Chester, PA).

### **6.2.2. Biosensor device fabrication**

The device consisted of a PDMS top and bottom structure with fluid channel and an electrode array, respectively. The molds for PDMS structures were designed using SolidWorks (Dassault System Solidworks Corp., Waltham, MA) and printed with a 3D printer (Form 2, Formlabs, Somerville, MA) using standard resin. The printed molds were washed several times under isopropyl alcohol bath and dried at room temperature overnight. The surface of the mold was cured under UV light for one hour. Silicone elastomer curing agent and base were mixed with a ratio of 1:10 and poured into the mold until the channel and electrode guidelines were fully submerged. The molds filled with semi-solid PDMS mixture were placed in the vacuum chamber to remove the bubbles inside and then baked at 65°C for 1 h. The solidified PDMS layers were peeled off the mold. The negatively printed stations for electrical connections were filled with conductive silver paste and cured at 65°C for 20 min.

Figure 6.1 shows schematic drawing of the fluidic device, which consists of DEP generator and detector electrodes, and a photograph of fabricated device. There are 80-gaps negative DEP microelectrodes array exposed within the fluid channel. The electrode width was

800  $\mu\text{m}$  and the gap between adjacent electrode strips was 400  $\mu\text{m}$ . The width and height of the fluid channel were 1 mm and 100  $\mu\text{m}$ , respectively.

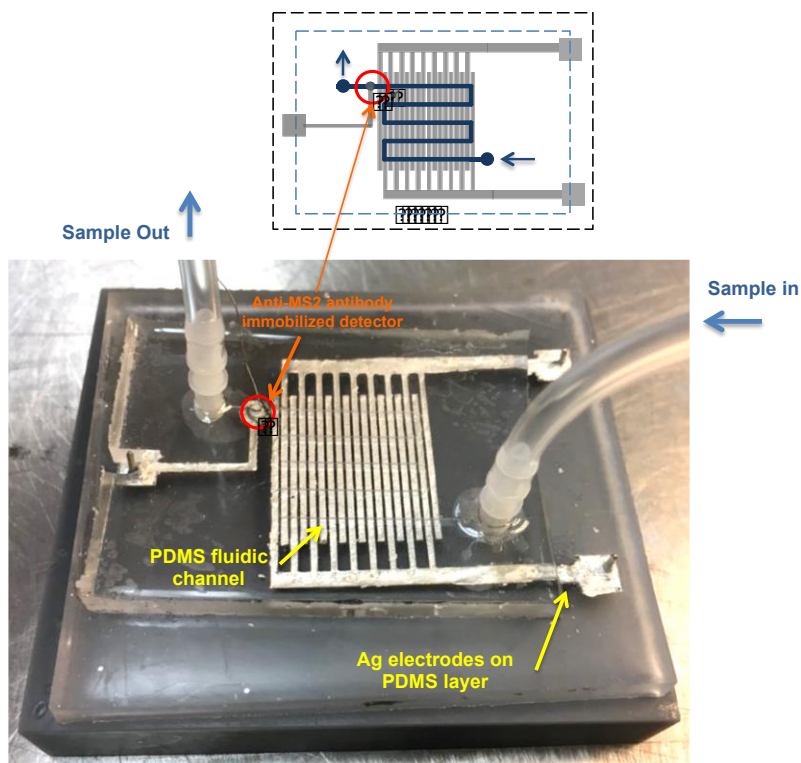


**Figure 6.1** A schematic of the fluidic device, which consists of the PDMS-fluidic channel (Blue), Ag electrode array for the DEP generator, and the anti-MS2 IgG immobilized on the SWCNTs coated electrode (Red). The fluid channel has 1mm of the width and 100  $\mu\text{m}$  of the height. The width of each strip of DEP generator electrode array was 800  $\mu\text{m}$ , and the gap between strips was 400  $\mu\text{m}$ .

### 6.2.3. Antibody immobilization on the detector

The detector was placed at the end of the fluid channel and was also filled with conductive silver paste. The anti-MS2 IgG was immobilized on the NHS-ester activated SWCNTs by covalent linking according to Gomes-Filho et al.'s procedure (Gomes-Filho et al., 2013) with slight modification. Ten mg of carboxylic acid functionalized SWCNTs were

dispersed in 5 mL of DMF by sonication under water bath for 2 h. The SWCNT-COOH suspension was activated with a mixture of 4 mM EDC and 10 mM NHS in 5 mL of 0.1 M MES buffer at room temperature for 1 h. Anti-MS2 IgG and BSA were individually diluted in 10 mM PBS solution (pH 7.2). The detector electrode was firstly coated with 3  $\mu$ L of 10% PEI in ethanol and dried at 65 °C for 20 min. NHS-ester activated SWCNTs (3  $\mu$ L) was dropped on the PEI film and dried at same temperature and time. An aliquot of 2  $\mu$ L anti-MS2 IgG (2.8 mg/mL) was placed on the surface of SWCNT-COO<sup>-</sup>/PEI/Ag and allowed the peptide coupling between the carboxyl group on SWCNTs and amine group on antibodies at 4 °C for 30 min. Unbound antibodies washed out with 0.01 M PBS solution. Then, antibody immobilized electrode was incubated with 3  $\mu$ L of 2% BSA solution at 4°C for 4 hours to block the non-specific binding sites where is not occupied by anti-MS2 IgG. Two layers were combined and placed in the refrigerator until use.

#### **6.2.4. Bacteriophage MS2 propagation**

An *E. coli* FAMP strain and MS2 cultures were obtained from Food Microbiology Lab at the University of Hawaii. An inoculant (100  $\mu$ L) of the frozen stock was transferred to 25 mL of TSB and incubated overnight at 37 °C. The culture amounting to 100  $\mu$ L was inoculated with another 25 mL of TSB and incubated at the same temperature for 3-4 hours until the optical density was between 0.2-0.3 at 600 nm, which is the value indicating the logarithmic growth phase. One mL of MS2 culture was added to *E. coli* FAMP culture and incubated overnight at 37 °C. The mixture of *E. coli* FAMP and MS2 was centrifuged at 6,000 rpm for 10 min, and the supernatant was filtered using a 0.2  $\mu$ m syringe filter to remove *E. coli* FAMP cells. The bacteria-free MS2 sample was serially diluted in 10 mM PBS.



### **6.2.5. Bacteriophage MS2 qualification by plaque assay**

The viable viral particle counts were determined by plaque counting method on double layer of 0.6% and 1.5% tryptic soy agar (TSA). 100  $\mu$ L of the *E. coli* FAMP cultures, which was in the logarithmic growth phase, was inoculated in the pre-melted 0.6% TSA tube and swirled in the water bath approximately 50 °C. After adding the equal amount of MS2 sample solution to *E. coli* FAMP contained TSA tube, they were mixed by rolling in the palm. The mixture was poured out in the pre-warmed 1.5% TSA plates. The plates were incubated at 37 °C for 24 h, and the plaques were counted.

### **6.2.6. Electrochemical measurement**

Cyclic voltammetry (CV) and electrochemical impedance spectroscopy (EIS) were used for characterization of the functionalized surface on the detector electrode. They were carried out using a  $\mu$ Autolab III/FRA2 (Metrohm Autolab USA Inc., Riverview, FL) controlled by NOVA 1.6 software. The CV experiment was conducted at a potential scan rate of 100 mV/s, the step height of 2.4 mV, and applied potential from 1V to -1V in an electrolyte solution consisting of 5 mM  $K_3Fe(CN)_6$ , 5 mM  $K_4Fe(CN)_6$ , and 0.1 M KCl. In the EIS measurement, a frequency range was from 0.1 to 100 kHz with a DC offset of 200 mV and AC amplitude of 10 mV in the same electrolyte solution.

### **6.2.7. Dielectrophoretic MS2 detection**

A syringe pump (Chemyx Inc., Stafford, TX) was used to induce flow rate 0.1 mL/mL. A function generator (3220A, Agilent Technologies, Santa Clare, CA) was applied to on the interdigitated Ag electrode array to produce the non-uniform electric field in the fluidic channel

with a voltage of 10 V<sub>pp</sub> and a frequency of 1 MHz. Figure 6.2 depicts strategy for MS2 capture on the biorecognition site using a negative DEP manipulation in the fluidic channel. Electrical current signal ( $I$ ) on the detector was measured using a picoammeter (6485, Keithley, Cleveland, Ohio, USA) with an applied voltage of 0.2 V. The background current measurement ( $I_{\text{antibody}}$ ) was conducted with 10 mM PBS. One mL of MS2 sample solution allowed passing through the detector. By flowing 1 mM PBS into the channel, the unbound MS2 particles washed out from the detector. The current signal after MS2 binding reaction ( $I_{\text{antibody-MS2}}$ ) was obtained in 10 mM PBS. The changes in current ( $\Delta I$ ) in response to MS2 capture on the detector was calculated as  $I_{\text{antibody-MS2}} - I_{\text{antibody}}$ .

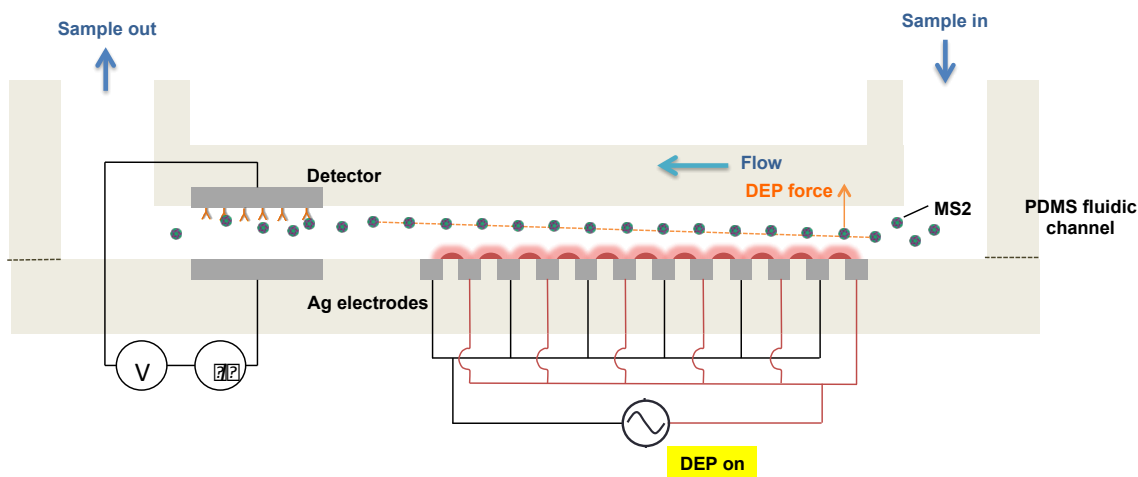


**Figure 6.2** A concept design for a negative DEP manipulation of MS2 particles to biorecognition site in the fluidic channel. The MS2 particles randomly react with antibodies when no DEP force applied. The MS2 experience the negative DEP force, which repel from higher electric field gradient, can travel toward the bottom of the fluidic channel and then bind to the antibody immobilized on the detector electrode.

### **6.2.8. Statistical analysis**

Data is collected from triplicate experiments reproduced on three separate MS2 dilutions. The mean and standard deviations of  $\Delta I$  were calculated for the serial dilutions of MS2 stock culture. The differences between the means were analyzed based on Duncan's multiple range tests using a single factor analysis of variance (ANOVA) offered by Statistical Analysis Software (SAS version 9.4, SAS Institute Inc., Cary, NC) at 95% confidence level ( $p \leq 0.05$ ). The independent sample t-test was conducted using a SPSS statistics 20.0 at 95% confidence level to compare the  $\Delta I$  means from the MS2 detection results with and without anti-MS2-IgG or DEP effect.

## **6.3. Results and discussion**

### **6.3.1. Characterization of SWCNTs-antibody functionalized surface and MS2 detection**

Unlike the antibody immobilization procedure by the non-covalent binding in previous studies, the MS2 antibodies were immobilized on the SWCNTs-COOH network via covalent bonding. Therefore, the surface modification process was characterized by CV and EIS measurement in the presence of the  $[\text{Fe}(\text{CN})_6]^{3-/4-}$  redox probe. Covalent bonding is one of the conjugation strategies for biological molecules, such as immunoglobulins, to CNTs structure (Venturelli et al., 2011). It has excellent stability, and better binding selectivity than non-covalent bonding due to the difficulty in dissociation of the biomolecules from the nanostructure (Fujigaya & Nakashima, 2015). The carboxyl group of oxidized CNT binds to the amine group of antibody through an amide linkage. The first layer of PEI is a highly cationic polymer, which contains a large number of amine groups reacting with the COOH groups of CNTs. Also, the PEI film can offer stable binding of CNTs to the electrode surface. The residues of COOH group on

CNTs can also link to  $\text{NH}_2$  group of the antibody resulting in the immobilization of antibody on the electrode. Figure 6.3 present cyclic voltammograms of PEI coated, PEI/SWCNTs surface and PEI/SWCNTs/anti-MS2-IgG/BSA coated Ag electrodes, and MS2 captured electrode. Cyclic voltammograms of the Ag/PEI/SWCNTs electrode showed an increase in the redox peaks in  $E_{pa} = -0.53 \text{ V}$  and  $E_{pc} = 0.3 \text{ V}$ . The voltammetry was decreased in the magnitude of redox peaks after antibody immobilization, followed by MS2 attachment.  $E_{pa}$  is the anodic peak potential reached when all of the substrates at the surface of the electrode has been oxidized, and  $E_{pc}$  is the cathodic peak potential achieved when all of the substrates at the surface of the electrode has been reduced.

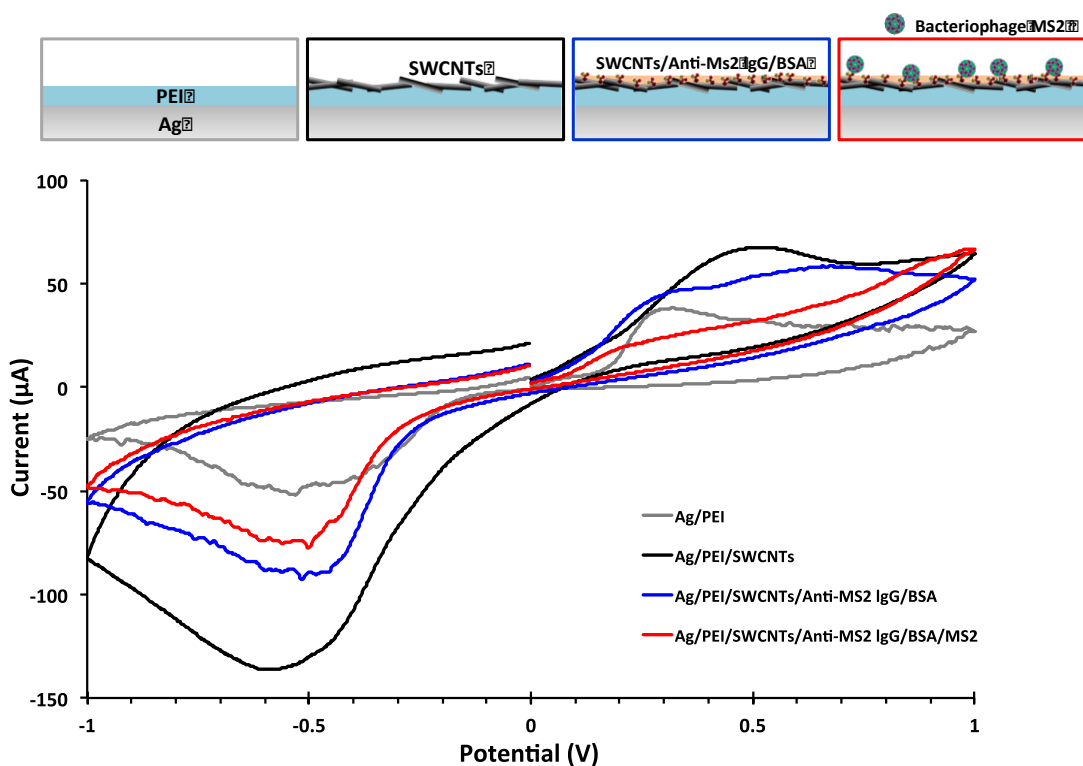


**Figure 6.3** Cyclic voltammograms of the detector in each modification step when the potential ranged from 1V to -1V at a scan rate of 100 mV/s in an electrolyte solution consisting of 5 mM  $\text{K}_3\text{Fe}(\text{CN})_6$ , 5 mM  $\text{K}_4\text{Fe}(\text{CN})_6$ , and 0.1 M KCl.

The increase in the redox current peaks by incorporation of CNTs into PEI networks can be explained by the CNTs natural high conductivity which leads to a higher electron transfer to the electrodes, imparting an enhanced conductivity at sensor surface (Zeng et al., 2006). The addition of biomolecules and MS2 particles contributed to reduction in the redox peaks due to their insulating properties that can prevent the load diffusion to the electrode surface (Yun et al., 2007).

The electrochemical impedance spectra of the modified electrode are shown in Figure 6.4. The diameter of the semicircle indicates that the electron transfer resistance was reduced by SWCNTs functionalization and gradually enlarged after antibody immobilization and MS2 attachment to the electrode. This result agrees with the changes in peak current in CV measurement. When the data was applied to Nyquist plots fitted with a Randle's equivalent circuit model (Figure 2.2), Ag/PEI electrode exhibits a high electron transfer resistance ( $R_{et}$ ) of about 24.0 k $\Omega$ . The SWCNTs layer affects the reduction in  $R_{et}$  value of Ag/PEI/SWCNTs electrode to 5.04 k $\Omega$ , which corresponds to increased redox peaks. As further modification and MS2 capture progressed, the  $R_{et}$  values were increased from 7.30 k $\Omega$  for Ag/PEI/SWCNTs/anti-MS2-IgG/BSA electrode to 8.99 k $\Omega$  for Ag/PEI/SWCNTs/anti-MS2-IgG/BSA/MS2 electrode.

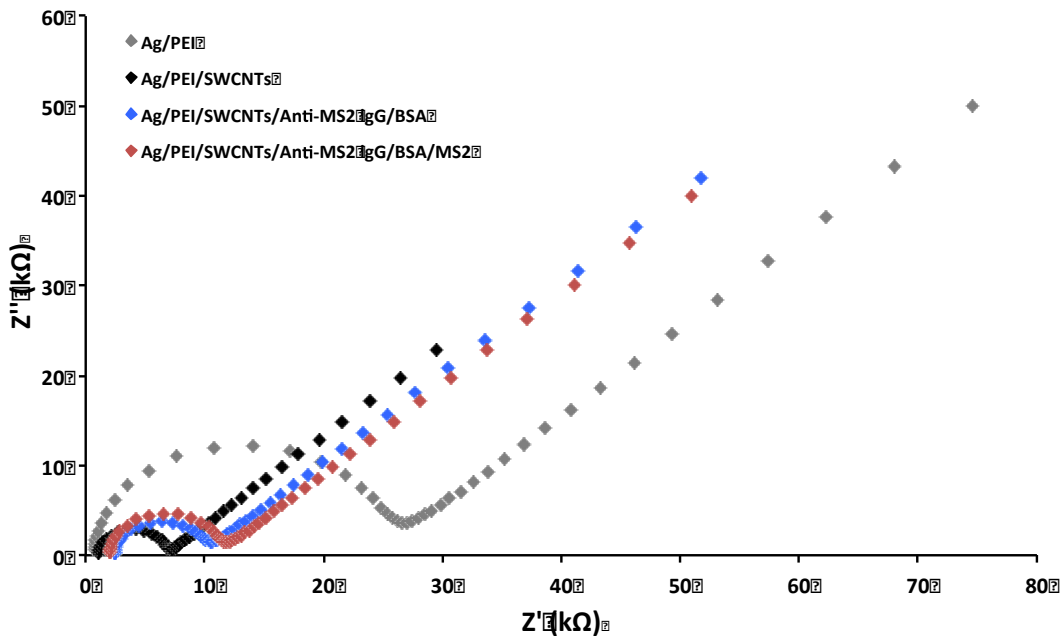


**Figure 6.4** Impedance spectra corresponding to each modification step on the detector electrode in the presence of 5 mM  $[\text{Fe}(\text{CN})_6]^{3-/4-}$  as a redox probe.

Some studies for electrochemical characterization regarding SWCNTs functionalized electrode showed a similar trend to the results in this study (Gomes-Filho et al., 2013; Weber et al., 2011). The enhanced current and decreased charge transfer resistance values by CNTs modification and shifts of the electrical signals by addition of biological molecules were observed.

Figure 6.5 indicates the effect of anti-MS2-IgG on the change in the current in response to the MS2 attachment on the detector. The detector electrodes with and without anti-MS2-IgG were incubated with the MS2 solution containing a concentration of around  $10^{10}$  PFU/mL. Averaged change in current values was observed to be  $0.438 \pm 0.130 \mu\text{A}$  in the absence of the anti-MS2-IgG on the surface of detector electrode. The averaged  $\Delta I$  of immunosensor dramatically increased to  $2.806 \pm 0.470 \mu\text{A}$ . However, this study's primary objective was to verify immunosensing between antigen and antibody immobilized on the SWCNTs modified

electrode in a new device. Therefore, further research including antibody titration and optimization of the functionalization parameters should be conducted.

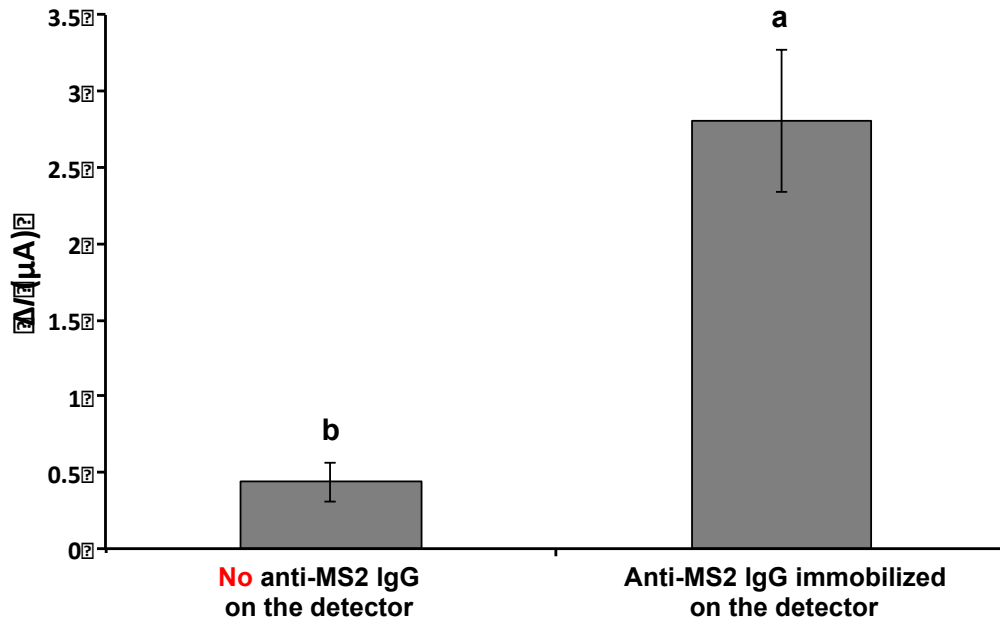


**Figure 6.5** Change in current in response to captured MS2 on the detector with and without MS2 antibody on the surface of detector electrode. The electrical current responses were measured with 10  $\mu\text{L}$  of MS2 solution ( $\sim 10^{10}$  PFU/mL) on the detector in stationary mode. Means with different letters are significantly different at 95% confidence level.

### 6.3.2. Effect of DEP concentration on change in signal response

Figure 6.6 shows the result of  $\Delta I$  with and without the proposed DEP concentration stage applied with MS2 solution concentration of  $\sim 10^7$  PFU/mL. The average  $\Delta I$  after DEP concentration was  $0.930 \pm 0.182 \mu\text{A}$  that is approximately 1.5 times higher without DEP applied. Hamada et al. (2013) studied bacterial detection using both positive and negative DEP. The *E. coli* cells moved toward the impedance detector following negative DEP forces. The peak value of conductance with the nDEP concentration was roughly two times higher than values obtained without nDEP concentration.

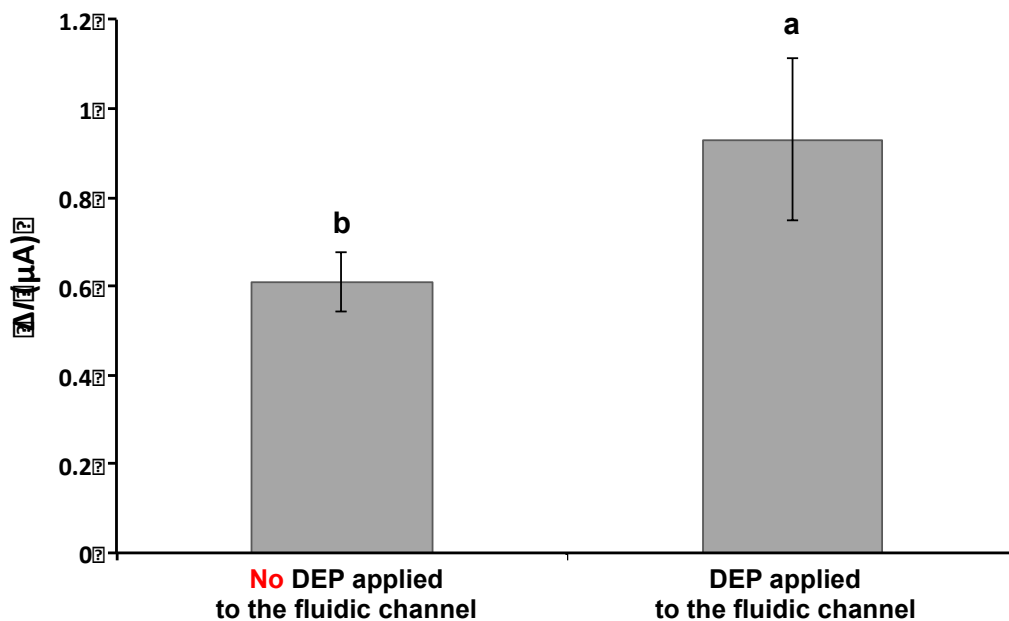


**Figure 6.6** Effect of DEP on current change in response to captured MS2 on the detector. DEP was applied at 10 V<sub>pp</sub> with a frequency of 1 MHz. The current signals were obtained from the detector filled with PBS after the 1mL of MS2 solution (~ 10<sup>7</sup> PFU/mL) passed through the biorecognition site at the flow rate of 0.1 mL/min.

Means with different letters are significantly different at 95% confidence level.

Similar to bacterial cell manipulation, DEP forces acting on a viral particle depends on its size, shape, conductivity, and permittivity, as well as applied electric field strength, frequency, and suspending medium properties. In this study, a single DEP condition was used at 10V<sub>pp</sub> and 1 MHz with 10 mM PBS (a conductivity of 1.5 S/m) as the suspending medium. This condition is referenced in several DEP studies for viral particle manipulation (Ermolina et al., 2006; Grom et al., 2006; Müller et al., 1996). However, the control of virus particles by DEP effect remains a challenge due to their small size (Madiyar et al., 2013). To achieve enhanced virus concentration, DEP forces and the drag forces, (i.e., A hydrodynamic force acting upon particles due to flow characteristics and is proportional to the volume of the radius ( $r^3$ ) and the radius ( $r$ ) of the



particle) can be balanced out with proper application of stronger electric field strengths. However, the applicable frequencies and electrical potentials within this study are hardware limited, thus field strengths are ranged limited. Another approach to enhance virus concentration can be to increase the conductivity of suspending medium. When the conductivity of particle is lower than that of the suspending medium, the particle is less polarizable than the medium and experiences negative DEP. Also, the behavior of viral particle can shift depending on the other factors. Therefore, more studies for DEP effect on virus manipulation are required toward biosensor device specific.

### **6.3.3. Detection of bacteriophage MS2 in the continuous flow mode**

The electrical current of PBS solution with various MS2 concentrations ranging from  $10^2$  to  $10^7$  PFU/mL was measured at a DC potential of 0.2 V. Before conducting test with the MS2 sample solution; the background current of pure PBS solution was measured. The change in current of each MS2 concentration compared to the control solution is shown in Figure 6.7. The  $\Delta I$  value increased with respect to the rising MS2 concentration and a linear relationship was observed between the logarithmic values of the  $\Delta I$  and MS2 concentration with  $R^2$  being 0.9803 in the range of  $10^2 - 10^8$  PFU/mL. This implies that an increase in the presence of anti-MS2-IgG and MS2 complexes on the detector.

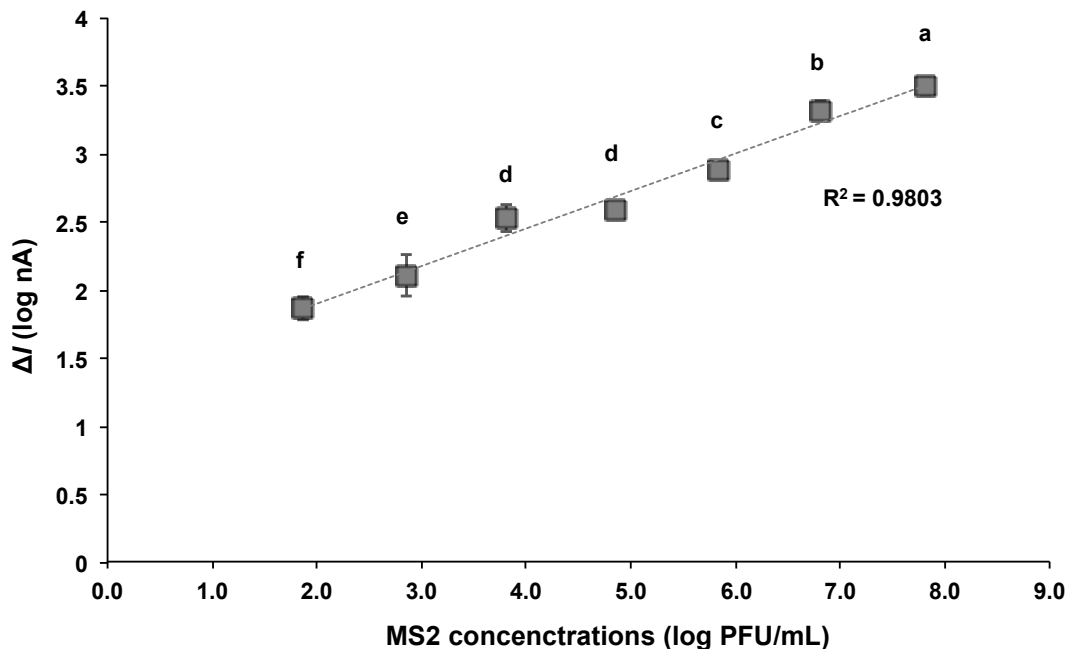


**Figure 6.7** Relationship between logarithmic values of change in current ( $\Delta I$ ) and concentrations of MS2 bound to the detector with DEP applied at 10 Vpp and 1 MHz. The current was measured at 0.2 V<sub>DC</sub>. Averaged logarithmic  $\Delta I$  values with different letters are significantly different at 95% confidence level.

Some studies have reported successful detection of MS2 using biosensors. For example, a paramagnetic bead-based electrochemical immunoassay detected MS with a detection limit of 90 ng/mL which corresponds to  $1.5 \times 10^{10}$  particles/mL. This was accomplished using an interdigitated array electrode in the PDMS fluidic channel (Thomas et al., 2004). Another electrochemical bead-based immunoassay in fluidic system reported a detection limit of  $1.6 \times 10^{11}$  particle/mL for MS2 (Kuramitz et al., 2006). A Carbon nanotube-based chemiresistive biosensor detected MS2 at  $10^3$  PFU/mL with a response time of 5 min (García-Aljaro et al., 2010). Sensitive detection of MS2 was achieved at 6 PFU/mL using porous silicon membrane-modified electrodes for voltammetric detection (Reta et al., 2016). Compared to the electrochemical biosensors in the fluidic system mentioned above, the proposed biosensor in this

study is able to provide detection of MS2 at concentration ranges as low as log 10 PFU/mL. In addition, the total assay can be accomplished within 15 min including particle concentration and current measurement.

#### **6.4. Conclusion**

In this study, a flow-based dielectrophoretic biosensor was fabricated as a proof-of-concept for detection of foodborne pathogenic viruses. The newly developed biosensor was evaluated to assess the sensor's performance when detecting bacteriophage MS2. Incorporation of immobilized antibodies and the SWCNT-modified sensing platform into the biosensor shows great promise for the capture of MS2 by immunoreaction on the detector electrode. Also, the DEP forces applied to the MS2 suspensions provide the potential for virus particle manipulation in the fluidic system. The proposed biosensor was able to detect MS2 in the range of  $10^2$  -  $10^8$  PFU/mL ( $R^2 = 0.9803$ ) with a total assay time of 15 min. Since this study is the initial step for virus detection using the newly fabricated flow-type sensor, more studies should be conducted. Therefore, the future study would be focused on the improvement of sensor's sensitivity by optimization of functionalization procedure and the DEP condition for viral particle manipulation. Also, other molecular-based virus detection method might be used for validation.

## **Chapter 7.**

### **CONCLUSIONS AND FUTURE WORKS**

#### **7.1. Conclusions**

The overall goal of this study was to develop bio- and nano-materials functionalized electrochemical immunosensor assisted with DEP and fluidic technology for rapid and reliable detection of potentially harmful microorganisms in food. The results achieved with the fabricated biosensors in this study regarding detection range, limit, and time with respect to target microorganisms are summarized in Table 7.1. The developed microwire-based electrochemical immunosensor (MEI sensor) with DEP-assisted cell trapping has a potential for fast, simple, and selective detection of low levels of target bacteria in the presence of mixed bacteria communities and food matrix. The CNTs functionalization and continuous flow assay could offer advances in sensitivity and detection time. The proposed sensing technology and device can offer a beneficial influence on food industries by providing rapid detection of multiple pathogens in foods as an early warning detection tool. It can also result in new approaches to the monitoring and control of biological hazards, which may be incorporated into food production and processing facilities to improve the safety of our food products.

**Table 7.1** Summary of dynamic detection range, limit of detection, and assay time achieved for each technical research objective and corresponding chapter

	<b>Objective 1 (Ch. 3)</b>	<b>Objective 2 (Ch. 4)</b>	<b>Objective 3 (Ch. 5)</b>	<b>Objective 4 (Ch. 6)</b>	
	Selective detection of target from non-target bacteria	Selective detection of target from non-target materials in spinach extract	Simultaneous detection of two different bacteria	Viral detection	
<b>Sensing platform</b>	Functionalized MEI sensor	Functionalized MEI sensor	Continuous flow multi-junction biosensor	Flow-based dielectrophoretic biosensor	
<b>Target microorganisms</b>	<i>E. coli</i> K12 <i>S. aureus</i>	<i>E. coli</i> K12 <i>S. Typhimurium</i>	<i>E. coli</i> K12 <i>S. aureus</i>	Bacteriophage MS2	
<b>Detection range and limit</b>	<i>E. coli</i> sensor	8.33 × 10 <sup>2</sup> - 7.97 × 10 <sup>5</sup> CFU/g with surface contamination (R <sup>2</sup> = 0.972) 1.05 × 10 <sup>3</sup> - 8.83 × 10 <sup>5</sup> CFU/g with internalized contamination (R <sup>2</sup> = 0.989) LOD: 10 <sup>3</sup> CFU/g	2.0 × 10 <sup>2</sup> - 10 <sup>5</sup> CFU/mL in pure solution (R <sup>2</sup> = 0.994) and in mixed solution (R <sup>2</sup> = 0.932) LOD: 10 <sup>3</sup> CFU/mL	-	
	<i>S. aureus</i> sensor	-	2.1 × 10 <sup>2</sup> - 10 <sup>5</sup> CFU/mL in pure solution (R <sup>2</sup> = 0.978) and in mixed solution (R <sup>2</sup> = 0.988) LOD: 10 <sup>2</sup> CFU/mL	-	
	<i>Salmonella</i> sensor	-	1.43 × 10 <sup>3</sup> - 1.67 × 10 <sup>7</sup> CFU/g with surface contamination (R <sup>2</sup> = 0.942) LOD: 10 <sup>4</sup> CFU/g	-	-
	MS2 sensor	-	-	-	10 <sup>2</sup> - 10 <sup>8</sup> PFU/mL (R <sup>2</sup> = 0.9803) LOD: 10 <sup>2</sup> PFU/mL
<b>Assay time</b>	10 min	10 min	2 min	15 min	

However, the specificity of the developed biosensors is still questionable when in the presence of more than three non-target bacteria. Single-cell detection, which might be essential to identify some pathogens, is not possible with the developed biosensors yet. It was also perceived that some food samples, which can alter the conductivity of suspending medium and nano-scale analytes may present major challenges for the integration of dielectrophoretic concentration into the biosensor. More in-depth studies on the optimization of antibody immobilization and microbial cell capture assistance via DEP and continuous flow strategies are also required.

## **7.2. Future works**

Based on the observed challenges and potentials, future studies should be conducted to extend the understanding of the pathogen detection mechanism with electrochemical immunosensor and to accomplish better detection efficiency based upon the following aspects.

### **7.2.1. Optimization of immunocapture: Antibody selection and immobilization**

In immunosensor-based analysis, the epitope types on the target analyte, types of the antibody, and assay format can affect the sensor's ability to detect and quantify low numbers of microbial cells and to differentiate specific strains of interest in microflora and to bind the target antigens with high-affinity strength. Antibodies recognize and bind to conformational or linear epitopes in the surfaces of antigens, which are part of the proteins and carbohydrates present within the microbial cell structure. Monoclonal, polyclonal, or recombinant antibodies are incorporated into biosensor platforms in a variety of different assay formats, such as the capture of antigen as a primary antibody, the capture of the antibody as a secondary one, or sandwich

format with both capture and detection antibodies (Byrne et al., 2009). The strategy for immunocapture in this study was to get bacteria or viruses to bind to the surface of the electrode's immobilized polyclonal antibodies on the SWCNTs structures by avidin-biotin complex formation or covalent bonding. The epitopes on the surface, flagella, and capsule of a bacterial cell or capsid structure of virus interacted with fragment antigen-binding domain (Fab domain, the arms of the IgG) of the antibody used as capture function. The fragment crystallizable region (Fc region) of the antibody coupled with biotin was linked to streptavidin on the SWCNTs structures via non-covalent interaction between protein and ligand. Otherwise, the anti-MS2 antibody was incorporated into carboxylic acid functionalized SWCNTs through the amide linkage. To enhance the immunocapture efficiency, the active antigen-binding region on the surface of the electrode should be stable and spacious allowing them maximum target microbial attachment and minimum signal noise from non-specific binding. The ideal structure considering the economical aspect would be in the form of monolayer antibodies with open two Fab domains throughout the biorecognition surface of the electrode. Therefore, the further studies should address the characterization of transducer surface and antigen binding activity accompanying antibody titration, which is a complexity of antibody concentration and affinity to provide the most reliable signal with the lowest background. In addition, resistance of the electrode surface should be tested to temperature and pH changes. An attempt for a self-assembled monolayer of organic molecules to immobilize the antibodies on the transducer electrode can be an alternative approach also.

### 7.2.1. Study on other physical effects on the particles in the electric field

There are a number of physical effects acting on a cell particle suspended within a fluid medium under an electric field. The behavior and movement of microbial cells can be influenced directly using induced polarization effects and indirectly through the hydrodynamic viscous drag exerted by suspension media. As a result, the cells will exhibit rotations and translations combined with other effects such as Brownian motion, diffusion and buoyancy force. DEP forces should be the dominant factor dictating cell motion to successfully achieve dielectrophoretic particle positioning and motion to a specific area. However, the hydrodynamic drag force ( $F_{\text{drag}}$ ) may play an important role depending on the system. It can be expressed as  $F_{\text{drag}} = -6\pi r_p \eta v$ , where  $r_p$  is a radius of the particle,  $\eta$  is the dynamic viscosity of the suspending medium, and  $v$  is the particle velocity relative to the medium. If the Brownian motion and buoyancy force can be considered negligible, the equation for particle motion with mass  $m$  can be described as  $m(dv/dt) = F_{\text{DEP}} + F_{\text{drag}}$  (Brownian motion may become a significant force as particle size is decreased). Thus, other driving forces that can exert the movement of the microbial particle should also be considered as critical parameters for new biosensor design, especially within microfluidic device with continuous flow. Numerical studies and computer simulation can be used to predict particle behavior, which can detail specific states and trajectories of the particle motion in the fluid to enhance the attraction efficiency at the sensing sites. This can be achieved by comparing the result to experimental observations and by optimizing the operating parameters in the system associated with appropriate geometries and applied variables.



### **7.2.3. Dielectrophoretic separation of pathogens from food sample**

The DEP effect on the bacterial concentration in buffer solution was understood adequately in this study; however, more knowledge about bacterial cell behaviors is required for the DEP manipulation of bacterial cells in higher conductive food samples. The optimization of the sensing parameters including the medium conductivity, applied voltage and frequency, and DEP experience time for efficient separation of bacteria and viruses from food sample can be an area of further studies. Efficient DEP condition should be device-specific considering electrode configuration and electroactive sample loading size based on the comprehensive understanding of complex effects on the microbial particles in the DEP field as described above.

### **7.2.4. Dielectrophoretic concentration of pathogens in fluidic channel**

In the continuous flow system, the critical parameter for DEP manipulation can be the hydraulic retention time (HRT), which is the length of time that microbial cells in medium remain in the fluidic channel. The microbial cell has to have enough time to encounter substantial DEP force while it travels through the fluidic channel to be concentrated at the sensing place. HRT is defined as the volume of a reactor ( $\text{m}^3$ ) divided by influent flow rate ( $\text{m}^3/\text{s}$ ), for continuous flow biosensor devices the volume of the reactor can be recognized as the volume of the fluidic channel corresponding to DEP acting space. Therefore, as the influent flow rate decreases, causing the slower velocity of the particle, and as the channel size increases, the HRT can be extended; and consequently, this increases DEP exposure time. However, the DEP force rapidly diminishes with the increasing distance between the electrode and particle; thus the modification of channel size might be better achieved with lengthening parallel to flow direction rather than channel height in regards to the continuous flow biosensor presented here.

### 7.2.5. Portable device for detection of multiple pathogens

The proposed multianalyte analysis has significant advantages over single analyte tests regarding the cost per assay, working load, assay throughput and suitability. The time required for the comprehensive analysis can be reduced by simultaneous detection of multiple pathogens in a single run. The biosensor devices developed within this PhD program was fabricated on a micro-scale, but the instrument for DEP generation and electrical measurement are not field-deployable yet. Figure 7.1 illustrates the conceptual design for multiplexed detection using multi-electrodes biosensor equipped with a portable sized unit for DEP generation and impedance measurement. Microelectrodes will be functionalized with different antibodies and assembled into a PDMS-based electrode guide. They can be replaced by other pathogen-specific microelectrode depending on the sample and pathogens to be identified. DEP generation mode can also be made to be multiplexing to distinguish and detect the target pathogens in the sample.

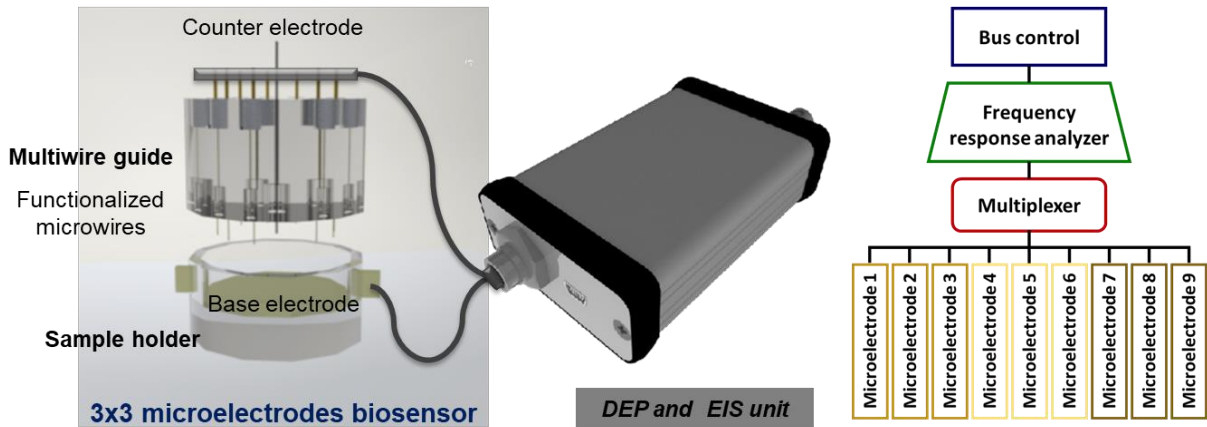


**Figure 7.1** The conceptual design for multiplexed detection using multi-electrodes biosensor connected to a field deployable unit. The proposed biosensor system consists of microwire sensing probes for cell concentration and collection, a sample container, and the combination unit of an electric power module for dielectrophoresis, and electronic sensor interface for multiplexed microbial detection. The multiplexed design will permit simultaneous measurement of nine different functionalized microelectrodes. It will incorporate a bus control, frequency response analyzer, and a multiplexer to switch the analyzer between nine microelectrodes.

## REFERENCES

- Abdel-Hamid, I., Ivnitski, D., Atanasov, P., & Wilkins, E. (1999). Highly sensitive flow-injection immunoassay system for rapid detection of bacteria. *Analytica Chimica Acta*, 399(1-2), 99-108.
- Abubakar, I., Irvine, L., Aldus, C. M., Wyatt, G., Fordham, R., Schelenz, S., Shepstone, L., Howe, A., Peck, M., & Hunter, P. (2007). A systematic review of the clinical, public health and cost-effectiveness of rapid diagnostic tests for the detection and identification of bacterial intestinal pathogens in faeces and food. *Health Technology Assessment*, 11, 1-216.
- Ahmed, A., Rushworth, J. V., Hirst, N. A., & Millner, P. A. (2014a). Biosensors for whole-cell bacterial detection. *Clinical Microbiology Reviews*, 27(3), 636-646.
- Ahmed, O. B., Asghar, A. H., EI-Rahim, I. H. A., & AI, H. (2014b). Detection of salmonella in food samples by culture and polymerase chain reaction methods. *Journal of Bacteriology & Parasitology*, 5(3), 187.
- Allen, B. L., Kichambare, P. D., & Star, A. (2007). Carbon nanotube field-effect-transistor-based biosensors. *Advanced Materials*, 19(11), 1439-1451.
- Ashiba, H., Sugiyama, Y., Wang, X., Shirato, H., Higo-Moriguchi, K., Taniguchi, K., Ohki, Y., & Fujimaki, M. (2017). Detection of norovirus virus-like particles using a surface plasmon resonance-assisted fluoroimmunosensor optimized for quantum dot fluorescent labels. *Biosensors and Bioelectronics*, 93, 260-266.
- Attar, A., Mandli, J., Ennaji, M. M., & Amine, A. (2016). Label-free electrochemical impedance detection of rotavirus based on immobilized antibodies on gold sononanoparticles. *Electroanalysis*, 28(8), 1839-1846.
- Bae, J., & Schwab, K. J. (2008). Evaluation of murine norovirus, feline calicivirus, poliovirus, and MS2 as surrogates for human norovirus in a model of viral persistence in surface water and groundwater. *Applied and Environmental Microbiology*, 74(2), 477-484.

- Bakthavathsalam, P., Rajendran, V., Saran, U., Chatterjee, S., & Jaffar Ali, B. (2013). Immunomagnetic nanoparticle based quantitative PCR for rapid detection of Salmonella. *An International Journal on Analytical Micro- and Nanochemistry*, 180(13), 1241-1248.
- Bally, M., Graule, M., Parra, F., Larson, G., & Höök, F. (2013). A virus biosensor with single virus-particle sensitivity based on fluorescent vesicle labels and equilibrium fluctuation analysis. *Journal for the Quantitative Biological Interface Data*, 8(1), 1-9.
- Barletta, F., Mercado, E., Lluque, A., Ruiz, J., Cleary, T., & Ochoa, T. (2013). Multiplex real-time PCR for detection of Campylobacter, Salmonella, and Shigella. *Journal of Clinical Microbiology*, 51(9), 2822.
- Bhunia, A. K. (2014). One day to one hour: how quickly can foodborne pathogens be detected? *Future Microbiology*, 9(8), 935-946.
- Borck, B., Stryhn, H., Ersbøll, A. K., & Pedersen, K. (2002). Thermophilic Campylobacter spp. in turkey samples: Evaluation of two automated enzyme immunoassays and conventional microbiological techniques. *Journal of Applied Microbiology*, 92(3), 574.
- Bozkurt, H., Souza, D. H., & Davidson, P. M. (2014). Thermal inactivation of human norovirus surrogates in spinach and measurement of its uncertainty. *Journal of Food Protection*, 77(2), 276.
- Byrne, B., Stack, E., Gilmartin, N., & Kennedy, R. (2009). Antibody-based sensors: Principles, problems and potential for detection of pathogens and associated toxins. *Sensors*, 9(6), 4407-4445.
- Canato, T., Magnani, M., Alves, J., & Hirooka, E. (2011). Multiplex PCR for the simultaneous detection of Salmonella spp. and Salmonella enteritidis in food. *International Journal of Food Science and Technology*, 46(7), 1502.
- Carnes, E., & Wilkins, E. (2005). The development of a new, rapid, amperometric immunosensor for the detection of low concentrations of bacteria Part I: Design of the detection system and applications. *American Journal of Applied Sciences*, 2(3), 597.

- Castillo-Fernandez, Ó., Uria, N., Muñoz, F. X., & Bratov, A. (2015). Cell concentration systems for enhanced biosensor sensitivity. In T. Rinken (Ed.), *Biosensors - Micro and Nanoscale Applications* (pp. Ch. 07). Rijeka: InTech.
- Caygill, R. L., Blair, G. E., & Millner, P. A. (2010). A review on viral biosensors to detect human pathogens. *Analytica Chimica Acta*, 681(1-2), 8-15.
- CDC. (2011). Estimates of foodborne illness in the United States. Retrieved from <https://www.cdc.gov/foodborneburden/2011-foodborne-estimates.html>
- CDC. (2017). List of selected multistate foodborne outbreak investigations. Retrieved from <https://www.cdc.gov/foodsafety/outbreaks/multistate-outbreaks/outbreaks-list.html>
- Chattopadhyay, S., Kaur, A., Jain, S., & Singh, H. (2013). Sensitive detection of food-borne pathogen Salmonella by modified PAN fibers-immunoassay. *Biosensors and Bioelectronics*, 45, 274-280.
- Chen, J., Zhang, L., Paoli, G. C., Shi, C., Tu, S.-I., & Shi, X. (2010). A real-time PCR method for the detection of Salmonella enterica from food using a target sequence identified by comparative genomic analysis. *International Journal of Food Microbiology*, 137(2), 168-174.
- Chen, Q., Wang, D., Cai, G., Xiong, Y., Li, Y., Wang, M., Huo, H., & Lin, J. (2016). Fast and sensitive detection of foodborne pathogen using electrochemical impedance analysis, urease catalysis and microfluidics. *Biosensors and Bioelectronics*, 86, 770-776.
- Cheng, X., Chen, G., & Rodriguez, W. R. (2009). Micro- and nanotechnology for viral detection. *Analytical and Bioanalytical Chemistry*, 393(2), 487-501.
- Cho, I.-H., & Irudayaraj, J. (2013). In-situ immuno-gold nanoparticle network ELISA biosensors for pathogen detection. *International Journal of Food Microbiology*, 164(1), 70-75.
- Cho, I.-H., Mauer, L., & Irudayaraj, J. (2014). In-situ fluorescent immunomagnetic multiplex detection of foodborne pathogens in very low numbers. *Biosensors and Bioelectronics*, 57, 143-148.

- Chung, S. H., Baek, C., Cong, V. T., & Min, J. (2015). The microfluidic chip module for the detection of murine norovirus in oysters using charge switchable micro-bead beating. *Biosensors and Bioelectronics*, *67*, 625-633.
- Croxen, M. A., Law Rj Fau - Scholz, R., Scholz R Fau - Keeney, K. M., Keeney Km Fau - Wlodarska, M., Wlodarska M Fau - Finlay, B. B., & Finlay, B. B. (2013). Recent advances in understanding enteric pathogenic Escherichia coli. *Clinical Microbiology Reviews*, *26*(4), 822-880.
- Dastider, S. G., Barizuddin, S., Yuksek, N. S., Dweik, M., & Almasri, M. F. (2015). Efficient and rapid detection of Salmonella using microfluidic impedance based sensing. *Journal of Sensors*, *2015*.
- Davis, J., Huw Vaughan, D., & Cardosi, M. F. (1995). Elements of biosensor construction. *Enzyme and Microbial Technology*, *17*(12), 1030-1035.
- Dawson, D. J., Paish, A., Staffell, L. M., Seymour, I. J., & Appleton, H. (2005). Survival of viruses on fresh produce, using MS2 as a surrogate for norovirus. *Journal of Applied Microbiology*, *98*(1), 203-209.
- Day, J. B., & Basavanna, U. (2015). Real-time PCR detection of Listeria monocytogenes in infant formula and lettuce following macrophage-based isolation and enrichment. *Journal of Applied Microbiology*, *118*(1), 233-244.
- de Freitas, C. G., Santana, Â. P., Da Silva, P. H. C., Gonçalves, V. S. P., Barros, M. d. A. F., Torres, F. A. G., Murata, L. S., & Perecmanis, S. (2010). PCR multiplex for detection of Salmonella Enteritidis, Typhi and Typhimurium and occurrence in poultry meat. *International Journal of Food Microbiology*, *139*(1), 15-22.
- Del Moral- Zamora, B., Punter- Villagrassa, J., Oliva- Brañas, A. M., Álvarez- Azpeitia, J. M., Colomer- Farrarons, J., Samitier, J., Homs- Corbera, A., & Miribel- Català, P. L. (2015). Combined dielectrophoretic and impedance system for on-chip controlled bacteria concentration: Application to Escherichia coli. *Electrophoresis*, *36*(9-10), 1130-1141.

- Di Biasio, A., Ambrosone, L., & Cametti, C. (2010). The dielectric behavior of nonspherical biological cell suspensions: An analytic approach. *Biophysical Journal*, *99*(1), 163-174.
- Duizer, E., Schwab, K. J., Neill, F. H., Atmar, R. L., Koopmans, M. P. G., & Estes, M. K. (2004). Laboratory efforts to cultivate noroviruses. *The Journal of general virology*, *85*(Pt 1), 79-87.
- Dürr, M., Kentsch, J., Müller, T., Schnelle, T., & Stelzle, M. (2003). Microdevices for manipulation and accumulation of micro- and nanoparticles by dielectrophoresis. *Electrophoresis*, *24*(4), 722-731.
- Dweik, M., Stringer, R. C., Dastider, S. G., Wu, Y., Almasri, M., & Barizuddin, S. (2012). Specific and targeted detection of viable Escherichia coli O157:H7 using a sensitive and reusable impedance biosensor with dose and time response studies. *Talanta*, *94*, 84-89.
- Ermolina, I., Milner, J., & Morgan, H. (2006). Dielectrophoretic investigation of plant virus particles: Cow Pea Mosaic Virus and Tobacco Mosaic Virus. *Electrophoresis*, *27*(20), 3939-3948.
- Evenson, M. L., Hinds Mw Fau - Bernstein, R. S., Bernstein Rs Fau - Bergdoll, M. S., & Bergdoll, M. S. (1988). Estimation of human dose of staphylococcal enterotoxin A from a large outbreak of staphylococcal food poisoning involving chocolate milk. *International Journal of Food Microbiology*, *7*(4), 311-316.
- Ezzati Nazhad Dolatabadi, J., & De La Guardia, M. (2014). Nanomaterial-based electrochemical immunosensors as advanced diagnostic tools. *Analytical Methods*, *6*(12), 3891-3900.
- FDA. (1997). HACCP principles & application guidelines. Retrieved from <https://www.fda.gov/Food/GuidanceRegulation/HACCP/ucm2006801.htm>
- Fedio, W. M., Jinneman, K. C., Yoshitomi, K. J., Zapata, R., Wendakoon, C. N., Browning, P., & Weagant, S. D. (2011). Detection of E. coli O157:H7 in raw ground beef by Pathatrix™ immunomagnetic-separation, real-time PCR and cultural methods. *International Journal of Food Microbiology*, *148*(2), 87-92.

- Fernández-Morales, F. H., Duarte, J. E., & Samitier-Martí, J. (2008). Bacterial handling under the influence of non-uniform electric fields: dielectrophoretic and electrohydrodynamic effects. *Anais da Academia Brasileira de Ciências*, 80, 627-638.
- Fintschenko, Y., & Wilson, G. (1998). Flow injection immunoassays: A review. *Microchimica Acta*, 129(1-2), 7-18.
- Fournier, P.-E., Drancourt, M., Colson, P., Rolain, J.-M., Scola, B. L., & Raoult, D. (2013). Modern clinical microbiology: New challenges and solutions. *Nature Reviews Microbiology*, 11(8), 574-585.
- Fujigaya, T., & Nakashima, N. (2015). Non-covalent polymer wrapping of carbon nanotubes and the role of wrapped polymers as functional dispersants. *Science and Technology of Advanced Materials*, 16(2), 024802.
- García-Aljaro, C., Cella, L. N., Shirale, D. J., Park, M., Muñoz, F. J., Yates, M. V., & Mulchandani, A. (2010). Carbon nanotubes-based chemiresistive biosensors for detection of microorganisms. *Biosensors and Bioelectronics*, 26(4), 1437-1441.
- Garrido, A., Chapela, M.-J., Román, B., Fajardo, P., Vieites, J. M., & Cabado, A. G. (2013). In-house validation of a multiplex real-time PCR method for simultaneous detection of *Salmonella* spp., *Escherichia coli* O157 and *Listeria monocytogenes*. *International Journal of Food Microbiology*, 164(1), 92-98.
- Gascoyne, P. R. C., & Vykoukal, J. (2002). Particle separation by dielectrophoresis. *Electrophoresis*, 23(13), 1973-1983.
- Gattuso, A., Gianfranceschi, M. V., Sonnessa, M., Delibato, E., Marchesan, M., Hernandez, M., De Medici, D., & Rodriguez-Lazaro, D. (2014). Optimization of a real time PCR based method for the detection of *Listeria monocytogenes* in pork meat. *International Journal of Food Microbiology*, 184, 106-108.
- Geng, P., Zhang, X., Meng, W., Wang, Q., Zhang, W., Jin, L., Feng, Z., & Wu, Z. (2008). Self-assembled monolayers-based immunosensor for detection of *Escherichia coli* using electrochemical impedance spectroscopy. *Electrochimica Acta*, 53(14), 4663-4668.



- Ghosh Dastider, S., Barizuddin, S., Dweik, M., & Almasri, M. F. (2012). *Impedance biosensor based on interdigitated electrode array for detection of E.coli O157:H7 in food products*. Paper presented at the Sensing for Agriculture and Food Quality and Safety IV.
- Gomes-Filho, S. L. R., Dias, A. C. M. S., Silva, M. M. S., Silva, B. V. M., & Dutra, R. F. (2013). A carbon nanotube-based electrochemical immunosensor for cardiac troponin T. *Microchemical Journal*, *109*, 10-15.
- Goode, J. A., Rushworth, J. V. H., & Millner, P. A. (2015). Biosensor regeneration: A review of common techniques and outcomes. *Langmuir*, *31*(23), 6267-6276.
- Gracias, K. S., & McKillip, J. L. (2004). A review of conventional detection and enumeration methods for pathogenic bacteria in food. *Canadian Journal of Microbiology*, *50*(11), 883-890.
- Grom, F., Kentsch, J., Müller, T., Schnelle, T., & Stelzle, M. (2006). Accumulation and trapping of hepatitis A virus particles by electrohydrodynamic flow and dielectrophoresis. *Electrophoresis*, *27*(7), 1386-1393.
- Gubitz, G., Schmid, M. G., Silviaeh, H., & Aboul-Enein, H. Y. (2001). Chemiluminescence flow-injection immunoassays. *Critical Reviews in Analytical Chemistry*, *31*(3), 167-174.
- Hamada, R., Takayama, H., Shonishi, Y., Mao, L., Nakano, M., & Suehiro, J. (2013). A rapid bacteria detection technique utilizing impedance measurement combined with positive and negative dielectrophoresis. *Sensors and Actuators B: Chemical*, *181*, 439-445.
- Hartwell, S., & Grudpan, K. (2010). Flow based immuno/bioassay and trends in micro-immuno/biosensors. *Microchimica Acta*, *169*(3-4), 201-220.
- He, X., Hu, C., Guo, Q., Wang, K., Li, Y., & Shangguan, J. (2013). Rapid and ultrasensitive Salmonella Typhimurium quantification using positive dielectrophoresis driven on-line enrichment and fluorescent nanoparticles label. *Biosensors and Bioelectronics*, *42*, 460-466.

- Hill, W., & Wachsmuth, K. (1996). The polymerase chain reaction: Applications for the detection of foodborne pathogens. *Critical Reviews in Food Science and Nutrition*, 36(1-2), 123-173.
- Hoffmann, S. A. (2015). *Economic burden of major foodborne illnesses acquired in the United States*: Washington, D.C. : United States Department of Agriculture, Economic Research Service.
- Hong, S. A., Kwon, J., Kim, D., & Yang, S. (2015). A rapid, sensitive and selective electrochemical biosensor with concanavalin A for the preemptive detection of norovirus. *Biosensors and Bioelectronics*, 64, 338-344.
- Huang, J., Yang, G., Meng, W., Wu, L., Zhu, A., & Jiao, X. (2010). An electrochemical impedimetric immunosensor for label-free detection of *Campylobacter jejuni* in diarrhea patients' stool based on O-carboxymethylchitosan surface modified Fe<sub>3</sub>O<sub>4</sub> nanoparticles. *Biosensors and Bioelectronics*, 25(5), 1204-1211.
- Hübner, Y., Hoettges, K. F., McDonnell, M. B., Carter, M. J., & Hughes, M. P. (2007). Applications of dielectrophoretic/electrohydrodynamic "zipper" electrodes for detection of biological nanoparticles. *International journal of nanomedicine*, 2(3), 427-431.
- Ivnitski, D., Abdel-Hamid, I., Atanasov, P., & Wilkins, E. (1999). Biosensors for detection of pathogenic bacteria. *Biosensors and Bioelectronics*, 14(7), 599-624.
- Jaemin, A., Jangwon, L., Youngho, K., Byungkyu, K., & Sangho, L. (2008, 6-9 Jan. 2008). *Analysis of cell separation efficiency in dielectrophoresis-activated cell sorter*. Paper presented at the 2008 3rd IEEE International Conference on Nano/Micro Engineered and Molecular Systems.
- Jain, S., Singh, S. R., Horn, D. W., Davis, V. A., Ram, M. K., & Pillai, S. (2012). Development of an antibody functionalized carbon nanotube biosensor for foodborne bacterial pathogens. *Journal of Biosensors & Bioelectronics*, S11:002.

- Joung, C.-K., Kim, H.-N., Lim, M.-C., Jeon, T.-J., Kim, H.-Y., & Kim, Y.-R. (2013). A nanoporous membrane-based impedimetric immunosensor for label-free detection of pathogenic bacteria in whole milk. *Biosensors and Bioelectronics*, *44*, 210-215.
- Kalyan Kumar, T., Murali, H., & Batra, H. (2010). Multiplex PCR assay for the detection of enterotoxigenic *Bacillus cereus* group strains and its application in food matrices. *The Official Publication of the Association of Microbiologists of India*, *50*(2), 165-171.
- Kang, I., Heung, Y. Y., Kim, J. H., Lee, J. W., Gollapudi, R., Subramaniam, S., Narasimhadevara, S., Hurd, D., Kirikera, G. R., Shanov, V., Schulz, M. J., Shi, D., Boerio, J., Mall, S., & Ruggles-Wren, M. (2006). Introduction to carbon nanotube and nanofiber smart materials. *Composites Part B: Engineering*, *37*(6), 382-394.
- Karoonuthaisiri, N., Charlermroj, R., Uawisetwathana, U., Luxananil, P., Kirtikara, K., & Gajanandana, O. (2009). Development of antibody array for simultaneous detection of foodborne pathogens. *Biosensors and Bioelectronics*, *24*(6), 1641-1648.
- Katz, E., & Willner, I. (2004). Biomolecule-functionalized carbon nanotubes: Applications in nanobioelectronics. *ChemPhysChem*, *5*(8), 1084-1104.
- Kentsch, J., Dürr, M., Schnelle, T., Gradl, G., Müller, T., Jager, M., Normann, A., & Stelzle, M. (2003). Microdevices for separation, accumulation, and analysis of biological micro- and nanoparticles. *IEE proceedings. Nanobiotechnology*, *150*(2), 82.
- Khoshmanesh, K., Baratchi, S., Tovar-Lopez, F. J., Nahavandi, S., Wlodkowic, D., Mitchell, A., & Kalantar-zadeh, K. (2011). On-chip separation of *Lactobacillus* bacteria from yeasts using dielectrophoresis. *Microfluidics and Nanofluidics*, *12*(1-4), 597-606.
- Kim, G. (2007). Nano-particle enhanced impedimetric biosensor for detection of foodborne pathogens. *Journal of Physics: Conference Series*, *61*(1), 555-559.
- Kim, J.-H., Hiraiwa, M., Lee, H.-B., Lee, K.-H., Cangelosic, G. A., & Chung, J.-H. (2013). Electrolyte-free amperometric immunosensor using a dendritic nanotip. *RSC Advances*, *3*(13), 4281-4287.

- Kim, N., & Park, I. S. (2003). Application of a flow-type antibody sensor to the detection of *Escherichia coli* in various foods. *Biosensors and Bioelectronics*, *18*(9), 1101-1107.
- Kim, S., Lu, L., Chung, J.-H., Lee, K., Li, Y., & Jun, S. (2011). A microwire sensor for rapid detection of *Escherichia coli* K-12 in fresh produce. *Innovative Food Science and Emerging Technologies*, *12*(4), 617-622.
- Kim, Y.-R., Czajka, J., & Batt, C. A. (2000). Development of a fluorogenic probe-based PCR assay for detection of *Bacillus cereus* in nonfat dry milk. *Applied and Environmental Microbiology*, *66*(4), 1453-1459.
- Kirk, M. D., Pires, S. M., Black, R. E., Caipo, M., Crump, J. A., Devleeschauwer, B., Döpfer, D., Fazil, A., Fischer-Walker, C. L., Hald, T., Hall, A. J., Keddy, K. H., Lake, R. J., Lanata, C. F., Torgerson, P. R., Havelaar, A. H., & Angulo, F. J. (2015). World Health Organization estimates of the global and regional disease burden of 22 foodborne bacterial, protozoal, and viral diseases, 2010: A data synthesis (Global disease burden of foodborne enteric disease). *12*(12), e1001921.
- Kothary, M. H., & Babu, U. S. (2001). Infective dose of foodborne pathogens in volunteers: A review. *Journal of Food Safety*, *21*(1), 49-68.
- Koyuncu, S., Andersson, M. G., & Haggblom, P. (2010). Accuracy and sensitivity of commercial PCR-based methods for detection of *Salmonella enterica* in feed. *Applied and Environmental Microbiology*, *76*(9), 2815-2822.
- Kuramitz, H., Dziewatkoski, M., Barnett, B., Halsall, H. B., & Heineman, W. R. (2006). Application of an automated fluidic system using electrochemical bead-based immunoassay to detect the bacteriophage MS2 and ovalbumin. *Analytica Chimica Acta*, *561*(1-2), 69-77.
- Lambertz, S. T., Nilsson, C., Hallanvuo, S., & Lindblad, M. (2008). Real-time PCR method for detection of pathogenic *Yersinia enterocolitica* in food. *Applied and Environmental Microbiology*, *74*(19), 6060-6067.

- Law, J. W., Ab Mutalib, N. S., Chan, K. G., & Lee, L. H. (2014). Rapid methods for the detection of foodborne bacterial pathogens: Principles, applications, advantages and limitations. *Frontiers in Microbiology*, *5*, 770.
- Lazcka, O., Campo, F. J. D., & Muñoz, F. X. (2007). Pathogen detection: A perspective of traditional methods and biosensors. *Biosensors and Bioelectronics*, *22*(7), 1205-1217.
- Leonard, P., Hearty, S., Brennan, J., Dunne, L., Quinn, J., Chakraborty, T., & O’Kennedy, R. (2003). Advances in biosensors for detection of pathogens in food and water. *Enzyme and Microbial Technology*, *32*(1), 3-13.
- Li, L., Mendis, N., Trigui, H., Oliver, J. D., & Faucher, S. P. (2014a). The importance of the viable but non-culturable state in human bacterial pathogens. *Frontiers in Microbiology*, *5*, 258.
- Li, M., Li, W. H., Zhang, J., Alici, G., & Wen, W. (2014b). A review of microfabrication techniques and dielectrophoretic microdevices for particle manipulation and separation. *47*(6), 063001.
- Lin, Y. H., Chen, S. H., Chuang, Y. C., Lu, Y. C., Shen, T. Y., Chang, C. A., & Lin, C. S. (2008). Disposable amperometric immunosensing strips fabricated by Au nanoparticles-modified screen-printed carbon electrodes for the detection of foodborne pathogen Escherichia coli O157:H7. *Biosensors and Bioelectronics*, *23*(12), 1832-1837.
- Linman, M. J., Sugerman, K., & Cheng, Q. (2010). Detection of low levels of Escherichia coli in fresh spinach by surface plasmon resonance spectroscopy with a TMB-based enzymatic signal enhancement method. *Sensors and Actuators B: Chemical*, *145*(2), 613-619.
- Liu, Y., Hu, J., Sun, J. S., Li, Y., Xue, S. X., Chen, X. Q., Li, X. S., & Du, G. X. (2014). Facile synthesis of multifunctional multi-walled carbon nanotube for pathogen *Vibrio alginolyticus* detection in fishery and environmental samples. *Talanta*, *128*, 311-318.
- López-Campos, G. (2012). *Microarray detection and characterization of bacterial foodborne pathogens*. New York: New York : Springer.

- Lu, L., Chee, G., Yamada, K., & Jun, S. (2013). Electrochemical impedance spectroscopic technique with a functionalized microwire sensor for rapid detection of foodborne pathogens. *Biosensors and Bioelectronics*, *42*, 492-495.
- Lu, L., & Jun, S. (2012). Evaluation of a microwire sensor functionalized to detect *Escherichia coli* bacterial cells. *Biosensors and Bioelectronics*, *36*(1), 257-261.
- Luka, G., Ahmadi, A., Najjaran, H., Alocilja, E., Derosa, M., Wolthers, K., Malki, A., Aziz, H., Althani, A., & Hoorfar, M. (2015). Microfluidics integrated biosensors: A leading technology towards lab-on-a-chip and sensing applications. *Sensors*, *15*(12), 30011-30031.
- Madic, J., Vingadassalon, N., de Garam, C. P., Marault, M., Scheutz, F., Brugere, H., Jamet, E., & Auvray, F. (2011). Detection of Shiga toxin-producing *Escherichia coli* serotypes O26:H11, O103:H2, O111:H8, O145:H28, and O157:H7 in raw-milk cheeses by using multiplex real-time PCR. *Applied and Environmental Microbiology*, *77*(6), 2035.
- Madiyar, F. R., Syed, L. U., Culbertson, C. T., & Li, J. (2013). Manipulation of bacteriophages with dielectrophoresis on carbon nanofiber nanoelectrode arrays. *Electrophoresis*, *34*(7), 1123-1130.
- Majumdar, T., Chakraborty, R., & Raychaudhuri, U. (2013). Development of PEI-GA modified antibody based sensor for the detection of *S. aureus* in food samples. *Food Bioscience*, *4*, 38-45.
- Maroto, A., Balasubramanian, K., Burghard, M., & Kern, K. (2007). Functionalized metallic carbon nanotube devices for pH sensing. *ChemPhysChem*, *8*(2), 220-223.
- Mazumdar, S. D., Hartmann, M., Kämpfer, P., & Keusgen, M. (2007). Rapid method for detection of *Salmonella* in milk by surface plasmon resonance (SPR). *Biosensors and Bioelectronics*, *22*(9), 2040-2046.
- Mello, L. D., & Kubota, L. T. (2002). Review of the use of biosensors as analytical tools in the food and drink industries. *Food Chemistry*, *77*(2), 237-256.

- Müller, T., Fiedler, S., Schnelle, T., Ludwig, K., Jung, H., & Fuhr, G. (1996). High frequency electric fields for trapping of viruses. *Biotechnology Techniques*, 10(4), 221-226.
- Nakano, M., Hisajima, T., Mao, L., & Suehiro, J. (2012, 28-31 Oct. 2012). *Electrical detection of norovirus capsid using dielectrophoretic impedance measurement method*. Paper presented at the Sensors, 2012 IEEE.
- Nakano, M., Obara, R., Zhenhao Ding, J., & Suehiro, J. (2013). Detection of norovirus and rotavirus by dielectrophoretic impedance measurement. 374-378.
- Nandakumar, V., La Belle Jt Fau - Reed, J., Reed J Fau - Shah, M., Shah M Fau - Cochran, D., Cochran D Fau - Joshi, L., Joshi L Fau - Alford, T. L., & Alford, T. L. (2008). A methodology for rapid detection of Salmonella Typhimurium using label-free electrochemical impedance spectroscopy. *Biosensors and Bioelectronics*, 24(4), 1045-1048.
- Neethirajan, S., Ahmed, S. R., Chand, R., Buoziš, J., & Nagy, E. (2017). Recent advances in biosensor development for foodborne virus detection. *Nanotheranostics*, 1(3), 272-295.
- O'Connell, K. P., Bucher, J. R., Anderson, P. E., Cao, C. J., Khan, A. S., Gostomski, M. V., & Valdes, J. J. (2006). Real-time fluorogenic reverse transcription-PCR assays for detection of Bacteriophage MS2. *Applied and Environmental Microbiology*, 72(1), 478-483.
- Oliwa-Stasiak, K., Kolaj-Robin, O., & Adley, C. C. (2011). Development of real-time PCR assays for detection and quantification of Bacillus cereus group species: Differentiation of B. weihenstephanensis and Rhizoid B. pseudomycoides Isolates from milk. *Applied and Environmental Microbiology*, 77(1), 80-88.
- Pankaj, K. (2013). Methods for rapid virus identification and quantification. *Materials and Methods*, 3.
- Park, M.-K., Park, J. W., Wikle, H. C., & Chin, B. A. (2013). Evaluation of phage-based magnetoelastic biosensors for direct detection of Salmonella Typhimurium on spinach leaves. *Sensors and Actuators B: Chemical*, 176, 1134-1140.

- Park, S., Zhang, Y., Wang, T. H., & Yang, S. (2011). Continuous dielectrophoretic bacterial separation and concentration from physiological media of high conductivity. *Lab Chip*, *11*(17), 2893-2900.
- Patel, M. M., Hall, A. J., Vinjé, J., & Parashar, U. D. (2009). Noroviruses: A comprehensive review. *Journal of Clinical Virology*, *44*(1), 1-8.
- Patel, S., Showers, D., Vedantam, P., Tzeng, T.-R., Qian, S., & Xuan, X. (2012). Microfluidic separation of live and dead yeast cells using reservoir-based dielectrophoresis. *Biomicrofluidics*, *6*(3), 034102.
- Pedrero, M., Campuzano S Fau - Pingarron, J. M., & Pingarron, J. M. (2009). Electroanalytical sensors and devices for multiplexed detection of foodborne pathogen microorganisms. *Sensors*, *9*(7), 5503-5520.
- Perfzou, M., Turner, A., & Merkoi, A. (2012). Cancer detection using nanoparticle-based sensors. *Chemical Society Reviews*, *41*(7), 2606-2622.
- Pohl, H. A. (1978). *Dielectrophoresis : The behavior of neutral matter in nonuniform electric fields*. Cambridge ; New York: Cambridge ; New York : Cambridge University Press.
- Punbusayakul, N., Talapatra, S., Ajayan, P. M., & Surareungchai, W. (2013). Label-free as-grown double wall carbon nanotubes bundles for Salmonella Typhimurium immunoassay. *Chemistry Central journal*, *7*, 102-102.
- Putzbach, W., & Ronkainen, N. (2013). Immobilization techniques in the fabrication of nanomaterial-based electrochemical biosensors: A review. *Sensors*, *13*(4), 4811-4840.
- Rabenau, H. F., Stürmer, M., Buxbaum, S., Walczok, A., Preiser, W., & Doerr, H. W. (2003). Laboratory diagnosis of norovirus: Which method is the best? *Intervirology*, *46*(4), 232-238.
- Radke, S. M., & Alocilja, E. C. (2004). Design and fabrication of a microimpedance biosensor for bacterial detection. *IEEE Sensors Journal*, *4*(4), 434-440.



- Radke, S. M., & Alocilja, E. C. (2005). A high density microelectrode array biosensor for detection of *E. coli* O157:H7. *Biosensors and Bioelectronics*, *20*(8), 1662-1667.
- Rasooly, A. (2006). Biosensors for the analysis of food- and waterborne pathogens and their toxins. *Journal of AOAC International*, *89*(3), 873-883.
- Reta, N., Michelmore, A., Saint, C., Prieto-Simon, B., & Voelcker, N. H. (2016). Porous silicon membrane-modified electrodes for label-free voltammetric detection of MS2 bacteriophage. *Biosensors and Bioelectronics*, *80*, 47-53.
- Rodriguez, B. A. G., Trindade, E. K. G., Cabral, D. G. A., Soares, E. C. L., Menezes, C. E. L., Ferreira, D. C. M., Mendes, R. K., & Dutra, R. F. (2015). Nanomaterials for advancing the health immunosensor. In T. Rinken (Ed.), *Biosensors - Micro and Nanoscale Applications* (pp. Ch. 12). Rijeka: InTech.
- Ronkainen, N. J., Halsall, H. B., & Heineman, W. R. (2010). Electrochemical biosensors. *Chem Soc Rev*, *39*(5), 1747-1763.
- Ruan, C., Yang, L., & Li, Y. (2002). Immunobiosensor chips for detection of *Escherichia coli* O157:H7 using electrochemical impedance spectroscopy. *Analytical Chemistry*, *74*(18), 4814-4820.
- Sadik, O. A., Aluoch Ao Fau - Zhou, A., & Zhou, A. (2009). Status of biomolecular recognition using electrochemical techniques. *Biosensors and Bioelectronics*, *24*(9), 2749-2765.
- Sails, A. D., Fox, A. J., Bolton, F. J., Wareing, D. R. A., & Greenway, D. L. A. (2003). A real-time PCR assay for the detection of *Campylobacter jejuni* in foods after enrichment culture. *Applied and Environmental Microbiology*, *69*(3), 1383-1390.
- Scallan, E., Hoekstra, R. M., Angulo, F. J., Tauxe, R. V., Widdowson, M. A., Roy, S. L., Jones, J. L., & Griffin, P. M. (2011). Foodborne illness acquired in the United States-major pathogens. *Emerging Infectious Diseases*, *17*(1), 7-15.

- Schwan, H. P. (1994). *Electrical properties of tissues and cell suspensions: Mechanisms and models*. Paper presented at the 6th Annual International Conference of the IEEE Engineering in Medicine and Biology Society.
- Sharma, H., Agarwal, M., Goswami, M., Sharma, A., Roy, S. K., Rai, R., & M.S., M. (2013). Biosensor: Tool for food borne pathogen detection. *Veterinary World*, 6, 968-973.
- Shen, Z., Hou, N., Jin, M., Qiu, Z., Wang, J., Zhang, B., Wang, X., Wang, J., Zhou, D., & Li, J. (2014). A novel enzyme-linked immunosorbent assay for detection of Escherichia coli O157:H7 using immunomagnetic and beacon gold nanoparticles. *Gut pathogens*, 6, 14.
- Shriver-Lake, L. C., Turner, S., & Taitt, C. R. (2007). Rapid detection of Escherichia coli O157:H7 spiked into food matrices. *Analytica Chimica Acta*, 584(1), 66-71.
- Siddiqui, S., Dai, Z., Stavis, C. J., Zeng, H., Moldovan, N., Hamers, R. J., Carlisle, J. A., & Arumugam, P. U. (2012). A quantitative study of detection mechanism of a label-free impedance biosensor using ultrananocrystalline diamond microelectrode array. *Biosensors and Bioelectronics*, 35(1), 284-290.
- Soria, M. C., Soria, M. A., & Bueno, D. J. (2013). A comparative study of culture methods and PCR assay for Salmonella detection in poultry drinking water. *Poultry Science*, 92(1), 225-232.
- Stannard, C. (1997). Development and use of microbiological criteria for foods. *Food Science and Technology Today*, 11(3), 137-176.
- Stevens, K. A., & Jaykus, L.-A. (2004). Bacterial separation and concentration from complex sample matrices: A Review. *Critical Reviews in Microbiology*, 30(1), 7-24.
- Subramanian, A., Irudayaraj, J., & Ryan, T. (2006). A mixed self-assembled monolayer-based surface plasmon immunosensor for detection of E. coli O157:H7. *Biosensors and Bioelectronics*, 21(7), 998-1006.

- Suehiro, J., Hamada, R., Noutomi, D., Shutou, M., & Hara, M. (2003). Selective detection of viable bacteria using dielectrophoretic impedance measurement method. *Journal of Electrostatics*, 57(2), 157-168.
- Suehiro, J., Ohtsubo, A., Hatano, T., & Hara, M. (2006). Selective detection of bacteria by a dielectrophoretic impedance measurement method using an antibody-immobilized electrode chip. *Sensors and Actuators B: Chemical*, 119(1), 319-326.
- Taitt, C. R., Shubin, Y. S., Angel, R., & Ligler, F. S. (2004). Detection of Salmonella enterica Serovar Typhimurium by using a rapid, array-based immunosensor. *Applied and Environmental Microbiology*, 70(1), 152-158.
- Tang, D., Tang, J., Su, B., Ren, J., & Chen, G. (2010). Simultaneous determination of five-type hepatitis virus antigens in 5 min using an integrated automatic electrochemical immunosensor array. *Biosensors and Bioelectronics*, 25(7), 1658-1662.
- Thisted Lambertz, S., Lindqvist, R., Ballagi-Pordány, A., & Danielsson-Tham, M. L. (2000). A combined culture and PCR method for detection of pathogenic Yersinia enterocolitica in food. *International Journal of Food Microbiology*, 57(1), 63-73.
- Thomas, J. H., Kim, S. K., Hesketh, P. J., Halsall, H. B., & Heineman, W. R. (2004). Bead-based electrochemical immunoassay for Bacteriophage MS2. *Analytical Chemistry*, 76(10), 2700-2708.
- Tlili, A., Abdelghani, A., Ameer, S., & Jaffrezic-Renault, N. (2006). Impedance spectroscopy and affinity measurement of specific antibody-antigen interaction. *Materials Science and Engineering C*, 26(2-3), 546-550.
- Trojanowicz, M. (2006). Analytical applications of carbon nanotubes: A review. *TRAC Trends in Analytical Chemistry*, 25(5), 480-489.
- Tully, E., Higson, S. P., & O’Kennedy, R. (2008). The development of a ‘labelless’ immunosensor for the detection of Listeria monocytogenes cell surface protein, Internalin B. *Biosensors and Bioelectronics*, 23(6), 906-912.

- Varshney, M., & Li, Y. (2007). Interdigitated array microelectrode based impedance biosensor coupled with magnetic nanoparticle-antibody conjugates for detection of Escherichia coli O157:H7 in food samples. *Biosensors and Bioelectronics*, 22(11), 2408-2414.
- Varshney, M., Li, Y., Srinivasan, B., & Tung, S. (2007). A label-free, microfluidics and interdigitated array microelectrode-based impedance biosensor in combination with nanoparticles immunoseparation for detection of Escherichia coli O157:H7 in food samples. *Sensors and Actuators B: Chemical*, 128(1), 99-107.
- Velusamy, V., Arshak K Fau - Korostynska, O., Korostynska O Fau - Oliwa, K., Oliwa K Fau - Adley, C., & Adley, C. (2010). An overview of foodborne pathogen detection: In the perspective of biosensors. *Biotechnology Advances*, 28(2), 232-254.
- Venturelli, E., Fabbro, C., Chaloin, O., Menard-Moyon, C., Smulski, C. R., Da Ros, T., Kostarelos, K., Prato, M., & Bianco, A. (2011). Antibody covalent immobilization on carbon nanotubes and assessment of antigen binding. *Small*, 7(15), 2179-2187.
- Viswanathan, S., Rani, C., & Ho, J. A. (2012). Electrochemical immunosensor for multiplexed detection of food-borne pathogens using nanocrystal bioconjugates and MWCNT screen-printed electrode. *Talanta*, 94, 315-319.
- Wanekaya, A. K., Chen, W., Myung, N. V., & Mulchandani, A. (2006). Nanowire-based electrochemical biosensors. *Electroanalysis*, 18(6), 533-550.
- Wang, H., Farber, J. M., Malik, N., & Sanders, G. (1999). Improved PCR detection of Campylobacter jejuni from chicken rinses by a simple sample preparation procedure. *International Journal of Food Microbiology*, 52(1), 39-45.
- Wang, R., Ruan, C., Kanayeva, D., Lassiter, K., & Li, Y. (2008). TiO<sub>2</sub> Nanowire Bundle Microelectrode Based Impedance Immunosensor for Rapid and Sensitive Detection of Listeria monocytogenes. *Nano Letters*, 8(9), 2625-2631.
- Wang, S., LeCroy, G. E., Yang, F., Dong, X., Sun, Y.-P., & Yang, L. (2015). Carbon nanotube-assisted capturing of bacterial pathogens. *RSC Advances*, 5(111), 91246-91253.

- Wang, Y., & Salazar, J. K. (2016). Culture-independent rapid detection methods for bacterial pathogens and toxins in food matrices. *Comprehensive Reviews in Food Science and Food Safety*, *15*(1), 183-205.
- Wang, Y., Ying, Y., & Ye, Z. (2012). New trends in impedimetric biosensors for the detection of foodborne pathogenic bacteria. *Sensors*, *12*(3), 3449-3471.
- Weber, J. E., Pillai, S., Ram, M. K., Kumar, A., & Singh, S. R. (2011). Electrochemical impedance-based DNA sensor using a modified single walled carbon nanotube electrode. *Materials Science and Engineering C*, *31*(5), 821-825.
- Wolffs, P., Norling, B., & Rådström, P. (2005). Risk assessment of false-positive quantitative real-time PCR results in food, due to detection of DNA originating from dead cells. *Journal of Microbiological Methods*, *60*(3), 315-323.
- Wu, W., Li, J., Pan, D., Li, J., Song, S., Rong, M., Li, Z., Gao, J., & Lu, J. (2014). Gold nanoparticle-based enzyme-linked antibody-aptamer sandwich assay for detection of Salmonella Typhimurium. *ACS Applied Materials & Interfaces*, *6*(19), 16974-16981.
- Wujcik, E. K., Wei, H., Zhang, X., Guo, J., Yan, X., Sutrave, N., Wei, S., & Guo, Z. (2014). Antibody nanosensors: A detailed review. *RSC Advances*, *4*(82), 43725-43745.
- Xu, M., Wang, R., & Li, Y. (2016). Rapid detection of Escherichia coli O157:H7 and Salmonella Typhimurium in foods using an electrochemical immunosensor based on screen-printed interdigitated microelectrode and immunomagnetic separation. *Talanta*, *148*, 200-208.
- Xu, M., Wang, R., & Li, Y. (2017). Electrochemical biosensors for rapid detection of Escherichia coli O157:H7. *Talanta*, *162*, 511-522.
- Yakes, B. J., Papafragkou, E., Conrad, S. M., Neill, J. D., Ridpath, J. F., Burkhardt, W., Kulka, M., & Degrasse, S. L. (2013). Surface plasmon resonance biosensor for detection of feline calicivirus, a surrogate for norovirus. *International Journal of Food Microbiology*, *162*(2), 152-158.

- Yamada, K., Choi, W., Lee, I., Cho, B. K., & Jun, S. (2016). Rapid detection of multiple foodborne pathogens using a nanoparticle-functionalized multi-junction biosensor. *Biosensors and Bioelectronics*, 77(1873-4235), 137-143.
- Yamada, K., Kim, C. T., Kim, J. H., Chung, J. H., Lee, H. G., & Jun, S. (2014). Single walled carbon nanotube-based junction biosensor for detection of Escherichia coli. *PLoS One*, 9(9), e105767.
- Yang, L. (2009). Dielectrophoresis assisted immuno-capture and detection of foodborne pathogenic bacteria in biochips. *Talanta*, 80(2), 551-558.
- Yang, L. (2012). A review of multifunctions of dielectrophoresis in biosensors and biochips for bacteria detection. *Analytical Letters*, 45(2-3), 187-201.
- Yang, L., & Bashir, R. (2008). Electrical/electrochemical impedance for rapid detection of foodborne pathogenic bacteria. *Biotechnology Advances*, 26(2), 135-150.
- Yang, L., Li, Y., & Erf, G. F. (2004). Interdigitated array microelectrode-based electrochemical impedance immunosensor for detection of Escherichia coli O157:H7. *Analytical Chemistry*, 76(4), 1107.
- Yazgan, I., Noah, N. M., Toure, O., Zhang, S., & Sadik, O. A. (2014). Biosensor for selective detection of E. coli in spinach using the strong affinity of derivatized mannose with fimbrial lectin. *Biosensors and Bioelectronics*, 61, 266-273.
- Yoo, J., Cha, M., & Lee, J. (2008). *Bacterial concentration detection with dielectrophoresis and capacitive measurement* (Vol. 2).
- Yun, Y., Bange, A., Heineman, W. R., Halsall, H. B., Shanov, V. N., Dong, Z., Pixley, S., Behbehani, M., Jazieh, A., Tu, Y., Wong, D. K. Y., Bhattacharya, A., & Schulz, M. J. (2007). A nanotube array immunosensor for direct electrochemical detection of antigen–antibody binding. *Sensors and Actuators B: Chemical*, 123(1), 177-182.

- Zeng, B., Wei, S., Xiao, F., & Zhao, F. (2006). Voltammetric behavior and determination of rutin at a single-walled carbon nanotubes modified gold electrode. *Sensors and Actuators B: Chemical*, 115(1), 240-246.
- Zhan, X., Tang, W., Dou, W., & Zhao, G. (2013). Disposable immunosensor for Escherichia coli O157:H7 based on a multi-walled carbon nanotube-sodium alginate nanocomposite film modified screen-printed carbon electrode. *Analytical Letters*, 46(17), 2690-2704.
- Zhang, D., Yan, Y., Li, Q., Yu, T., Cheng, W., Wang, L., Ju, H., & Ding, S. (2012). Label-free and high-sensitive detection of Salmonella using a surface plasmon resonance DNA-based biosensor. *Journal of Biotechnology*, 160(3-4), 123-128.
- Zhang, S., Wright, G., & Yang, Y. (2000). Materials and techniques for electrochemical biosensor design and construction. *Biosensors and Bioelectronics*, 15(5), 273-282.
- Zhao, X., Lin, C. W., Wang, J., & Oh, D. H. (2014). Advances in rapid detection methods for foodborne pathogens. *Journal of Microbiology and Biotechnology*, 24(3), 297-312.